Elucidation of a Molecular Mechanism Controlling Inflammation during Bacterial Infection

INAUGURALDISSERTATION

zur
Erlangung der Würde eines Doktors der Philosophie
vorgelegt der
Philosophisch-Naturwissenschaftlichen Fakultät
der Universität Basel

von
Therese Tschon-Müller
aus Füllinsdorf, BL

BASEL, 2015

Genehmigt von der Philosophisch-Naturwissenschaftlichen Fakultät

auf Antrag von:

Prof. Dr. Cécile Arrieumerlou
        Dissertationsleiterin
Prof. Dr. Matthias Wymann
        Korreferent

Basel, den 11.11.2014

Prof. Dr. Jörg Schibler
        Dekan

Dedicated to

My husband, Dominik Tschon-Müller

Our daughters, Laura and Karina

My social parents, Susanne and Ruedi Weisskopf-Ruetz

Abstract

Recently we described a mechanism of gap junction-mediated communication between infected and uninfected epithelial cells that potentiates innate immunity during infection by the enteroinvasive bacterium *Shigella flexneri*. We showed that although *S. flexneri* secretes multiple effector proteins that downregulate inflammation in infected epithelial cells, NF-κB and the MAP kinases p38, JNK and ERK are activated in uninfected cells surrounding the sites of infection. The propagation of these proinflammatory signals leads to massive secretion of proinflammatory cytokines such as interleukin-8 (IL-8) by uninfected bystander cells. A genome wide RNAi-screen on *Shigella*-induced bystander activation confirmed the roles of the proteins TAK1 and NF-κB. Besides this, new candidates for bystander activation were found, including Na^+/K^+-ATPase (ATP1A1), the TRAF-interacting protein with a FHA domain (TIFA) and the TNF receptor-associated factor 6 (TRAF6). These proteins together with NOD1 and RIPK2, members of the NOD1 signaling pathway, which is induced by invasive *Shigella*, were studied in more detail. To our surprise we found that signals underlying cell-cell communication are produced independently of the receptor NOD1 and the downstream signaling proteins RIPK2, TAK1 and NF-κB as well as independent of TIFA and TRAF6. Unexpectedly, in bystander cells NOD1 and RIPK2 contribute to the proinflammatory response, whereas TAK1, NF-κB, TIFA and TRAF6 are indispensable for the production of cytokines. Furthermore, TIFA and TRAF6 are upstream of TAK1 and are required for TAK1 activation. In addition, selective stimulation of TIFA or TRAF6 depleted cells with the NOD1 ligand iE-DAP unraveled that TIFA and TRAF6 contribute to NOD1 signaling in bystander cells of *S. flexneri* infection. And finally, we propose a link between intercellular calcium signaling triggered by invasive *S. flexneri* and bystander IL-8 expression, since inhibition of calcium signals via a calcium chelator or inhibition of the IP_3-receptor or phospholipase C (PLC) lead to a decreased bystander IL-8 response.

Thesis Statement

The work presented here was performed in the group of Prof. Cécile Arrieumerlou in the Focal Area of Infection Biology at the Biozentrum of the University of Basel, Switzerland. My PhD was supervised by a thesis committee consisting of:

Prof. Cécile Arrieumerlou
Prof. Christoph Dehio
Prof. Matthias Wymann

The present thesis is written in a classical format consisting of the following parts: an abstract summarizing the presented work, followed by an introduction covering the topics of my research, a results part, presenting the major findings of my research, a materials and methods section, and a discussion and outlook section. For reasons of readability, not all abbreviations are written out in full, but instead a comprehensive glossary of abbreviations can be found at the end of the thesis.

Contents

Contents

I   Introduction

1 *Shigella* causative agent of shigellosis and model organism to study host pathogen interactions

1.1 Shigellosis or acute bacillary dysentery

Shigellosis or bacillary dysentery is a global human health problem especially in developing countries, with poor hygiene and bad water supplies. However, shigellosis also occurs in industrialized countries where children in day-care centers, travelers, migrant workers or persons infected with HIV most often are affected. In 1999, it was estimated that annually more than 165 million *Shigella* episodes occur worldwide, with 99% occurring in developing countries. 1.1 million deaths were attributed to *Shigella* infections annually. The highest incidence and case-fatality rates were found in children below the age of five years [1]. Recently, by reviewing the literature from 1990 to 2009, a similar incidence rate was found for shigellosis but the number of cases with fatal outcome was 98% lower compared to the earlier estimate. The authors of the new study speculate that nonspecific interventions including measles vaccination, vitamin A supplementation and improved nutrition could be the reason for the reduced number of deaths in shigellosis patients [2]. However, shigellosis remains a global health burden due to the high incidence rate and the emerging number of multi-drug resistant *Shigella* strains [3].

Bacillary dysentery is caused by *Shigella* species that are highly adapted to primates and humans. The genus *Shigella* belongs to the family of *Enterobacteriaceae*. There are four major species of *Shigella* classified by biochemical, antigenetic and clinical characteristics: *S. dysenteriae, S. flexneri, S. boydii* and *S. sonnei* [4]. The majority of all infections is caused by *S. flexneri* and *S. sonnei*, whereas *S. dysenteriae* is responsible for the most severe form of dysentery and therefore causes the majority of fatal shigellosis cases.

Bacteria are transmitted directly via the feco-oral route or indirectly through contaminated water or food. The pathogen is highly contagious, as few as 100 microorganisms are sufficient to cause the disease [5]. *Shigella* species invade the human colon and rectum where they cause an acute mucosal inflammation. Patients suffer from diarrhea, mucoid bloody stool, fever and abdominal cramps. Shigellosis is usually a self-limited illness. But depending on the virulence potential of the strain and the nutritional status of the individual, shigellosis can progress to severe disease [6].

Even though, oral rehydration would be sufficient as therapy, an additional antibiotic treatment is advantageous and recommended by the World Health Organisation (WHO 2005) guidelines [7]. On one hand it shortens the duration of the disease, in serious cases it might be life-saving and the spreading of the disease can be limited. A major problem, however, is the increasing number of multidrug-resistant *Shigella* strains [8]. Therefore, an effective *Shigella* spp. vaccine may have substantial benefits, but so far there is no vaccine available.

1.2   Cellular pathogenesis of *Shigella* infections

Shigella spp. are enteroinvasive, gram-negative, rod-shaped, non-motile, uncapsulated, and facultative anaerob bacteria that belong to the family *Enterobacteriaceae*. *Shigella* spp. evolved from non-pathogenic *E. coli* by the acquisition of a large virulence plasmid and chromosomal pathogenicity islands (PAI). Comparative genomics between *E. coli* K-12 and *Shigella* spp. revealed sequence differences of about 1.5% only. To date the complete sequences of the virulence plasmids and the chromosomes of various *Shigella* strains are available [9].

The PAIs together with the virulence plasmid encoded genes are responsible for the invasive phenotype of *Shigella* spp.. These genes allow *Shigella* to kill macrophages, to invade intestinal epithelial cells (IECs) and to trigger the acute inflammation response typical for shigellosis. pWR100, the 213-kb virulence plasmid of *S. flexneri* strain M90T (serotype 5) harbors about 100 genes and many insertion sequences [10]. The core of the plasmid is the conserved 31-kb entry region, where genes are clustered, that are required and sufficient to invade IECs and to induce pyroptosis in macrophages. This gene cluster encodes for Mxi and Spa proteins that are required for assembly and regulation of the type 3 secretion system (T3SS), the transcription factors VirB and MxiE, chaperones (IpgA, IpgC, IpgE, and Spa15), the translocators IpaB and IpaC and the secreted effector proteins (IpaD, IpgB1, IpgD and IcsB) [11-13]. Other substrates of the T3SS are encoded by genes scattered throughout the virulence plasmid and are listed in Table I.1.

Table I.1 *S. flexneri* T3SS translocated effectors encoded on the virulence plasmid.

Effector	Biochemical activity	Host cell target(s)	Virulence function and/or phenotype
IpaA	Vinculin activation	Vinculin, β_1-integrins, Rho signaling	Efficient invasion, actin cytoskeleton rearrangements, disassembly of cell-matrix adherence
IpaB	Membrane fusion	Cholesterol, CD44, caspase-1	Control of type III secretion, translocon formation, phagosome escape, macrophage apoptosis
IpaC	Actin polymerization	Actin, β-catenin	Translocon formation, filopodium formation, phagosome escape, disruption of EC tight junctions
IpaD			Control of type III secretion, membrane insertion of translocon
IpaH7.8			Efficient phagosome escape
IpaH9.8	E3 ubiquitin ligase	Splicing factor U2AF, MAPK kinase, NEMO/IKKγ ABIN-1, NF-κB pathway	Host cell transcriptome modulation, reduction of inflammation
IpaH0722	E3 ubiquitin ligase	TRAF2	Inhibition of NF-κB activation, dampening of inflammatory response
IpaJ	Cysteine protease	ARF1	Inhibition of Golgi cargo transport, Golgi fragmentation
IcsA (VirG)		N-WASP, vinculin	Recruitment of actin-nucleating complex required for actin-based motility and intercellular spread
IcsB		Atg5	Camouflage of IcsA for autophagic evasion
IcsP*a*	Serine protease		Cleavage of IcsA, modulation of actin-based motility
IpgB1	RhoG mimicry	ELMO protein	Induction of Rac1-dependent membrane ruffling, regulation of inflammation
IpgB2	RhoA mimicry	RhoA ligands	Induction of actin stress fiber-dependent membrane ruffling
IpgD	Phosphoinositide 4-phosphatase	Phosphatidylinositol 4,5-bisphosphate, leads to connexin hemichannel blockage	Facilitation of entry, promotion of host cell survival, prevents termination of EGFR signaling, down-regulates inflammation by preventing ATP secretion
OspB		Retinoblastoma Protein, GEF-H1, NF-κB pathway	Reduction of inflammation
OspC1		Nucleus and cytoplasm	Induction of PMN migration
OspC3	Caspase-4 binding, prevents p19/p10 heterodimerization	Caspase-4	Reduction of cell death, increased bacterial replication

Table I.1 Continued on next page

Effector	Biochemical activity	Host cell target(s)	Virulence function and/or phenotype
OspD1			T3SS substrate, unknown function in host cells, antiactivator of MxiE
OspE1/E2		ILK, Focal contacts	Maintenance of EC morphology, stabilization of focal adhesion
OspF	Phosphothreonine lyase	MAPKs Erk and p38	Inhibition of histone phosphorylation and NF-κB-dependent gene expression, reduction of PMN recruitment
OspG	Protein kinase, ubiquitination inhibitor	Ubiquitin-conjugating enzymes	Downregulation of NF-κB activation, reduction of inflammation
OspI	Glutamine deamidase	Ubiquitin-conjugating enzymes	Downregulation of NF-κB activation, reduction of inflammation
OspZ		NF-κB	blockage of NF-κB subunit p65 nuclear translocation, downregulation of IL-8 expression, redcues PMN transepithelial migration
PhoN2*a*	Apyrase		Unipolar localization of IcsA
SepA*a*	Serine protease		Promotion of intestinal tissue invasion and destruction
VirA	Cysteine protease	α-Tubulin	Facilitation of entry and intracellular motility by degradation of microtubules, Golgi fragmentation Calpain activation, cell death

Adapted with modifications from PhD Thesis from C. Schmutz.

Contact with host cell membranes triggers the insertion of the translocators IpaB and IpaC into the host cell membrane, where they form a pore through which they are themselves exported together with other effector proteins [14-16]. Expression of the genes of the virulence plasmid is tightly regulated. The regulatory cascade is triggered in response to environmental changes such as temperature shift to 37°C after uptake by the host, pH, osmolarity and iron concentration [17-20]. Upon encountering such changes, the virulence plasmid encoded transcription factors VirF and VirB are expressed, which in turn induce the expression of the entry region and the first set of effector proteins (IpaA-D, IpgB1, IpgD, IcsB, OspC2-4, OspD1/2,OspB, OspF, OspC1 and VirA) of the virulence plasmid [12, 17]. Increased transcription of the first set proteins during secretion triggers the expression of a second set of effectors (OspB, OspC1, OspE1/2, OspF, VirA, OspG and IpaH4.5/7.8/9.8) under the control of the transcription factor MxiE and the chaperone IpgC, acting as a co-activator [21].

Once ingested *Shigella* species survive the acidic milieu of the stomach because they harbor acid resistance systems [22]. In addition, *Shigella* species are able to down-regulate the expression of antimicrobial peptides in the intestine [23]. After passing the small intestine, *Shigella* spp. reach the colon and rectum. Since *Shigella* spp. are not able to effectively invade epithelial cells directly from the luminal side, invasion occurs through the basolateral pole of colonic epithelial cells [24]. In order to get access to the submucosal space *Shigella* spp. exploit microfold cells (M-cells), specialized epithelial cells in the follicular associated epithelium (FAE) that overlie lymphoid tissue [25, 26]. M-cells allow intact *Shigella* to traverse into the underlying subepithelial pocket where macrophages reside and phagocytose invading bacteria. *Shigella* escape from the phagosome, enter the macrophage cytosol, where they replicate and induce pyroptosis [27]. Prior to cell death, infected macrophages release large amounts of the proinflammatory cytokines interleukin-1β (IL-1β) and IL-18 through the direct activation of caspase-1 by *Shigella* [27, 28]. Secretion of these cytokines results in the acute and massive inflammatory response, a hallmark of shigellosis [29]. IL-18 induces an effective antibacterial response by attracting natural killer (NK) cells and by inducing the production of interferon γ (INF-γ). IL-1β release results in the recruitment of polymorphonuclear cells (PMNs) from the blood stream to the site of infection [30, 31]. PMNs are phagocytes that efficiently kill bacteria. Invading PMNs cross the epithelial layer and thereby disrupt the integrity of the epithelium. This, in turn, allows more lumenal bacteria to translocate into the subepithelial space [32] and gives *Shigella* access to the basolateral pole of epithelial cells [24]. By the use of the T3SS, *Shigella* delivers effector proteins into the host cell. One set of the translocated effectors interfere with cytoskeletal components, induce the formation of membrane ruffles that engulf the bacteria and lead to their macropinocytotic uptake [9]. After having lysed the phagosomal membrane, *Shigella* reach the host cell cytosol where they start to replicate. By means of actin based motility, they spread to neighboring cells [33, 34]. Infected IECs recognize *Shigella* mainly via the cytosolic pattern recognition receptor NOD1 [35]. Upon binding of peptidoglycan moieties released from replicating bacteria, NOD1 gets activated, which is followed by the activation of the NF-κB and MAPK signaling pathways resulting in the expression of proinflammatory genes [36, 37] (Table I.2).

Table I.2 Up-regulated genes in *S. flexneri* infected IECs.

Category of genes	Description of genes	Fold increase*
Chemokines and cytokines	Interleukin-8	304.79
	CXCL1	133.74
	CCL20	38.67
	CXCL2	13.17
	TNF-*α* inducible protein A20	4.23
	CXCL3	3.12
	TNF-α[ρ]	3.06
	B94 protein	1.66
Colony-stimulating factors	GM-CSF	33.24
	IEX-1	1.88

*Gene expression of *S. flexneri* infected CaCo-2 cells compared to gene expression in uninfected CaCo-2 cells. *Adapted with modifications from* [36]

Amongst these genes, IL-8, another chemoattractant of PMNs, is highly expressed during *Shigella* infection [38]. *Shigella* use another set of effector proteins including OspF, OspG, OspI, OspZ, IpaH0722 and IpaH9.8 to interfere with host cell signaling cascades thereby dampening the inflammatory response in infected cells (described in more detail in section 2.3). Infected cells in turn, counteract the inhibitory effect of bacterial effector proteins by propagating inflammatory signals to uninfected bystander cells, which produce large amounts of proinflammatory cytokines, such as IL-8 (described in detail in section 3.3) (Figure I.1) [39].
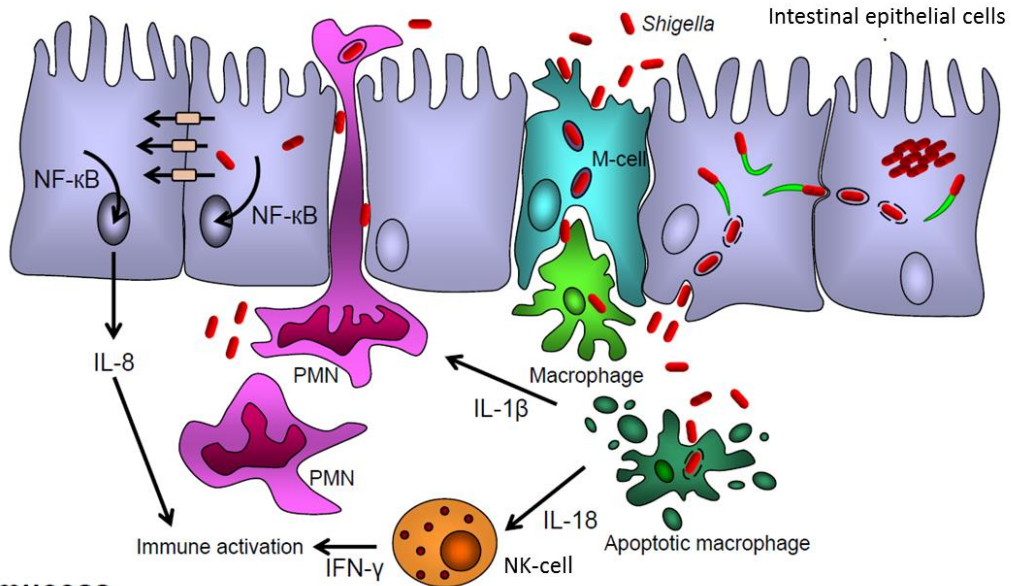
1.3 Induction of pyroptosis in macrophages

After having crossed the intestinal epithelial layer via M-cells, *Shigella* reaches the submucosal space where macrophages reside. Macrophages are phagocytes that take up and degrade cellular debris, foreign substances and invading pathogens. Several bacterial pathogens have developed different strategies to escape from macrophage killing. *S. flexneri*, for instance, kills macrophages and thereby gets access to the basolateral side of IECs, which comprise the replicative niche of *Shigella*. To do so, *S. flexneri* induces pyroptosis in macrophages. Pyroptosis is a form of programmed cell death (PCD) that is characterized by the activation of NLR inflammasomes, multi-protein complexes described in more detail in section 2.1.2. Inflammasomes mediate the activation of caspase-1, which mediates the proteolytic maturation of the cytokines IL-1β and pro-IL-18 and induces pyroptotic cell death [40, 41]. Cytokine secretion is followed by a massive inflammation response including the attraction of PMNs to the site of infection. Invading PMNs destabilize the integrity of the intestinal epithelial barrier and favor *Shigella* invasion.

1.4 *Shigella* adherence and uptake into intestinal epithelial cells

Once released form dying macrophages, *S. flexneri* have access to the basolateral side of IECs. Here they adhere to host cells at the sites of lipid rafts [42], which are subdomains of the plasma membrane that contain high concentrations of cholesterol, sphingolipids and glycosphingolipids [43]. Furthermore, this lipid rafts contain clusters of specific receptor proteins, which are connected to the actin cytoskeleton and to proteins

Figure I.1 Stages of *Shigella flexneri* infection. Lumenal bacteria traverse the colonic epithelial cell layer via endocytic M-cells that transcytose the bacteria into the submucosal space, where they are phagocytosed by macrophages. After escaping from the phagosome, *Shigella* induces pyroptosis in macrophages, leading to the release of the proinflammatory cytokines IL-1β and IL-18. Upon escape from dying macrophages, *Shigella* bacteria trigger their uptake into IECs, escape from the vacuole, replicate in the host cytosol and use actin based motility to spread to adjacent IECs. IECs sense bacteria via pattern recognition receptors that activate the NF-κB signaling pathway. The proinflammatory signals are propagated from infected to uninfected bystander cells, which produce large amounts of IL-8. The secreted cytokines from macrophages and IECs, IL-1β and IL-8, attract PMNs to the site of infection. PMNs phagocytose the bacteria and are responsible for the clearance of the infection. IL-18 stimulates NK cells to produce IFN-γ. Altogether contribute to the induction of the acute intestinal inflammation characteristic for shigellosis. IEC, intestinal epithelial cell; IFN-γ, interferon gamma; NK-cell, natural killer cell; PMN, polymorph nuclear cell. *Adapted with modifications from PhD Thesis from C. Schmutz and from [9]*

localized at the cytoplasmic side of the plasma membrane [44]. Thus, lipid rafts act as signaling platforms that control endocytosis, intracellular vesicle trafficking and activation of the immune response and apoptosis [45-48]. The CD44 hyaluronan and $\alpha_5\beta_1$ integrin receptor, are two proteins that are clustered in lipid rafts and both are administered by *S. flexneri* for adhesion [49, 50]. IpaB interacts with CD44, whereas the $\alpha_5\beta_1$ integrin receptor is bound by IpaB, IpaC and IpaD. Recently, the outer membrane protein IcsA, known to be required actin based motility, in addition, was found to function as an adhesin that was necessary and sufficient to promote contact with IECs [51]. So far, the host receptor for IcsA could not be identified. Contact with host cells induces T3SS dependent secretion of effector proteins into the host cell cytosol. The concerted action of pore-forming proteins and effectors triggers massive actin polymerization. This leads to the formation of large membrane protrusions that engulf the bacteria and allow the macro-pinocytotic internalization of bacteria into non-phagocytic host cells. Reorganization of the eukaryotic actin cytoskeleton is controlled by small Rho GTPases (including RHOA, RHOG, CDC42 and RAC1) and tyrosine kinases (e.g. SRC family members). The *S. flexneri* effector IpgB1, by mimicking activated RhoG, activates the RAC1-ELMO-DOCK180 pathway leading to membrane ruffling [52]. IpgB2, by mimicking activated RhoA, mediates stress fibers and membrane ruffling [53]. However, its role in the invasion process of *S. flexneri* is not completely understood. The pore-forming protein IpaC of *S. flexneri* induces SRC-dependent actin nucleation and ruffle formation in the vicinity of the bacteria [54, 55]. Secreted IpaA binds to the cytoskeleton associated protein vincullin, thus promoting depolymerization of actin filaments, which results in the weakened adhesion of the host cell to the extracellular matrix [56]. And finally, the injected phosphoinositide phosphatase IpgD uncouples the plasma membrane from the actin cytoskeleton thereby facilitating the remodeling of membranes and actin [57].

1.5 Phagosome escape, replication and intra - and intercellular dissemination

Within less than 15 minutes *S. flexneri* lysis the macropinocytic vacuole and escapes into the host cell cytosol [58]. Membrane lysis is mediated by the T3SS translocator proteins IpaB, IpaC and IpaD [59-61]. Furthermore, IpaH7.8 has been shown to be involved in phagosome escape in macrophages by a yet unknown mechanism [62]. Liberated *S. flexneri* bacteria start to replicate in the host cell cytosol, protected from immune system components present in the extracellular environment. In order to evade

from the intracellular host defense *S. flexneri* follows two strategies: (I) spreading from cell to cell and (II) the manipulation of host cell immune signaling, which is described in section 2.3.

S. flexneri exploits the host cell actin assembly machinery to move through the cytoplasm and into adjacent epithelial cells. The effector protein IcsA (VirG) is localized at one pole of the bacterium and mediates actin polymerization by binding to the host protein N-WASP[34, 63, 64]. Emerging actin filaments localized at one pole of the bacterium generate propulsive forces and allows *S. flexneri* to propel through the cytoplasm of the host cell. The movement of the bacterium through the cell is supported by the action of the T3SS substrate VirA, which degrades α-tubulin to weaken the intracellular microtubule network [65]. In addition, intracellular replication and motility of the bacteria depends on the ability of *S. flexneri* to escape from the host's autophagy machinery. Autophagy is a crucial process for survival of cells and mediates the degradation of undesirable cellular components including invasive microbes in double-membrane compartments. The effector protein IcsB protects *S. flexneri* from autophagy recognition [66, 67]. By binding to IcsA, IcsB masks the autophagy-inducing-recognition site of IcsA, and thus the bacteria cannot be engulfed by autophagic vacuoles and are therefore protected from degradation. When moving bacteria contact the host cell membrane, membrane protrusions into the adjacent cell are formed, which are actively endocytosed by the neighboring cell in a myosin light chain kinase and cadherin dependent process [68, 69]. Inside, the new host cell *S. flexneri* starts a new replication cycle after having lysed the vacuole.

2 Innate Immunity

Vertebrates are constantly exposed to microorganisms or toxic substances through contact, ingestion and inhalation. The immune system evolved to protect multicellular organisms from environmental stresses. The evolutionary older innate immune system comprises the first line of defense against invasive pathogens in a rapid but non-specific manner. There are several strategies how this is achieved, including formation of physical barriers at epithelial surfaces, complement activation, induction of an inflammatory response, removal of pathogens by PMNs and macrophages and finally the activation of the adaptive immune system, which elicits a specific response to the invading pathogen and provides immune memory.

2.1 Innate immune receptors: sensors of invading microbes

Fast pathogen recognition and the initiation of an inflammatory response are crucial for the successful elimination of invading pathogens. This is achieved by germ line encoded pattern recognition receptors (PPRs), which are expressed by hematopoietic cells of myeloid origin including dendritic cells, macrophages and neutrophils as well as non-hematopoietic cells such as epithelial cells. PRRs detect conserved components expressed uniquely by microbes, so called pathogen-associated molecular patterns (PAMPs), e.g. lipopolysaccharide (LPS), lipoproteins or muramylpeptides (MDPs) [70]. There is emerging evidence that these receptors are also able to recognize endogenous molecules originating from injured or dying cells, termed damage associated molecular patterns (DAMPs), e.g. ATP or DNA [71]. Up to now, four different families of PRRs have been identified. Members of the Toll-like receptors (TLRs) family and the C-type lectin receptor (CLR) family are transmembrane proteins. Receptors belonging to these two families are located at plasma and endosomal membranes to survey the extracellular compartment and the endosomes for the presence of PAMPs and DAMPs. Members of the Retinoic acid-inducible gene (RIG)-I-like receptor (RLR) family and NOD-like receptor (NLR) family are cytoplasmic receptors [70]. These receptors sense the presence of intracellular PAMPs and DAMPs. Invading bacteria are recognized by TLRs and NLRs, whereas RLRs detect nucleic acids from viruses and CLRs sense fungal PAMPs [70] (Figure I.2). Upon activation of these receptors, various signaling cascades are triggered that control transcription factors such as NF-κB, AP-1, Elk-1, ATF2 and members of the interferon regulatory factor (IRF) family [72-74].

Activation of these transcription factors in turn leads to the expression of proinflammatory genes such as chemokines including IL-8 and CCL2 that attract other immune cells to the site of infection, as well as cytokines such as IL-1β, IL-6 and TNFα that modulate the immune response.
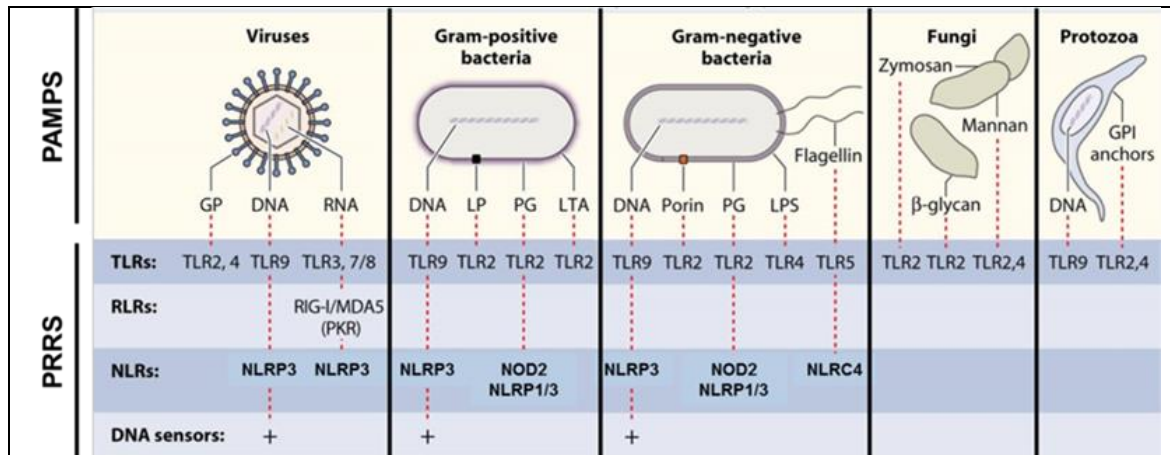
Figure I.2 PRRs recognize PAMPs derived from different classes of pathogens. Viruses, bacteria, fungi, and protozoa expose various PAMPs, some of which are shared between different classes of pathogens. Main PAMPs are nucleic acids, including DNA, dsRNA and ssRNA, as well as surface glycoproteins (GP), lipoproteins (LP), and membrane components such as peptidoglycan (PG), lipoteichoic acid (LTA), lipopolysaccharide (LPS), and GPI anchors. These diverse PAMPs are recognized by different families of PRRs including TLRs (Toll-like recpetors), RLRs (RIG-I-like receptors), NLRs (NOD-like receptors) and DNA sensors. *Adapted with modifications from* [75]

2.1.1 Toll like receptors

Members of the TLR family are the most extensively studied class of PRRs. To date 13 mammalian TLRs have been identified [76]. They are integral membrane proteins that expose leucin-rich-repeat (LRR) domains to an extracellular or luminal compartment and a cytoplasmic Toll/interleukin-1 (IL-1) receptor homology (TIR) domain into the cytosol. The LRR domain is responsible for molecular recognition, whereas the TIR domain transduces signals to intracellular adaptor proteins leading to the activation of downstream signaling pathways that control an effective immune response to invading organisms [77]. TLRs interact with a variety of PAMPs derived from bacteria, viruses, fungi and parasites (Table I.3) and DAMPs derived from injured cells (Table I.4).

Table I.3 PAMPs recognized by TLRs, NLRs and other PRRs.

Species	PAMP	TLRs	NLRs, other PRRs
Bacteria	LPS	TLR4	
	Lipoproteins, PDG, LTA, Lipoarabinomannan	TLR2/1, TLR2/6	NOD1, NLRP3, NLRP1
	MDP		NOD2, NLRP1
	Flagellin	TLR5	NLRC4
	DNA	TLR9	AIM2
	RNA	TLR7/TLR13	NLRP3
Viruses	DNA	TLR9	AIM2, DAI, IFI16
	RNA	TLR3, -7, -8	RIG-I, MDA5, NLRP3
	Structural protein	TLR2, -4	
Fungi	Zymosan	TLR2, -6	Dectin-1
	β-glucan	TLR2, -6	Dectin-1, NLRP3
	Mannan	TLR2, -4	
	DNA	TLR9	
	RNA	TLR7	
Parasites	tGPI-mutin (*Trypanosoma*)	TLR2	
	Glycoinositolphospholipids (*Trypanosoma*)	TLR4	
	DNA	TLR9	
	Hemozoin (*Plasmodium*)	TLR9	NLRP3
	Profilin-like molecule (*Trypanosoma* gondii)	TLR11	

Adapted from [76, 78, 79] and NLR nomenclature according to nomenclature standards defined by [80]

Table I.4 DAMPs sensed by PRRs.

DAMP	Putative sensor
HMGB1	TLR2, TLR4, TLR9, RAGE and CD24
HSPs	TLR2, TLR4, CD91, CD24, CD14 and CD40
S100 proteins	RAGE
SAP130	CLEC4E
RNA	TLR3
DNA	TLR9 and AIM2
Uric acid and MSU crystals	NLRP3
ATP	NLRP3
Hyaluronan	TLR2, TLR4 and CD44
Biglycan	TLR2 and TLR4
Versican	TLR2
Heparan sulphate	TLR4
Formyl peptides (mitochondrial)	FPR1
DNA (mitochondrial)	TLR9
CPPD crystals	NLRP3
β-amyloid	NLRP3, CD36 and RAGE
Cholesterol crystals	NLRP3 and CD36
IL-1α	IL-1R
IL-33	ST2

Adapted with modifications from [71]

TLR1, -2, -4, -5, -6, and 11 are localized at the cell surface where they mainly recognize extracellular cell wall products that are unique to microbes. Other TLRs, such as TLR3, -7, -8, -9 and -13, are located at intracellular vesicles such as endosomal or lysosomal membranes detecting nucleic acids derived from viruses or bacteria being degraded in the lysosom. Discrimination between self and non self is achieved rather by the localization of the ligands in endosomal compartments than by a specific sequence, modification or species origin [81, 82].

Following ligand binding, TLRs undergo homo- or heterodimerization. Depending on the individual stimulus and the corresponding TLR, different TIR domain containing adaptor proteins are recruited to the receptor complex. To date, five adaptor proteins are known including myeloid differentiation factor 88 (MYD88), MYD88-adaptor like (MAL), TIR domain containing adaptor inducing IFN-β (TRIF), TRIF-related adaptor molecule (TRAM), and sterile alpha and HEAT-Armadillo motifs (SARM) [83]. According to the adaptor molecules that are engaged to the TLRs, two major intracellular signaling pathways can be activated. One is referred to as the MYD88 dependent pathway, which is activated by all TLRs, except TLR3, and is mediated via IRAK-1 and IRAK-4, TNF receptor-associated factor 6 (TRAF-6), and results in MAP kinase activation and the activation of the IkB kinase (IKK) complex. Subsequently, the transcription factors AP-1 and NF-κB are activated, which control the expression of proinflammatory genes. The second pathway, known as TRIF pathway, gets activated downstream of TLR3 or TLR4, when recruited to endosomal membranes, and leads to the activation of the interferon regulated factors (IRF) family of transcription factors resulting in the synthesis of interferon (IFN) [77] (Figure I.3).
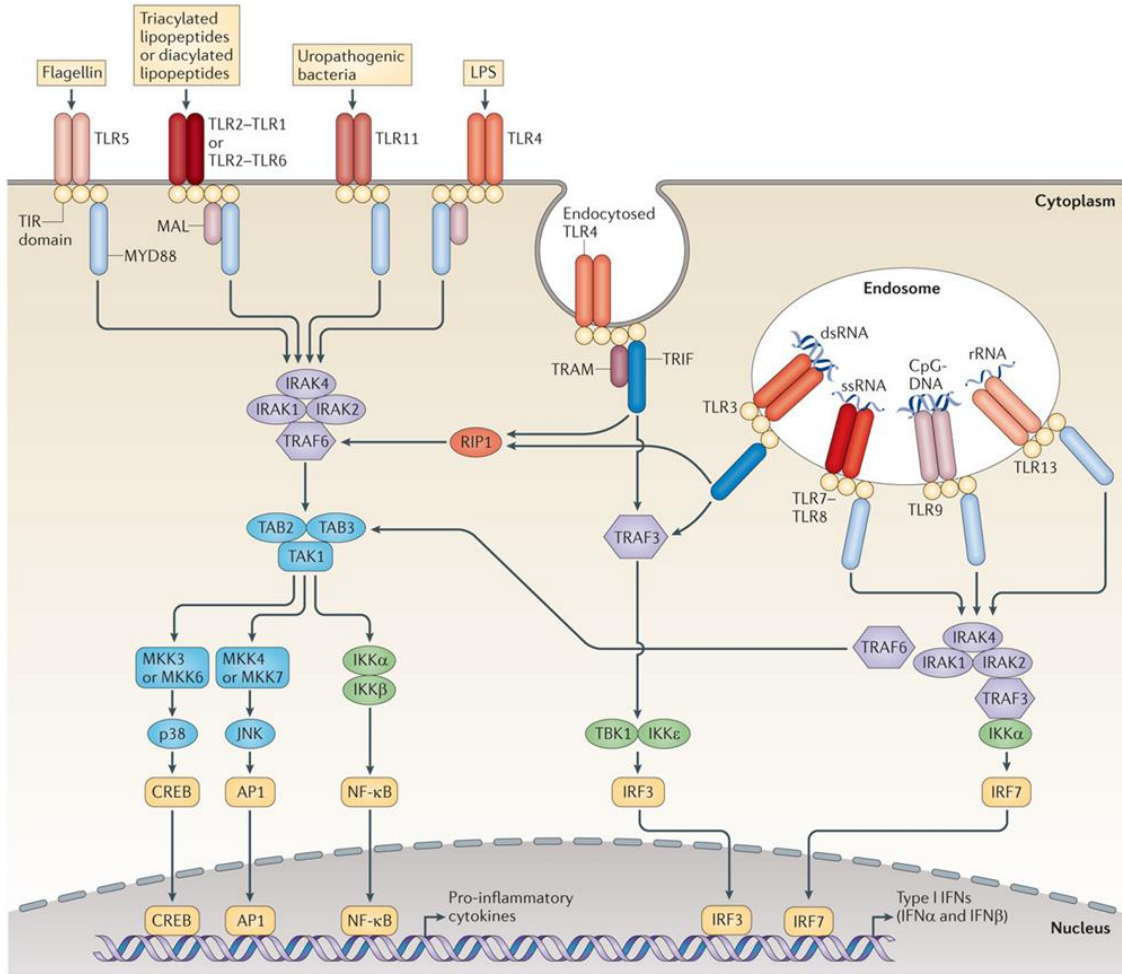
Figure I.3 Mammalian TLR downstream signaling. TLR5, TLR11, TLR4, and the heterodimers of TLR2/TLR1 or TLR2/TLR6 are localized at the cell surface to sense extracellular microbial components. TLR3, TLR7/TLR8, TLR9 and TLR13 localize to the endosomes, where they detect nucleic acids. TLR4 localizes at both, the plasma membrane and the endosomes. Ligand-binding induces the dimerization of the receptors and allows the recruitment of the adaptor proteins including MYD88, MAL, TRIF, or TRAM via homotypic interaction of the TIR domains. Receptor binding of the adaptor proteins stimulates downstream signaling pathways that are mediated by IRAK proteins and TRAF proteins leading to the activation of the MAP kinases JNK and p38, and to the activation of transcription factors including NF-κB, IRF3, IRF7, AP-1 and CREB. Activation of the TLR signaling pathway leads to the expression of proinflammatory cytokines, and in the case of the endosomal TLRs to the expression of type I interferon (IFN). CREB, cyclic AMP-responsive element-binding protein; IRAKs, IL-1R-associated kinases; JNK, JUN N-terminal kinase; MAL, MYD88-adaptor-like protein; MAPKs, mitogen-activated protein kinases; MYD88, myeloid differentiation primary-response protein 88; dsRNA, double-stranded RNA; IKK, inhibitor of NF-κB kinase; LPS, lipopolysaccharide; MKK, MAP kinase kinase; RIP1, receptor-interacting protein 1; rRNA, ribosomal RNA; ssRNA, single-stranded RNA; TAB, TAK1-binding protein; TAK,1 TGFβ-activated kinase 1; TBK1, TANK-binding kinase 1; TRAF, TNF receptor-associated factor; TRAM, TRIF-related adaptor molecule; TRIF, TIR domain-containing adaptor protein inducing IFN-β. *Adapted from* [76]

2.1.2   NOD like receptors

The human NOD-like receptor (NLR) family consists of 22 members that are characterized by a modular domain organization (Figure I.4). They are composed of a *C*-terminal leucine-rich repeat (LRR) domain involved in ligand sensing, a central nucleotide-binding and oligomerization (NBD) domain required for nucleotide binding and self-oligomerization and finally a *N*-terminal protein-protein binding domain, that interacts with downstream adaptor proteins. Based on the *N*-terminal effector domain, NLRs are classified into subfamilies: NLRA, NLR containing an acidic domain (CIITA), NLRB, NLR with baculovirus inhibitor of apoptosis repeat (BIR) domains (NAIP), NLRC consisting of NLRs with a caspase activation and recruitment (CARD) domain (NOD1, NOD2, NLRC3, NLRC4/IPAF, NLRC5), NLRP, NLR with a pyrin domain (PYD) (NLRP1 to NLRP14) and finally, NLRX, NLR with no strong homology to the N-terminal domain of any other NLR subfamily member [80]. NLRs are intracellular sensors of PAMPs and DAMPs. Upon activation of NLRs, diverse signaling cascades are triggered. Some NLRs control the inflammasome-dependent activation of caspase-1 that processes IL-1β and IL-18 [84] and induce caspase-1 dependent pyroptotic cell death [85]. Another set of NLRs activate the NF-κB and MAP kinase signaling pathways and thereby induce the transcription of proinflammatory genes [86]. Some NLR receptors trigger autophagy [87] and some induce type I interferon signaling [88].

2.1.2.1   Non-inflammasome NLRs: NOD1 and NOD2

NOD1 and NOD2 are the first characterized and best studied members of the NLRC subfamily of NLRs. NOD1 and NOD2 harbor besides their LRR and NBD domain one or two caspase recruitment domains (CARD), respectively. They are intracellular sensors for fragments of the bacterial cell wall component PDG, representing a PAMP. NOD1 detects γ-D-glutamyl-meso-diaminopimelic acid (iE-DAP), which is found primarily in the PDG of gram-negative bacteria, but also in certain gram-positive bacteria such as *Listeria* spp*.* and *Bacill*us spp. [89, 90]. Nevertheless, NOD1 is seen as sensor for gram-negative bacteria. In contrast, NOD2 detects intracellular muramyl dipeptide(MDP), which is ubiquitously present in bacteria and therefore NOD2 is referred to as a general sensor of bacteria [91]. NOD1 is expressed ubiquitously in antigen-presenting cells (APCs) including macrophages and dendritic cells and in epithelial cells, whereas NOD2 is mainly expressed in APCs [92]. Furthermore, NOD2
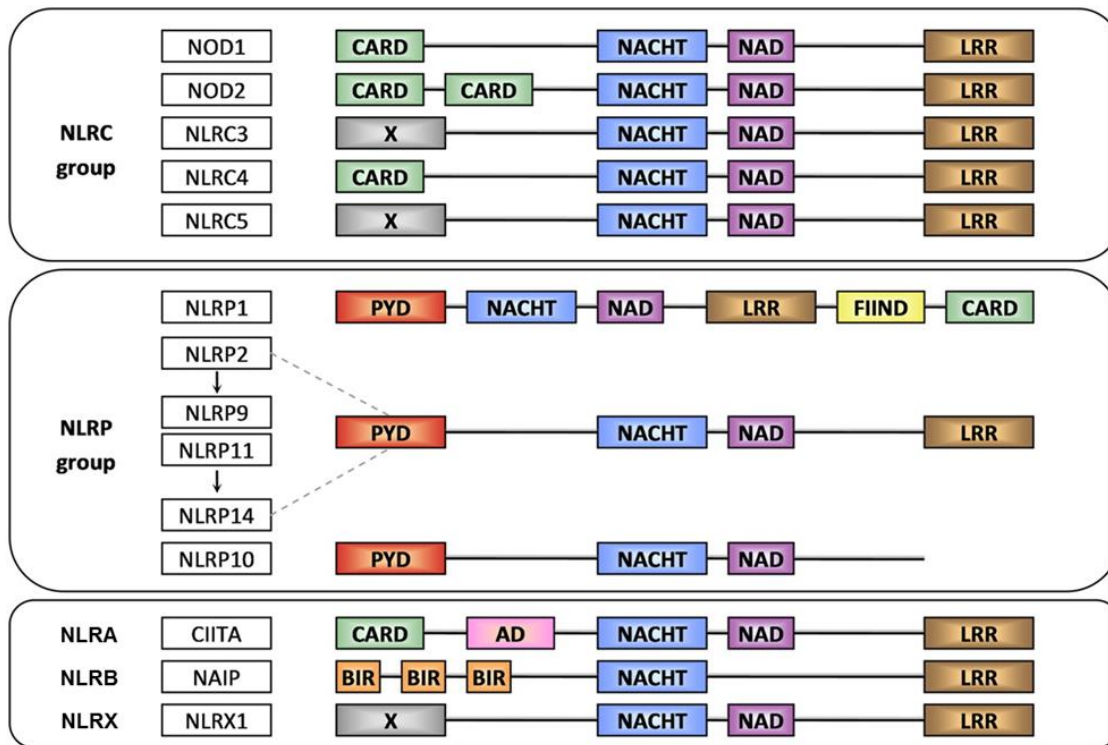
Figure I.4 Domain organization of the Nod-like receptor (NLR) family proteins. The overall structure of NLRs is a *C*-terminal leucine-rich repeat (LRR) domain, a central nucleotide binding domain (NBD) consisting of a NACHT and NAD domain and a variable *N*-terminal effector domain. The 22 NLR family members are grouped into subfamilies according to their *N*-terminal effector domain. NLRC members contain a CARD domain, NLRP members a PYD domain, NLRA members an AD domain, NLRB members BIR domains and finally, NLRX members possess an undefined *N*-terminal domain. AD, acid transactivation domain; BIR, baculoviral inhibitory repeat; CARD, caspase recruitment domain; FIIND, function-to-find domain; NAD, NACHT-associated domain; NAIP, neuronal apoptosis inhibitor protein; PYD, pyrin domain; X, undefined domain. *Adapted with modifications from* [93]

has been reported to be present in intestinal epithelial cells [94], where its expression can be modulated by diverse stimuli [95, 96]. NOD1/2 recognize intracellular iE-DAP or MDP, respectively, originating from replicating bacteria. It is estimated that dividing gram-negative bacteria recycle only 30-60% of the cleaved PDG during their replication cycle, implying that a substantial amount of PDG is released during bacterial replication [97]. But NOD proteins are not only sensors for intracellular bacteria. Some extracellular bacteria deliver PDG moieties to the cytoplasm of host cells. For instance, *Helicobacter pylori* uses a T4SS for the delivery of PDG to the host cytosol and thereby triggers NOD1 signaling [98]. *Staphylococcus aureus* inserts pore-forming toxins into the cell membrane of targeted cells and thereby delivers PDG to the host cytosol to induce NOD2 [99]. Furthermore, NOD1/2 ligands can be endocytosed [100, 101] or be

internalized by oligopeptide transporters, e.g. pH-sensing regulatory factor of peptide transporter (PEPT1) [101].

Recently, it has been shown, for NOD1 [102] and for NOD2 [103, 104], that both receptors directly bind to their cognate ligands. Upon ligand sensing, NOD1 and NOD2 undergo conformational changes that allow self-oligomerization and the subsequent recruitment of the serine/threonine kinase RIPK2 via CARD-CARD protein interactions [105]. Receptor bound RIPK2 gets conjugated with lysine 63 (K63)-linked polyubiquitin chains. Ubiquitination is a three step process in which an ubiquitin activating enzyme (E1) loads an ubiquitin moiety on an ubiquitin-conjugating enzyme (E2) that together with an ubiquitin ligase (E3) transfers ubiquitin molecules onto a target protein (Figure I.5). Variations in the linkage of the linear polyubiquitin chains determine the fate of target proteins. K48-linked polyubiquitin chains mark a protein for degradation by the proteasome, whereas K63-linked polyubiquitin chains stabilize signaling complexes by providing signaling platforms. Various E3 ubiquitin ligases have been suggested to be involved in mediating NOD1 and NOD2 activation to NF-κB including XIAP, TRAF2, TRAF5, TRAF6, cIAP1 and cIAP2 [106-110]. Polyubiquitinated RIPK2 allows the se-
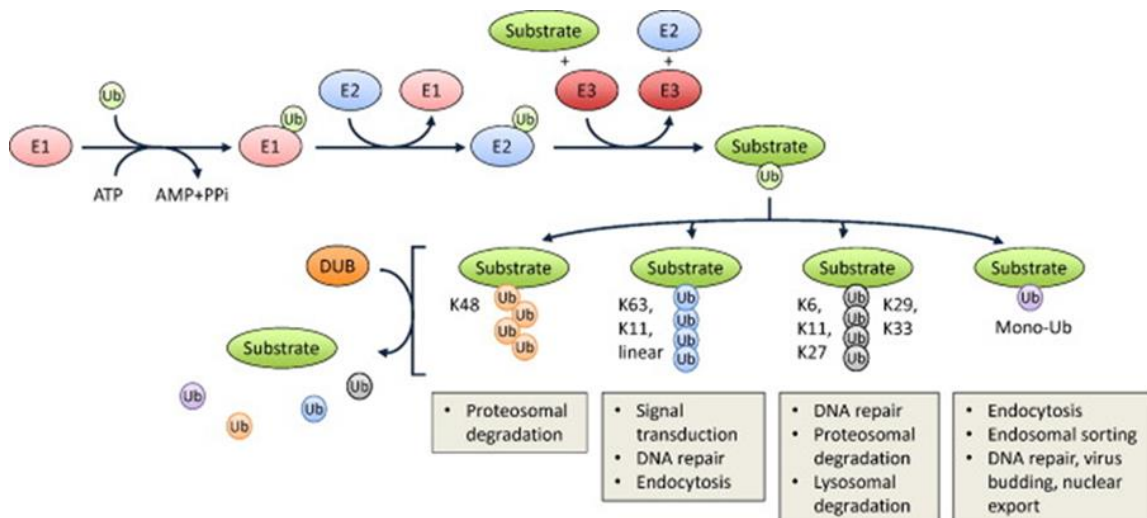
Figure I.5 The Ubiquitination system. Ubiquitination is a post translational modification and involves the covalent attachment of an ubiquitin (Ub) molecule or Ub-chains to target proteins in a three step process. First an Ub-activating enzyme (E1) loads an Ub protein, second this Ub is transferred from E1 to an Ub-conjugating enzyme (E2) and third, an Ub-ligase (E3) associates with the Ub-loaded E2 enzyme and the substrate and attaches the Ub-molecule to the substrate. In this process single Ub molecules or various Ub chains are attached to the substrate. Ubiquitin polymers are built by linking one of the seven lysin residues of one Ub with the C-terminal glycin of the following Ub. The type of linkeage determines the fate of the substrate protein. *Adapted from* [111]

quential association and activation of the TAK1-TAB1-TAB2 and IKKα-IKKβ-NEMO/IKKγ complexes. Activated IKK phosphorylates the NF-κB inhibitor-α (IκBα) thereby marking it for K48-linked ubiquitination and subsequent proteasomal degradation. Liberated NF-κB dimers translocate to the nucleus and induce transcription of target genes [112]. TAK1 belongs to the family of MAP3 kinases and, as such, activates, besides the IKK protein complex, the MAP kinases p38 and JNK [112, 113]. JNK controls the activation of the transcription factor AP-1 [114], whereas p38 mediates histone H3 phosphorylation, thereby making DNA accessible for the activated transcription factors [115]. The activation of the NF-κB and the MAPK signaling pathways downstream of NOD1 and NOD2 receptors results in the expression of proinflammatory cytokines, such as TNF-α and IL-6, chemokines including, IL-8, CXCL1, CXCL2 and CCL2, and antimicrobial peptides, including defensins [105, 116-118] (Figure I.6).
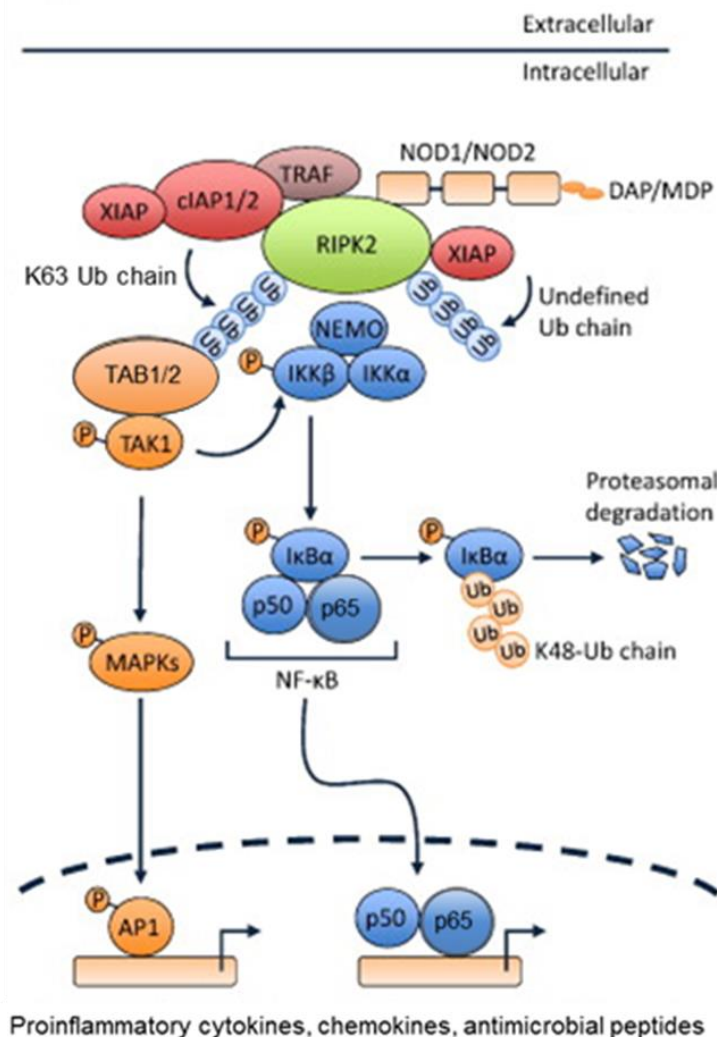
Figure I.6 NOD1/2 signaling pathway. Upon ligand binding NOD1/2 recruits RIPK2 and various E3 ligases to the receptor complex. K63 Ub-chains are attached to RIPK2 leading to the recruitment and the activation of the TAK1 and IKK complexes. IKK posphorylates IκBα, and thereby marks it for K48-linked polyubiquitination and subsequent degradation by the proteasome. NF-κB (p50/p65) is no longer sequestered in the cytosol and translocates to the nucleus to induce gene expression. TAK1 also activates MAP kinases which in turn activate AP-1 another transcription factor that contributes to the expression of proinflammatory genes. *Adapted with modifications from* [111]

In addition to activation by cognate ligands, NOD1 and NOD2 can be activated independent of ligand binding. NOD1 has been shown to sense cytosolic microbes by sensing the activation state of small Rho GTPases in an *in vitro Salmonella enterica* serovar Typhimurium infection model. The *Salmonella* effector protein SopE, harboring GEF activity, induces membrane ruffle formation by activating RAC1 and CDC42. NOD1 was shown to be recruited to the activated RHO GTPases and triggered NF-κB activation in a RIPK2-dependent manner. Furthermore, ectopic expression of constitutively active RHOA, RAC1 and CDC42, was sufficient to activate the NOD1 signaling pathway [119]. Moreover, it has been shown that ARHGEF2 (also known as GEF-H1), which triggers RHOA activation, potentiates NOD1 and NOD2 signaling independent of ligand binding [120, 121].

There are other pathways that are triggered by NOD1 and NOD2. One is autophagy that is an important cellular mechanism to remove invading microbes. Recent research has unraveled that NOD1 and NOD2 recruit the autophagy protein ATG16L1 to the entry site of bacteria, mediating the degradation of invading pathogens [87]. NOD1 and NOD2 are also involved in the activation of the adaptive immunity and the expression of type I INF genes [88, 122, 123].

2.1.2.2   The inflammasomes

Inflammasomes contribute to innate immunity and have been shown *in vivo*, to participate in the antimicrobial immune response [41]. Inflammasomes are multi protein complexes that are assembled from NLRs that form platforms for the activation of inflammatory caspase-1. Some NLRs including NLRP1 and NLRP3, require the adaptor protein ASC for the recruitment of caspase-1, others like NLRC4 directly bind and activate caspase-1. Furthermore, NAIP proteins have been shown to associate to certain NLRs providing ligand specificity. Caspase-1 activation by inflammasomes results in the proteolytic maturation and controlled secretion of proinflammatory cytokines such as IL-1β and IL-18 [124-126]. Moreover, activated caspase-1 induces pyroptosis, a form of programmed cell death (PCD) frequently observed during microbial infections. It combines characteristics of apoptosis, such as nuclear condensation and DNA fragmentation, and of necrosis, including pore formation in the plasma membrane, followed by cell swelling and osmolytic lysis [127, 128]. Recently, caspase-11 was as well associated with inflammasome activation in response to gram-negative bacteria, leading to pyroptosis and release of cytokines such as IL-1α independently of caspase-1 activation [129, 130]. Inflammasome activation requires two

signals. The first is a priming signal, which is mediated by TLRs, NLRs, TNF receptors or IL-1 receptors and leads to NF-κB activation resulting in the synthesis of the pro-forms of IL1-β and IL-18 and of NLRs required for inflammasome formation [131, 132]. The second signal depends on specific DAMPs and PAMPs that induce inflammasome formation and promote caspase-1 or caspase-11 activation followed by cytokine secretion and pyroptosis.

There are several inflammasomes described so far of which the NLRP3 (also known as NALP3) and the NLRC4 (also known as IPAF) inflammasomes are the best studied. NLRP3 and NLRC4 are mainly expressed in myeloid cells. NLRP3 is activated in response to bacteria, viruses and fungi by multiple stimuli, including PAMPs, DAMPs and toxins [84] (Tables I.3 and I.4), whereas NLRC4 senses several pathogenic gram-negative bacteria that are equipped with a T3SS or a T4SS including *Salmonella enterica* ser. Typhimurium, *Shigella flexneri*, *Legionella pneumophila*, and *Pseudomonas aeruginosa* [84] which deliver flagellin or rod components of the T3SS (PrgJ, Mxil) to the host cell cytosol [29, 133].

2.2 Role of the intestinal mucosa in innate immunity

The intestine forms the biggest surface in the body in contact with the environment. Besides functioning in the uptake of nutrients, it has to ensure tolerance to commensal bacteria and, at the same time, protect the body against invasion of pathogenic microorganisms. A single layer of epithelial cells forms a physical and a biochemical barrier that separates the body from the intestinal microbiota and from pathogenic microorganisms. The intestinal epithelium consists of a majority of intestinal epithelial cells (IEC), which are connected by tight junctions and form an impermeable barrier between the body and the luminal contents. IEC have a dual function. They are responsible for the uptake of nutrients and they are part of the innate immune system. Their immune functions are to produce antimicrobial peptides that are secreted into the lumen and to act as sentinels of the immune system that recognize invading pathogens and induce an immune response. Besides IECs, the epithelium includes specialized cells. One kind are M-cells, that are localized above the Peyer's patches or above isolated lymphoid follicles. M-cells sample luminal antigens directly to the submucosal space and present these microbiota-derived antigens to macrophages and dendritic cells. Finally there are the goblet cells, which secrete the protective mucus layer and Paneth cells that reside in the crypts of the small intestine but not of the colon and secrete high amounts of antimicrobial peptides.

2.2.1 Expression and localization of PRRs at the intestinal epithelium

The mucosa of the large intestine is constantly exposed to the commensal microbiota. Even though the commensal bacteria are separated from IECs by a thick mucus layer, large amounts of surface components including LPS, PDG or flagellin from replicating bacteria are released. Therefore the difficulty of PRR function at the intestinal epithelium is to discriminate between pathogenic microorgansims and the commensal microbiota. Tolerance to commensal bacteria can be achieved by the expression pattern and the localization of PRRs. For example, some of the surface exposed TLRs are expressed and localized exclusively in the crypt epithelial cells [134, 135] and thus far away from the gut flora. TLR4 sensing of LPS is not possible because the essential co-receptor MD-2 is poorly expressed in IECs [134]. In addition, TLR4 is sequestered in the golgi and has been found to respond to internalized LPS [136, 137]. TLR5, the sensor for bacterial flagellin, is expressed only in the colon at the basolateral side of IECs [138]. Another strategy for tolerance to commensal bacteria is represented by the NLRs that are cytosolic PRRs. In IECs, NOD1 and NOD2 are expressed and provide the first line of defense against pathogens that avoid immune recognition by TLRs [94, 139].

2.3 *S. flexneri* infection of epithelial cells: recognition and manipulation of host signaling

Upon invasion into epithelial cells, *S. flexneri* is recognized by NOD1 [35]. NOD1 is recruited to phagosomal membrane remnants produced after the bacteria escape from the vacuole to reach their main replicative niche, the cytosol of IECs. NOD1 activation leads to RIPK2 and TAK1 mediated activation of the NF-κB and MAP kinase pathways as described in section 'Noninflammasome NLRs: NOD1 and NOD2'. Only recently, it became evident that the vacuolar membrane remnants produced by *S. flexneri* are recognized as DAMPs and activate NF-κB and the MAP kinases. At bacterial entry sites diacylgylcerol (DAG) accumulation in host membranes was observed and subsequent activation of a protein complex consisting of CARD-BCL10-MALT1 (CBM), followed by TRAF6 and TAK1 activation resulting in the activation of NF-kB and the MAP kinases [140]. It is assumed that PKC mediates DAG dependent assembly of the CBM complex.

S. flexneri by delivering many different effector proteins via the T3SS into IECs, effectively counteracts host signaling and dampens inflammation by targeting the NF-κB and the MAP kinase pathways [141, 142] (Figure I.7). The effector protein IpaH9.8
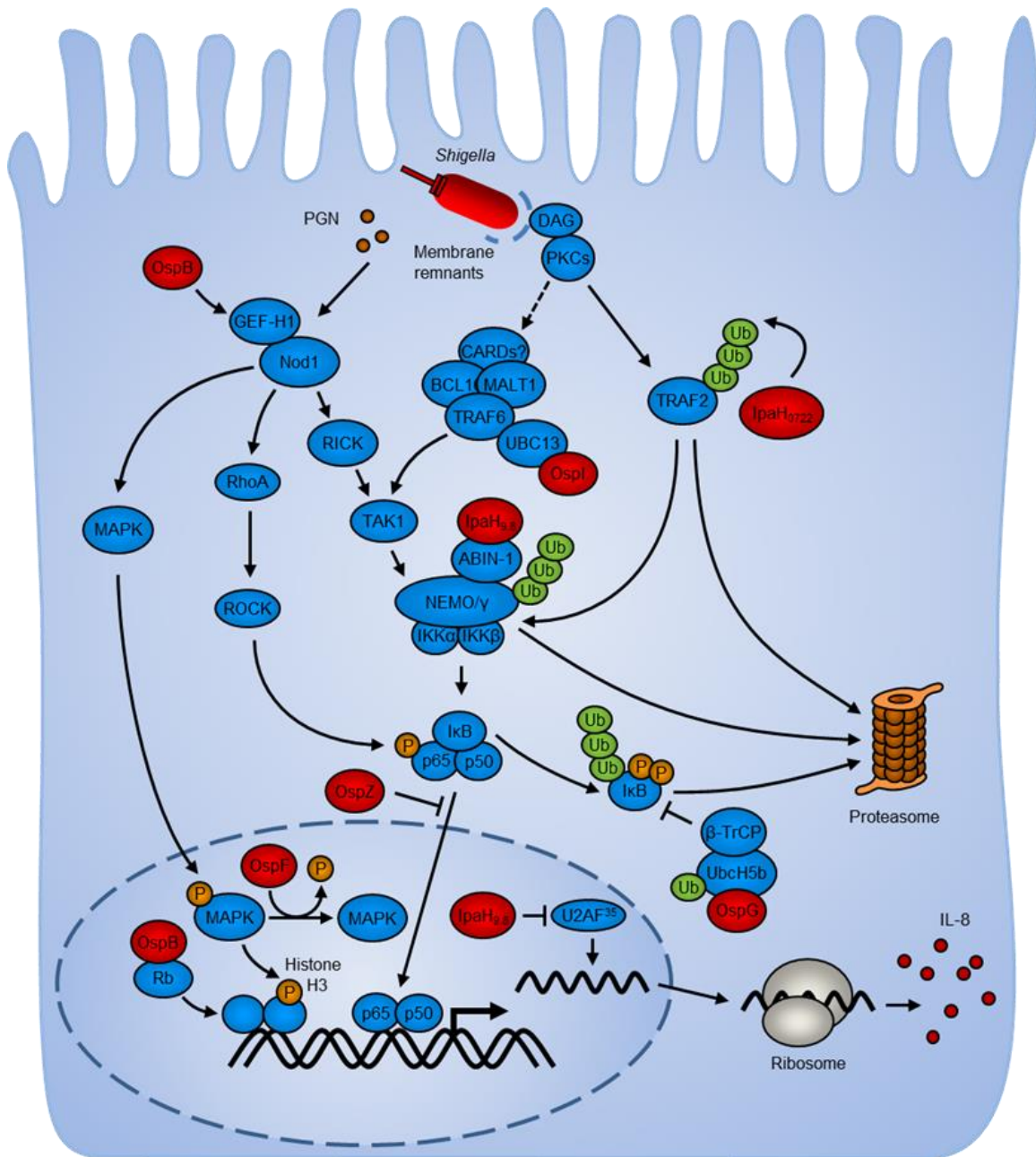
Figure I.7 Manipulation of host signaling by *S. flexneri*. *Shigella* effector proteins injected via the T3SS into the host cell cytosol interfere with host signaling pathways and dampen inflammation. PDG released from replicating *Shigella* triggers the NOD1 signaling pathway, whereas vacuolar membrane remnants act as DAMPs and induce the TRAF6-TAK1 pathway. Both pathways together activate NF-κB and the MAPKs that control the expression of proinflammatory genes. The injected bacterial effector proteins interfere with host signaling proteins and suppress inflammation. For more details refer to the text. *Adapted with modifications from PhD Thesis from C. Schmutz and [141].*

having E3 ligase activity, when secreted into host cells acts in the cytoplasm and in the nucleus of target cells. Cytoplasmic IpaH9.8 targets the NF-κB pathway by polyubiquitinating the regulatory IKKγ subunit of the IKK protein complex, resulting in its degradation and thereby NF-κB remains sequestered in the cytosol [143]. In the nucleus, IpaH9.8 inhibits the mRNA splicing factor U2AF, which again results in a reduced inflammatory response [144]. Recently, another IpaH E3 ubiquitin ligase family protein, IpaH0722, was shown to inhibit the PKC mediated activation of NF-κB. IpaH0722 was found to polyubiquinate TRAF2, a protein downstream of PKC, and thereby marking it for proteasomal degradation [145]. The serine/threonine kinase OspG inhibits NF-κB activation by binding to the E2 ubiquitin conjugating enzyme UbcH5b, thereby preventing the polyubiquitination of phospho-IkB and its subsequent degradation [146]. Consequently, NF-κB is sequestered in the cytoplasm and target genes are not expressed. Furthermore, the effector protein OspZ has been reported to inhibit NF-κB activation in TNFα or IL-1 stimulated cells ectopically expressing OspZ [147]. The precise mechanism remains elusive. The MAP kinases p38 and ERK are targeted by the effector protein OspF. OspF is a phosphothreonine lyase that translocates to the nucleus and irreversibly dephosphorylates the MAP kinases p38 and ERK. The role of OspB is controversial. One group reported that OspB potentiated NOD1 dependent signaling to NF-κB in an ARHGEF2 (GEF-H1) dependent manner [120], whereas in another study, OspB was found to dampen inflammation by interacting with the retinoblastoma protein [148]. Recently, it was reported, that the effector protein OspI, a glutamine deamidase, interferes with the DAMP induced NOD1 independent-TRAF6-NF-κB signaling pathway. OspI selectively deamidates UBC13, an E2 ubiquitin conjugating enzyme, that is required to activate the E3 ubiquitin ligase TRAF6. As a consequence TRAF6 mediated NF-κB activation is impaired in response to *S. flexneri* infection. [140].

Finally, it has been shown that during *Shigella* infection the expression of anti-microbial peptides (AMP), including LL-37 and β-defensin, is reduced in human rectal epithelium of patients [23]. How *Shigella* dampens the production of AMPs remains currently unknown. Some data indicate that the *Shigella* transcription factor MxiE could be responsible for the suppressing effect suggesting that effector proteins could be involved [149]. However, during *Shigella* infection massive amounts of the cytokine IL-8 are produced [38]. IL-8 is a potent chemoattractant for PMNs, which migrate from the periphery to the site of infection. At early stages of *Shigella* infection, the invasion of PMNs destabilizes the integrity of the intestinal epithelium and thereby favors *Shigella*

invasion. But at later stages of infection, they mediate the clearance of infection [150, 151]. In section 3.3, the host mechanism that allows counteracting the immune suppressive activity of bacterial effector proteins is presented.

3   Cellular communication

Multicellular organisms use cell-cell communication to coordinate their behavior to the benefit of the entire organism. The communication mechanisms depend on signaling molecules that are produced to communicate with neighboring cells but also to signal to distant tissues. Signaling molecules, including small peptides, amino acids, nucleotides or nitric oxide, are sensed by receptors that are located at cell membranes or in the cytosol of cells. Upon binding of their cognate ligands, they engage a variety of intracellular signaling proteins that direct the signal to the appropriate parts of the cell. Intracellular signaling proteins are scaffolding proteins, kinases, phosphatases, GTP-binding proteins, ubiquitin ligases and many more. At the end of signaling cascades are target proteins, which are altered after activation of the pathway, and allow the cell to change its behavior in response to environmental changes. Depending on the target protein, different cellular processes are affected including metabolic queues, gene expression, cell shape or movement.

3.1   Principles of cellular communication

There are different mechanisms that allow cell-cell communication. Some allow communication over long distances such as endocrine and synaptic signaling, whereas other mechanisms such as juxtacrine (also known as contact dependent), autocrine and paracrine signaling allow communication over short distances to coordinate localized responses. Such communication over short distances is important during the initial stages of immune responses. When a signaling molecule is secreted and diffuses over a short distance to act on neighboring cells, this is called paracrine signaling. If such a secreted molecule binds to receptors on the cell that produced the signaling molecule, this is called autocrine signaling. A prerequisite for juxtacrine signaling is direct contact between cells or cells and the extracellular matrix. There exist three types of juxtacrine signaling: (I) A signal protein bound to the surface of the signaling cell binds to a cell membrane receptor of an adjacent cell; (II) communication via gap junctions that connect adjacent cells and allow diffusion of small signaling molecules from the signaling cell to neighboring cells and (III) interaction of extracellular matrix glycoproteins that interact with a cell membrane receptor.

3.2 Gap junction mediated cell-cell communication

Gap junctions are channels that connect the cytoplasm of adjacent cells. The channels allow the direct exchange of small (< 1–2 kDa in molecular weight), hydrophilic molecules, such as metabolites (e.g. ATP), nutrients (e.g. glucose), and second messengers (e.g. cAMP, IP_3 and Ca^{2+}) between cells, which is called gap junctional intercellular communication (GJIC) [152]. Gap junctions are formed by two hemichannels or connexons, one contributed by each of the communicating cells (Figure I.8). Each connexon is assembled by six connexin (CX) proteins. There exist 21 connexin proteins in humans. They share a common architecture consisting of four membrane-spanning domains, two extracellular loops and the cytosolic *N*-terminal and *C*-terminal part and one cytosolic loop [153]. The cytosolic domains allow the interaction with connexin interacting proteins that regulate the assembly, function and degradation of gap junctions [154]. There exist many connexin interacting proteins including cytoskeletal proteins (microtubules, actin or actin-binding proteins), adherence junctional proteins (cadherins), tight junctional proteins (ZO-1, ZO-2) and enzymes (kinases and phosphatases). Connexin proteins are expressed in a cell- and tissue specific manner. The most abundant connexin in humans is CX43. Most cells communicate via gap junctions with a few exceptions such as skeletal muscle cells, erythrocytes and circulating lymphocytes [155].
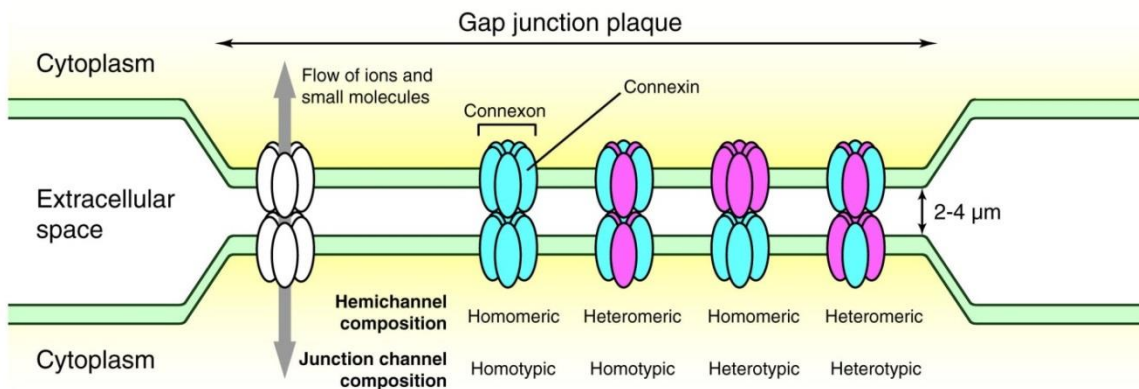
Figure I.8 Architecture of gap junctions. Gap junctions are clusters of transmembrane channels that form gap junction plaques. Two connexons, or hemichannels, in the opposed membranes of neighboring cells form a channel for ions and small molecules (< 1-2kDa). Each connexon is composed of six connexin subunits. Hemichannels can be either homomeric or heteromeric, and gap junctions can be either homotypic or heterotypic based on the composition of constituent connexons. *Adapted from* [156].

As gap junctions allow the intercellular exchange of metabolites and signaling molecules, they control various cellular processes, such as maintenance of tissue homeostasis, gene expression, induction of apoptosis, growth control and allow the coordinated behavior of a group of cells [157, 158]. A proposed mechanism of how various cell types communicate with each other to coordinate and synchronize their activity are intercellular calcium waves (ICWs), i.e. propagation of increases in intracellular calcium concentration through adjacent cells [158]. ICWs have been observed in many different cell types including neurons, hepatocytes, smooth muscle cells and epithelial cells and are associated with various physiological processes for instance, the coordination of airway epithelial ciliary activity or pathological processes such as brain ischemia. The current hypothesis for the communication of ICWs is, that a local stimulus leads to IP_3 production in the challenged cell. IP_3 binds to the IP_3 receptor at the endoplasmatic reticulum (ER) and induces an intracellular calcium wave. Moreover, IP_3 diffuses via gap junctions to neighboring cells, binds to the IP_3 receptor and initiates consecutive intracellular calcium waves in the bystander cells. In addition, or alternatively, the stimulated cell releases ATP via hemichannels or vesicular release, which diffuses to adjacent cells, activates P2 receptors (GPCRs), which in turn, stimulate IP_3 production to induce a calcium wave in the adjacent cell. Propagation may involve the regenerative release of ATP. Each mechanism can occur in isolation or synergistically (Figure I.9).
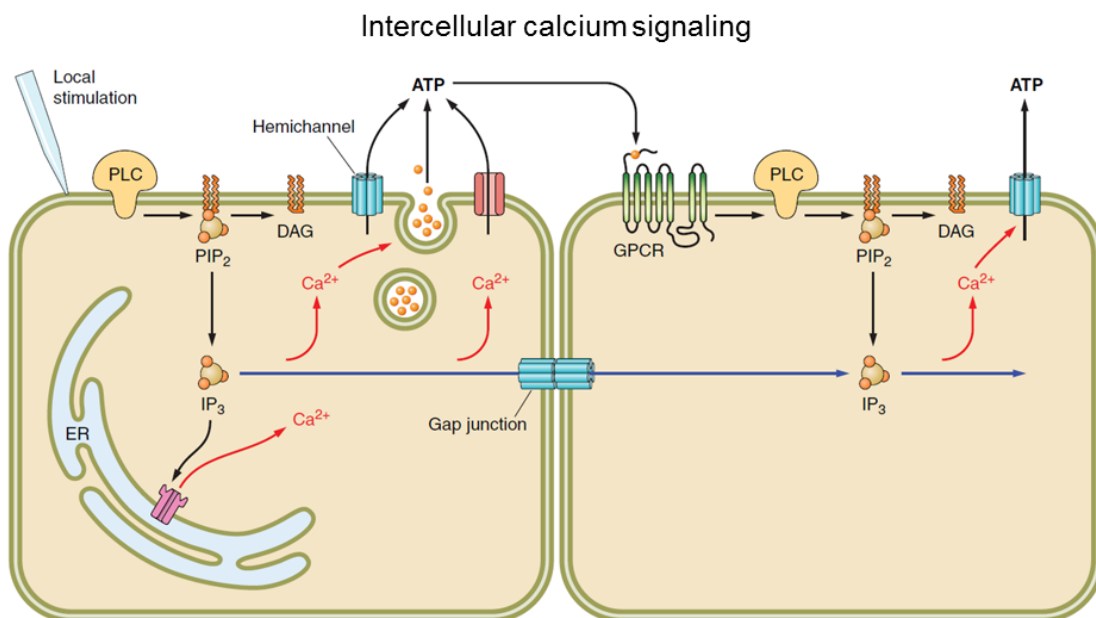

Figure I.9 Model of intercellular calcium waves. For details refer to text. *Adapted from* [158]

GJIC has also been linked to stress responses, where a single cell exposed to a stress induces a biological response in the adjacent healthy tissue. For instance, single irradiated cells secrete cytokines and propagate signals via gap junctions to trigger DNA damage in non-irradiated bystander cells [159]. Recently, we have shown that during bacterial infection of epithelial cells, GJIC mediates the propagation and amplification of proinflammatory signals from infected to uninfected bystander cells [39], which is described in more detail in the following section. Antiviral immune responses have as well been reported to be dependent on cell-cell communication mediated by gap junctions [160, 161]. One group observed that single cells stimulated with double-stranded (ds) DNA, induced interferon-β and TNFα expression in bystander cells [161]. Recently, Ablasser and colleagues discovered a mechanism for bystander activation in response to cytosolic DNA. DNA is sensed by a receptor called cyclic GMP-AMP (cGAMP) synthase (cGAS). Stimulated cGAS catalysis the production of the second messenger cGAMP, which binds to a receptor located at the ER called STING. STING activation results in the induction of an antiviral immune response, including the secretion of type I IFNs. cGAMP produced in dsDNA stimulated cells, was found to be delivered to bystander cells in a gap junction dependent manner and resulted in a STING mediated antiviral immune response [160].

3.3 Cell-cell propagation of proinflammatory signals during bacterial infection

By the use of secreted effector proteins, *S. flexneri* effectively elicits immune suppressive activity. Even though, in the rabbit-ligated ileal loop model of *S. flexneri* infection, as well as in rectal biopsies of *Shigella* infected patients, massive secretion of proinflammatory cytokines is observed [38, 162]. In a recent study, we described a mechanism of communication between infected and uninfected epithelial cells that potentiates innate immunity during infection by the enteroinvasive bacterium *S. flexneri* [39] (see V Appendix). We showed that NF-κB and the MAP kinases p38, JNK and ERK are activated in uninfected cells surrounding the sites of infection. The propagation of these proinflammatory signals leads to massive secretion of proinflammatory cytokines such as IL-8, tumor necrosis factor α (TNFα) and granulocyte-macrophage colony-stimulating factor (GM-CSF), by uninfected bystander cells. Bystander IL-8 production can be triggered by recognition of peptidoglycan and is mediated by gap junction communication between consecutive epithelial cells. Finally, bystander IL-8 expression

was also observed in response to other pathogens such as *S. enterica* ser. Typhimurium and *Listeria monocytogenes*.

In a parallel study, the mechanism of bystander activation induced by *L. monocytogenes* was investigated in a murine intestinal epithelial cell infection model. Similar to our findings, bystander activation induced by *L. monocytogenes* was independent of paracrine signaling. In contrast, whereas *S. flexneri* induced bystander activation required functional gap junctions, in the *Listeria* infection model, bystander activation was mediated by reactive oxygen intermediates (ROIs) produced by the NADPH oxidase (NOX) 4. Inhibition of ROI production resulted in abolished bystander activation and subsequently abolished production of proinflammatory cytokines including CXCL2 (also known as MIP-2, the mouse homolog of human IL-8) and CXCL5 in bystander cells. [163].

Altogether, this indicates that host organisms evolved strategies to counteract bacterial manipulation that suppresses the induction of an inflammation response and thereby ensure defense. In addition, the mechanism of bystander activation amplifies the immune response to invasive bacteria and might give the host an advantage in clearing bacterial infection.

4   Aim of the Thesis

While the innate immune response is effectively suppressed by *S. flexneri* injected effector proteins, massive IL-8 secretion is observed during shigellosis [38]. We have recently found a novel mechanism of cell-cell communication between infected and uninfected neighboring cells that allows an infected host to counteract bacterial manipulation and to amplify the immune response [39] (see V Appendix). By monitoring of proinflammatory signals at the single cell level during *S. flexneri* infection, we found that NF-κB and MAP kinase activation was propagated from infected to adjacent uninfected neighboring cells, which we called bystander cells. Uninfected bystander cells were found to be the main source of IL-8 secretion. In addition, we could show that signals between infected and bystander cells were mediated via gap junctions. Finally, we found by microinjecting the NOD1 ligand TriDAP into epithelial cells that activation of the NOD1 signaling pathway was sufficient to induce bystander IL-8 expression, suggesting that the recognition of Nod1 ligands in infected cells may be sufficient to generate the underlying signals that mediate IL-8 expression in bystander cells of *S. flexneri* infection (Figure I.10).

In order to dissect the molecular mechanism of cell–cell communication based propagation of proinflammatory signals during infection, we followed three strategies: a genome wide RNAi screen in HeLa cells (in collaboration with C.A. Kasper) a LC-HRMS screen for small metabolites and nucleotides (in collaboration with N. Delmotte and P. Kiefer from J.A. Vorholts group at the ETHZ) and a hypothesis driven approach. We aimed at identifying new candidate proteins that are involved in the process of bystander IL-8 expression during *Shigella* infection. Furthermore, we investigated signaling events taking place sequentially in infected and in bystander cells during infection. And finally we set out to identify the signaling molecule(s) responsible for the propagation of proinflammatory signals from infected to uninfected bystander cells.
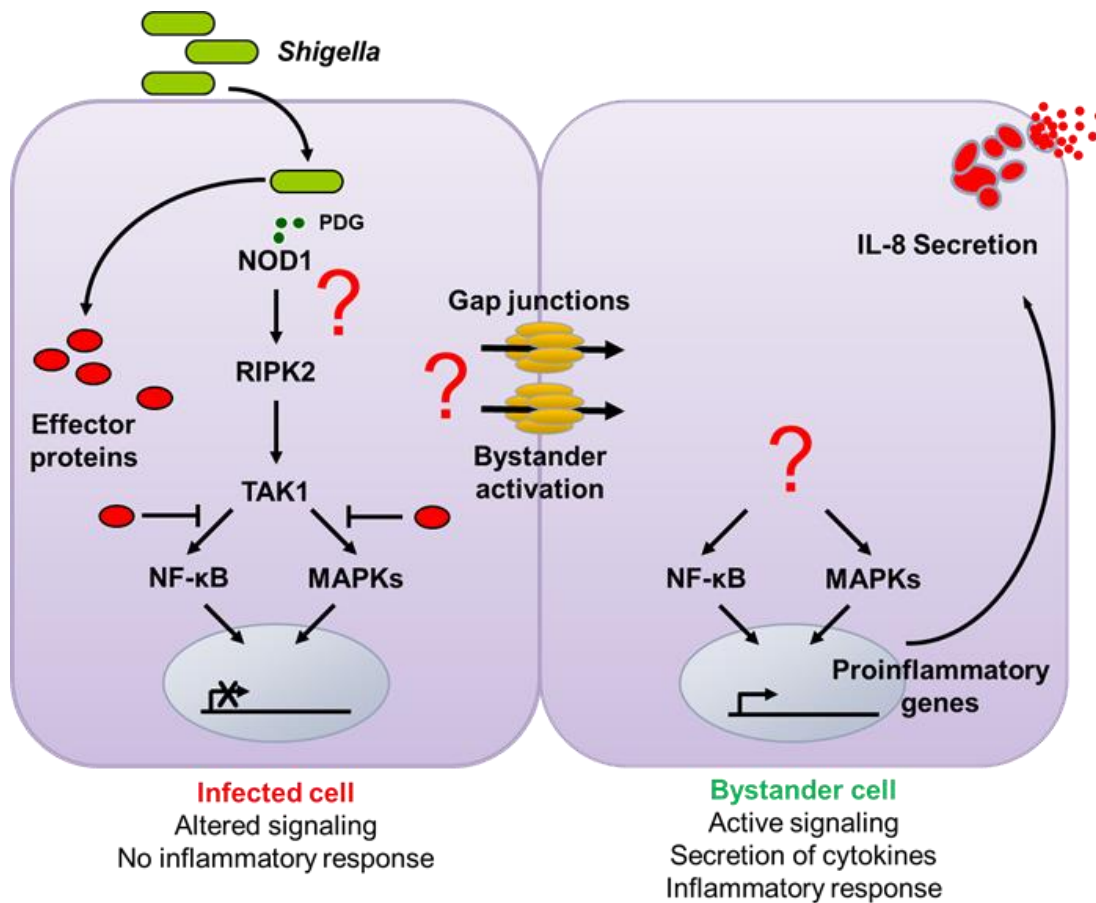
Figure I.10 Model of bystander activation. Invasive *S. flexneri* are detected in epithelial cells by sensing of PDG by the PRR NOD1. Activated NOD1 oligomerizes and recruits RIPK2 to the receptor complex. The subsequent polyubiquitination of RIPK2 allows association of the TAK1 and IKK protein complexes followed by the activation of NF-κB and MAPKs. Altogether control the expression of proinflammatory genes. Secreted bacterial effector proteins inhibit inflammatory signals in infected cells and suppress gene expression. Infected cells are able to propagate NF-κB and MAP kinase activation to adjacent cells leading to IL-8 secretion in bystander cells of infection. Cell-cell communication of proinflammatory signals is mediated via gap junctions and leads to massive amplification of the inflammation response.

II Results

1   Statement of contribution

I have performed most of the experiments in this chapter by myself. In addition, I did most of the quantifications that were based on image analysis. Quantification of mixed cell population assays and of U73122 treated HeLa cells were done by C.A. Kasper. I. Sorg performed Ca^{++}/iE-DAP costimulation experiments in HeLa cells and the in vitro infection assays of BAPTA treated HeLa cells.

2 Results

2.1 NF-κB and TAK1 are essential for IL-8 expression in bystander cells of *S. flexneri* infection

To unravel the molecular mechanism of bystander Il-8 expression, I addressed the two qustions: (I) what kind of signaling events in infected cells trigger bystander IL-8 expression? And (II) how are NF-κB and the MAP kinases activated in bystander cells? *S. flexneri* infecting epithelial cells are recognized by the PRR NOD1 that oligomerizes upon binding of peptidoglycan moieties derived from replicating bacteria [112, 164]. Downstream of NOD1 the MAP3 kinase TAK1 gets activated. From TAK1 signals diverge; one signaling branch leads to MAP kinase activation, whereas the second signaling branch leads to the activation of the transcription factor NF-κB that controls IL-8 expression. First the important function of NF-κB and TAK1 during *S. flexneri* infection was verified. To do so, I monitored the IL-8 response of HeLa cells depleted for NF-κB or TAK1 by means of RNA interference. Cell monolayers were infected at low multiplicity of infection (MOI) with *S. flexneri* Δ*virG* the non-motile deletion mutant [165]. This mutant was used throughout the study, to avoid infection of bystander cells by intercellular bacterial spreading. Newly synthesized IL-8 was trapped in the golgi apparatus by treating cells with monensin, a protein transport inhibitor. To visualize IL-8 accumulation in bystander cells of *S. flexneri* infected cells, immunofluorescence microscopy was performed followed by automated image analysis. As expected, HeLa cells depleted for NF-κB (Figure II.1, panel A left) or TAK1 (Figure II.1, panel A right and panel B) were not able to induce IL-8 expression in response to *S. flexneri* infection. In addition, I confirmed the TAK1 dependent nuclear translocation of the NF-κB subunit p65 by means of immunofluorescence microscopy and automated image analysis as described previously [39]. As expected, NF-κB p65 translocation in infected (Figure II.1, panel C left) and in bystander cells (Figure II.1, panel C right) during infection of HeLa cells depleted for TAK1 was strongly impaired compared to control cells.
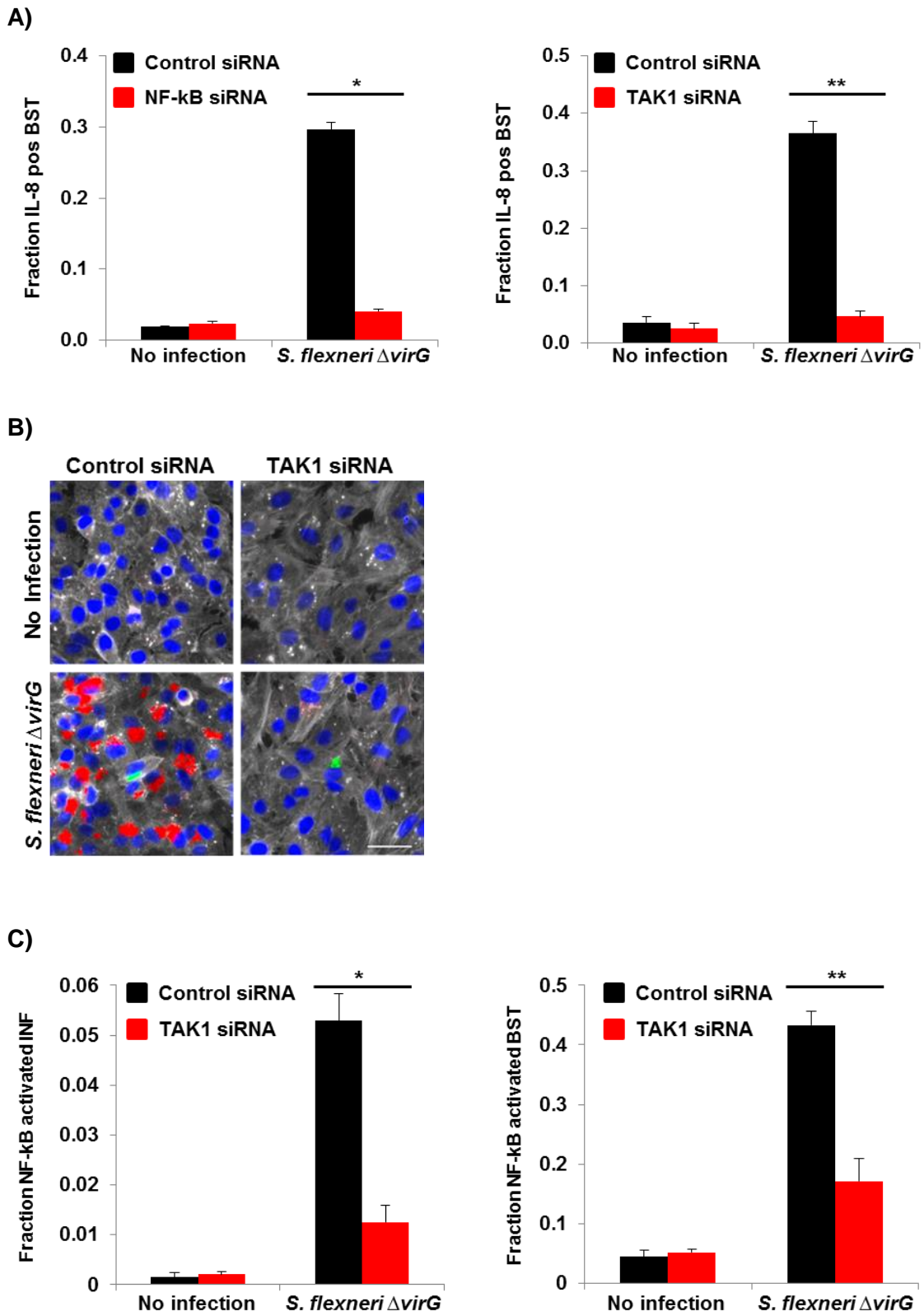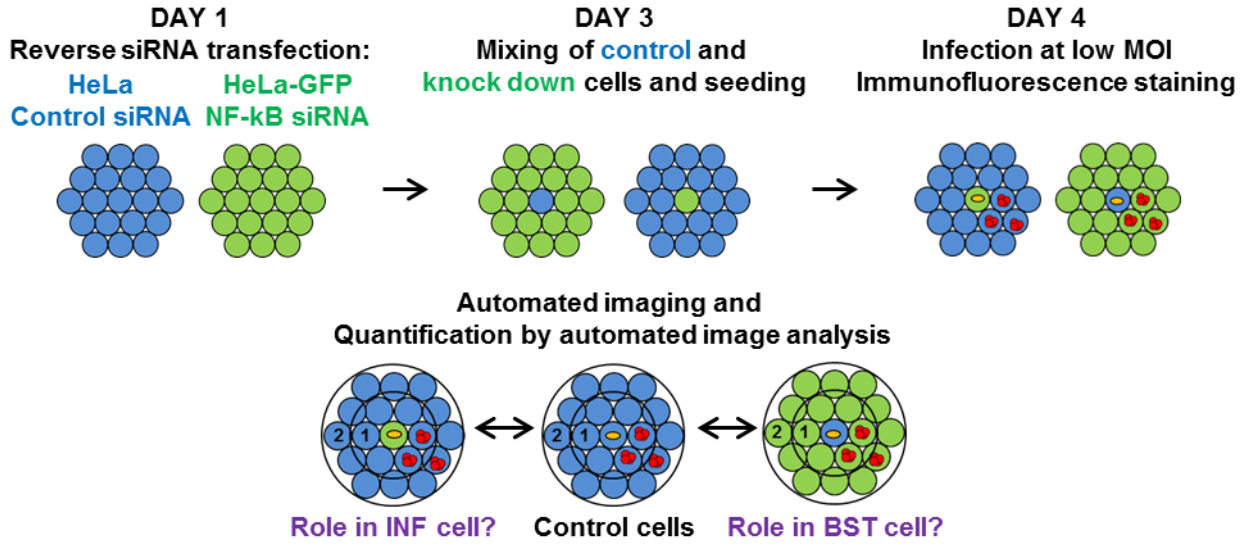
Figure II.1

A)

B)

C)

Figure II.1 NF-κB and TAK1 are essential for bystander IL-8 production during *S. flexneri* infection. (**A**) Effect of NF-κB or TAK1 siRNA knock down, on IL-8 production in bystander cells of *S. flexneri* infection. HeLa cells depleted for NF-κB (left) or TAK1 (right) by means of RNA interference for 72 hours and infected with *S. flexneri* (MOI=1). IL-8 staining of monensin treated cells after 3.5 hours of infection. Quantification was performed by automated image analysis based on the use of threshold intensity values for bacterial and IL-8 detection as described previously [39] (see V Appendix) (means ± SD of triplicate wells, graph representative of three independent experiments; *p = 6.4E-09; **p = 1.0E-08). (**B**) Effect of TAK1 depletion on IL-8 accumulation in bystander cells. TAK1 depleted HeLa cells were infected with *S. flexneri*. IL-8 staining of monensin-treated HeLa cells, 3.5 hours post infection (IL-8 in red, *S. flexneri* in green, Hoechst in blue, MOI=0.5). Scale bar, 50 µm. (**C**) TAK1 dependent NF-κB activation during *S. flexneri* infection. HeLa cells were transfected for 72 hours with TAK1 siRNA, and infected with *S. flexneri* at MOI=1 for 1 hour. The nuclear translocation of NF-κB p65 was monitored by immunofluorescence and quantified by automated image analysis. The nuclear/cytoplasmic p65 intensity ratio was calculated as described previously [39]. The data shown are mean values +/- SD of triplicate wells per condition; graph representative of 3 independent experiments; *p = 3.0E-08;**p = 5.0E-08. (BST = bystander cells)

Next, I investigated firstly whether NF-κB or TAK1 activation was required in *S. flexneri* infected cells for the production of a diffusible signaling molecule responsible for bystander activation and secondly whether NF-κB or TAK1 activation was required in bystander cells for IL-8 expression. For this purpose, the mixed cell population assay was designed, which is described in detail in Figure II.2, panel A and in material and methods. Mixed HeLa cell layers consisting of few cells depleted for NF-κB or TAK1, respectively, surrounded by a majority of control cells were infected at very low MOI to be able to analyze single infection sites. Automated analysis of immunofluorescence images was used to quantify the fraction of IL-8 producing control cells at bystander position one to five neighboring to either an infected control cell or an infected cell depleted for NF-κB or TAK1. It turned out that infected cells depleted for NF-κB (Figure II.2, panel B left) or TAK1 (Figure II.2, panel B right) induced the same fraction of IL-8 positive bystander cells at any given bystander position (red curve) when compared to infected control cells (black curve). This data indicates that NF-κB or TAK1 activation in infected cells is not required for the production of a diffusible signaling molecule responsible for bystander activation. Next, the role of NF-κB or TAK1 for IL-8 expression in bystander cells was investigated. Mixed cell layers consisting of few control cells embedded in a majority of cells depleted for NF-κB or TAK1, respectively, were infected at low MOI. Analysis of the propagation of IL-8 expression induced by an infected control cell in either control bystander cells or in bystander cells depleted for NF-κB or TAK1 revealed, as expected, that NF-κB (Figure II.2, panel C left) and TAK1 activation (Figure II.2, panel C right) are essential in bystander cells for IL-8 expression.

Figure II.2

A)

B)
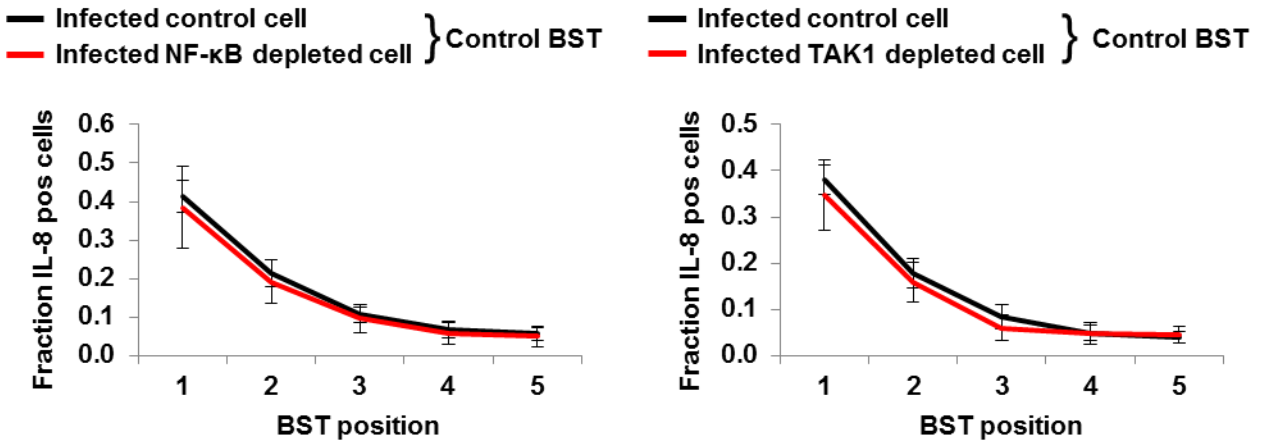
Figure II.2 NF-κB and TAK1 are required only in bystander cells for IL-8 expression. (**A**) Sketch of mixed cell population assay: At day1, two cell populations were reverse transfected by means of small interfering RNA: HeLa cells with a control siRNA (control cells; blue) and HeLa-GFP cells with specific siRNAs targeting e.g. NF-κB (green). At day 3 (after 48 hours), the two cell populations were harvested, mixed at ratios 1 to 5 and 5 to 1 and seeded. At day 4 (after 72 hours) the mixed cell layers were infected with *S. flexneri* at MOI=0.02 followed by an immunofluorescence staining: Hoechst to visualize cell nuclei, IL-8 was stained with a specific antibody and visualized by an Alexa Fluor 647-coupled secondary antibody, bacteria express dsRed and knock down cells express GFP. Quantification was performed by automated image processing as described previously [39]. (**B**) Spatial propagation of IL-8 expression triggered from either a *S. flexneri* infected control cell or HeLa-GFP cell depleted for NF-κB (left) or TAK1 (right) into control bystander cells. Each number corresponds to the fraction of IL-8 producing cells for a given bystander cell position. Quantification was performed by automated image analysis as described previously [39] (means ± SD of 18 wells, graph representative of 3 independent experiments; NF-κB: p > 0.18 at any given position; TAK1: p > 0.11 except at position 3 (p= 0.02)).

C)
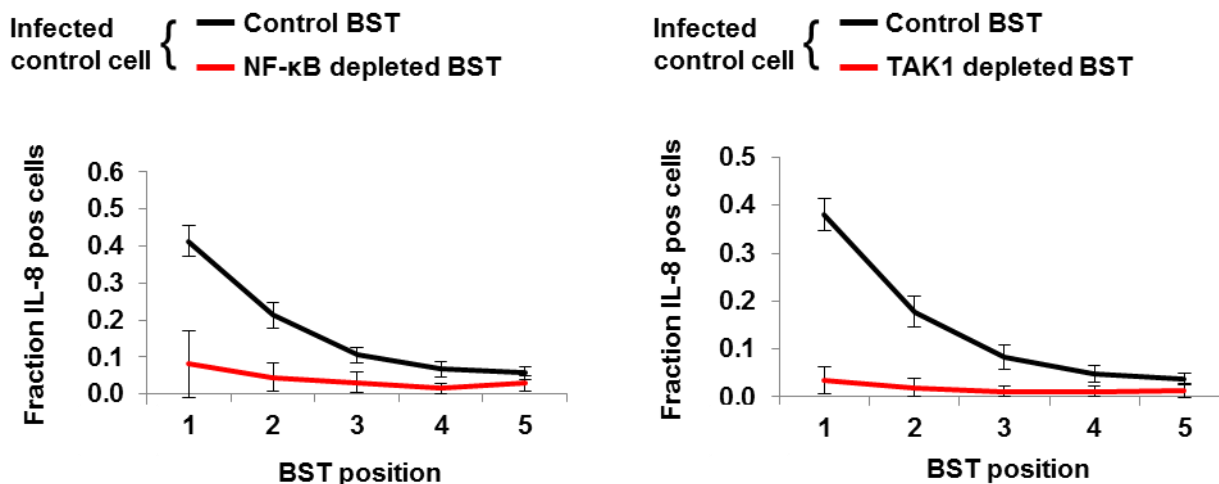
D)
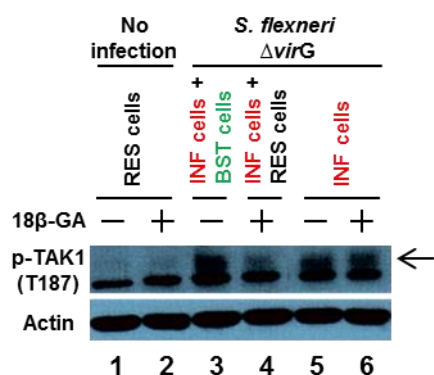
Figure II.2 Continued. (**C**) Spatial propagation of IL-8 production from a *S. flexneri* infected control cell into either control bystander cells or HeLa-GFP bystander cells depleted for NF-κB (left) or TAK1 (right). Each number corresponds to the fraction of IL-8 producing cells for a given bystander cell position. Quantification was performed by automated image analysis as described previously [39] (means ± SD of 18 wells, graph representative of 3 independent experiments; NF-κB: $p < 2E\text{-}04$ at any given position; TAK1: $p < 2E\text{-}06$). (**D**) TAK1 activation in bystander cells of *S. flexneri* infection. Whole cell lysates from HeLa cells untreated or treated with the gap junction inhibitor 18β-GA one hour prior to infection, and infected at MOI=4 (lane 3, 4) or at MOI=40 (lane 5, 6) with *S. flexneri* Δ*virG* for 45 minutes, were analyzed by immunoblotting using a phospho-specific antibody that detects TAK1 phosphorylated at threonine 187 (p-TAK1). Actin was used as loading control. (RES = resting cells; INF = infected cells; BST = bystander cells)

As it became evident that TAK1 plays a crucial role in bystander cells to mount a proinflammatory response, I aimed at confirming that TAK1 indeed was activated in bystander cells during *S. flexneri* infection. TAK1 activation during *S. flexneri* infection was monitored with a phosphospecific antibody that detects threonine 187 in the activation loop of TAK1 [166]. In order to distinguish between signaling events taking place in infected and in bystander cells, HeLa cells were either left untreated or treated

with the gap junction inhibitor 18β glycyrrethinic acid (18β-GA) prior to infection. In absence of treatment, cell layers consisted of around 50% infected cells and 50% bystander cells, whereas upon inhibition of gap junctions cell layers consisted of 50% infected cells and 50% resting cells. Resting cells did not show any TAK1 phosphorylation (Figure II.2, panel D, lanes 1 and 2). In contrast, when I infected all cells, I observed a strong activation of TAK1, which was not affected by the drug treatment, reflecting TAK1 activation induced by invasive *S. flexneri* (Figure II.2, panel D, lanes 5 and 6). In the condition of 50 % infected (and 50 % bystander or resting cells, respectively) in absence of drug treatment a strong band was observed representing TAK1 activation in infected and in bystander cells (Figure II.2, panel D, lane 3), whereas upon treatment with 18β-GA a weak band was observed, representing TAK1 activation in infected cells (Figure II.2, panel D, lane 4). These data demonstrate that TAK1 is activated in infected and in bystander cells during *S. flexneri* infection.

Taken together, my data confirmed the important role of NF-κB and TAK1 in mounting a proinflammatory response during *S. flexneri* infection. I showed the TAK1 dependent activation of NF-κB in infected and in bystander cells. Furthermore, there is evidence that NF-κB and TAK1 activation are not required in infected cells for the production of a signaling molecule that triggers bystander activation. As expected, NF-κB and TAK1 activation are essential in bystander cells for IL-8 expression during *S. flexneri* infection. Finally, I show that TAK1 is indeed activated in infected and in bystander cells of *S. flexneri* infection.

2.2 RIPK2 contributes to IL-8 expression in bystander cells of *S. flexneri* infection

Next, the question was addressed whether the activation of the NOD1 signaling pathway was required for the induction of a bystander IL-8 response during *S. flexneri* infection of HeLa cells. Because it was not possible to reduce the NOD1 mRNA levels sufficiently by means of RNA interference (data not shown), I depleted the adaptor protein RIPK2, which is required to mediate NOD1 activation to the TAK1 complex [108]. I used quantitative real time PCR (qRT-PCR) to control the siRNA mediated knock down efficiency and found a reduction of RIPK2 mRNA levels by more than 95% compared to control HeLa cells (Figure II.3, panel A). After infection of these cells with

Figure II.3

A)

B)   **C)**
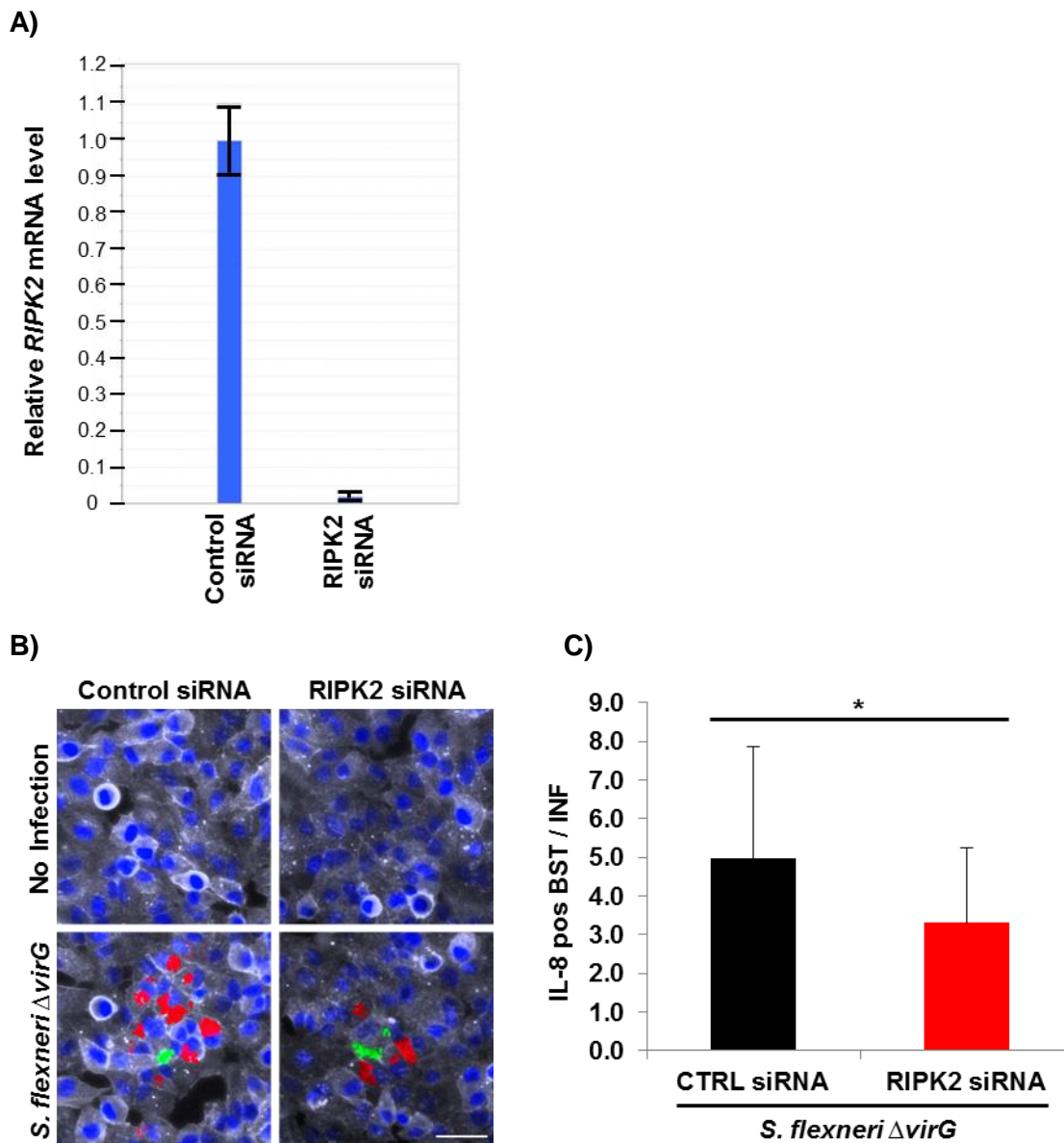
Figure II.3 RIPK2 contributes to IL-8 expression during *S. flexneri* infection. (**A**) RIPK2 mRNA level after siRNA mediated knock down. HeLa cells were transfected for 72 hours with control or RIPK2 siRNA, respectively. *RIPK2* mRNA levels were quantified by qRT-PCR. Values represent relative quantities (RQ) ± RQ max and RQ min of triplicate samples and indicate the *RIPK2* mRNA level of HeLa cells depleted for RIPK2 relative to HeLa control cells after normalization to *GAPDH* mRNA; graph representative of 3 independent experiments. (**B**) Effect of RIPK2 depletion on IL-8 accumulation in bystander cells. RIPK2 depleted HeLa cells were infected with *S. flexneri* (MOI=0.5). IL-8 staining of monensin-treated HeLa cells, 3.5 hours post infection, IL-8 in red, *S. flexneri* in green, Hoechst in blue, F-actin in grey). Scale bar, 50 µm. (**C**) Effect of RIPK2 knock down, on IL-8 production in bystander cells of *S. flexneri* infection. HeLa cells depleted for RIPK2 by means of RNA interference for 72 hours and infected with *S. flexneri* (MOI=1). IL-8 staining of monensin treated cells after 3.5 hours of infection. The number of IL-8 positive bystander cells per infection site was determined (means ± SD, N=112, representative of four independent experiments; *p = 1.1E-06).

S. flexneri at low MOI followed by automated fluorescence microscopy, the number of bystander cells per infection site was determined. In control cells an average of 5 ± 3 bystander cells per infection site was found. Interestingly, RIPK2 depleted bystander cells of infection were still able to respond to *S. flexneri* infection, but only an average of 3.3 ± 1.9 bystander cells per infection site were observed (Figure II.3, panel B and C). Furthermore, a mixed cell population assay was performed and the IL-8 response triggered by RIPK2 depleted infected cells was analyzed in control bystander cells. Data were not clear; either pointing to no role or a minor contribution of RIPK2 in infected cells in the generation of signals that trigger bystander IL-8 expression (Figure II.4, panel A). Analysis of the propagation of IL-8 expression induced by infected control cells in bystander cells depleted for RIPK2, revealed a consistently and significantly reduced, yet not completely blocked, fraction of IL-8 positive bystander cells at any given position (Figure II.4, panel B).

Figure II.4

A)   **B)**
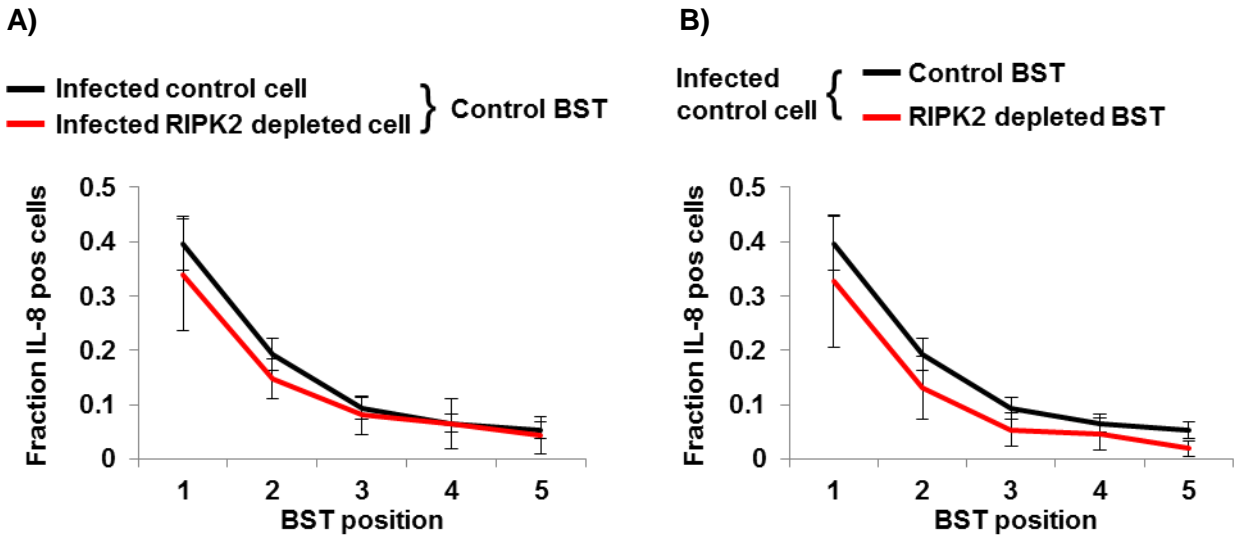
Figure II.4 RIPK2 contributes exclusively in bystander cells to IL-8 expression. (**A**) Spatial propagation of IL-8 expression triggered from either a *S. flexneri* infected control cell or HeLa-GFP cell depleted for RIPK2 into control bystander cells. Each number corresponds to the fraction of IL-8 producing cells for a given bystander cell position. Quantification was performed by automated image analysis as described previously [39] (means ± SD of 18 wells, graph representative of 3 independent experiments; p > 0.05 at any given position, except at BST position 2: p=5.2E-04). (**B**) Spatial propagation of IL-8 production from a *S. flexneri* infected control cell into either control bystander cells or bystander cells depleted for RIPK2. Each number corresponds to the fraction of IL-8 producing cells for a given bystander cell position. Quantification was performed by automated image analysis as described previously [39] (means ± SD of 18 wells, graph representative of 3 independent experiments; p < 0.04 at any given position).

C)
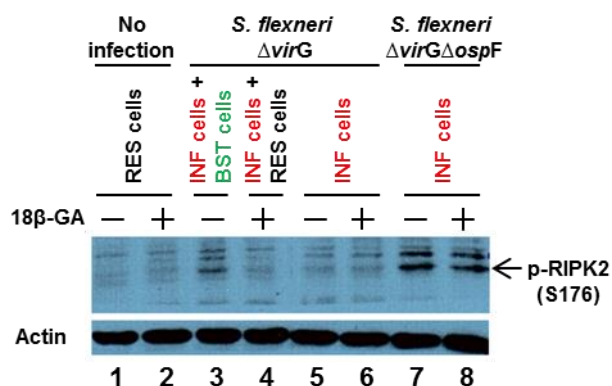
Figure II.4 Continued. (**C**) RIPK2 phosphorylation in bystander cells of *S. flexneri* infection. Whole cell lysates from HeLa cells untreated or treated with the gap junction inhibitor 18β-GA one hour prior infection, and infected at MOI=4 (lanes 3, 4) or at MOI=40 (lanes 5, 6, 7, 8) with *S. flexneri* Δ*virG* or *S. flexneri* Δ*virG*Δ*ospF* for 45 minutes, were analyzed by immunoblotting using a phospho-specific antibody that detects RIPK2 phosphorylated at serine 176 (p-RIPK2). Actin was used as loading control. (RES = resting cells; INF = infected cells; BST = bystander cells)

I next investigated the phosphorylation status of the serine/threonine kinase RIPK2. It has been shown that RIPK2 kinase activity is required to control protein stability and that in absence of kinase activity, NOD1 signaling and consequently inflammatory gene expression was impaired [167]. Therefore, the activation status of RIPK2 in infected and in bystander cells was examined. I performed immunoblotting with a phospho-specific antibody that detects RIPK2 phosphorylated at serine 176, which is a regulatory autophosphorylation site in the activation loop and, which can be used to monitor the activation state of RIPK2 [168]. HeLa cells were either left untreated or treated with the gap junction inhibitor 18β-GA prior to infection. Resting cells did not show any RIPK2 phosphorylation (Figure II.4, panel C, lanes 1 and 2). When infecting all cells with *S. flexneri* Δ*virG*, no phospho-RIPK2 was detected in both conditions, indicating that RIPK2 was not stabilized by autophosphorylation in infected cells (Figure II.4, panel C, lanes 5 and 6). In the condition of 50 % infected cells (and 50 % bystander or resting cells, respectively), in absence of drug treatment a p-RIPK2 band was observed, which was sensitive to 18β-GA, indicating that RIPK2 was exclusively phosphorylated in bystander cells of *S. flexneri* infection (Figure II.4, panel D, lanes 3 and 4). As positive control we used a *S. flexneri* mutant strain depleted for OspF, which is no longer able to suppress RIPK2 phosphorylation in infected cells [169] (Figure II.4, panel D, lanes 7 and 8).

In summary, these data indicated that RIPK2 contributes exclusively in bystander cells of *S. flexneri* infection to IL-8 expression but was not essential, implying the existence of a NOD1 independent signaling pathway that mediates bystander activation, or that NOD1 signaling was not exclusively mediated via RIPK2. Furthermore, we could show that RIPK2 was phosphorylated in bystander cells resulting in the stabilization of this protein. Hence, efficient NOD1 signaling could take place in bystander cells mediating IL-8 expression [167].

2.3 NOD1 is not required to trigger bystander activation but contributes to IL-8 expression in bystander cells of *S. flexneri* infection

In order to investigate whether the activation of the NOD1 signaling pathway was required in the mechanism of bystander activation, I made use of two commercially available cell lines: human embryonic kidney cells (HEK) 293 cells stably overexpressing NOD1 (HEK/hNOD1) and the parental HEK 293 cell line. Since HEK 293 cells express low levels of endogenous NOD1, residual NOD1 was depleted by means of small interfering RNA. These cells were used hereafter in my studies and referred to as HEK/null cells. I compared the mRNA levels of NOD1 in the two cell lines and found that they were reduced in HEK/null cells by more than 99% when compared to HEK/hNOD1 cells (Figure II.5, panel A). To be able to study NOD1 signaling, I wanted to validate that HEK/null cells indeed did not respond to the NOD1 ligand iE-DAP. Therefore, the responsiveness of both cell lines to the acyl modified NOD1 ligand, C_{12}-iE-DAP (lauroyl-γ-$_D$-iE-DAP) was tested. The accumulation of IL-8 was visualized by immunofluorescence microscopy followed by automated image analysis. Very low concentrations of C_{12}-iE-DAP (5 ng/ml) were sufficient to induced IL-8 production in HEK/hNOD1 cells, whereas HEK/null cells did not respond to the stimulus, even at very high concentrations such as 2.56 µg/ml (Figure II.5, panel B), showing that these two cell lines are a suitable model system to investigate the role of NOD1 in the molecular mechanism of bystander activation.

First, I confirmed the NOD1 dependent NF-κB activation of *S. flexn*eri infected HEK/hNOD1 and HEK/null cells by means of immunofluorescence. As expected, NF-κB activation was observed in most of infected HEK/hNOD1 cells, whereas in infected HEK/null cells, NF-κB activation was strongly reduced (Figure II.5, panel C).

Figure II.5

A)

B)

C)
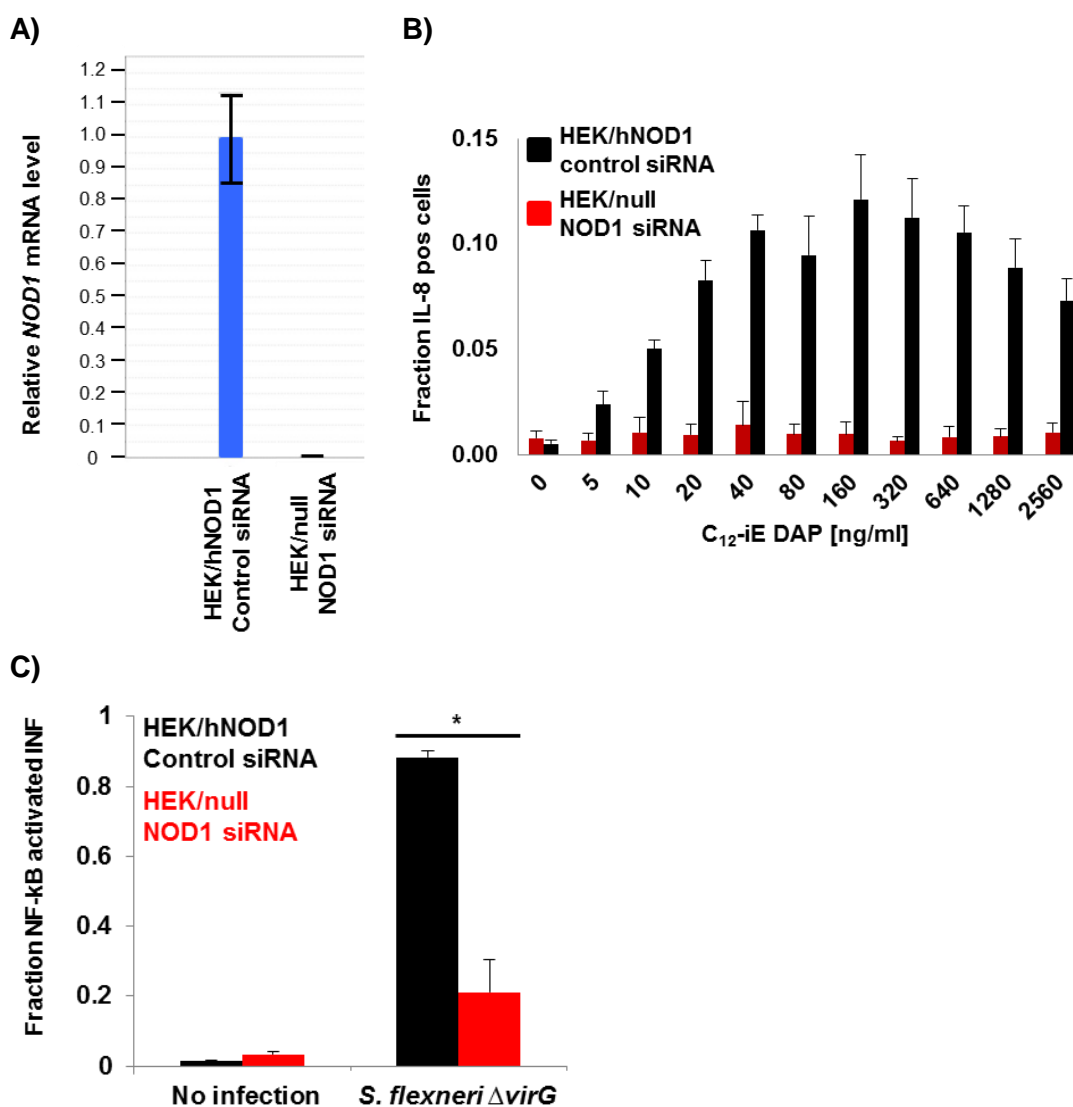
Figure II.5 NOD1 contributes to the activation of NF-κB and to bystander IL-8 expression during *S. flexneri* infection. (**A**) Comparison of *NOD1* mRNA levels between HEK 293 cells over-expressing NOD1 (HEK/hNOD1) and HEK 293 cells depleted for NOD1 (HEK/null). HEK/hNOD1 cells and HEK/null cells were transfected with control or NOD1 siRNA, respectively, for 72 hours and *NOD1* mRNA levels were measured by qRT-PCR. Values represent relative quantities (RQ) ± RQ max and RQ min of triplicate samples and indicate the *NOD1* mRNA level of HEK/null cells relative to HEK/hNOD1 cells after normalization to *GAPDH* mRNA; graph representative of 2 independent experiments. (**B**) Quantification of IL-8 accumulation in C_{12}-iE-DAP stimulated HEK cells depleted for NOD1. HEK/hNOD1 and HEK/null cells were transfected with control or NOD1 siRNA, respectively, for 72 hours followed by stimulation with increasing concentrations of C_{12}-iE-DAP for 5 hours. Immunofluorescence images were examined by automated image analysis (means ± SD of triplicate wells, graph representative of three independent experiments). (**C**) NOD1 dependent nuclear localization of NF-κB in infected HEK cells. HEK/hNOD1 cells were treated with control siRNA and HEK/null cells with NOD1 siRNA for 72 hours. Cell layers were infected for 50 minutes with *S. flexneri* (MOI=1) and stained with a p65 antibody. NF-κB translocation was detected by fluorescence microscopy and manually quantified (results represent the mean ± SD of triplicate wells; HEK/hNOD1: N= 154; HEK/null: N=195; graph representative of 3 independent experiments, *p = 2.5E-04).

Subsequently, single infection sites were investigated in order to determine the role of NOD1 in bystander cells. In HEK/hNOD1 cell layers an average of 9.9 ± 0.85 NF-κB positive bystander cells per infection site were found. HEK cells depleted for NOD1 were still able to respond to infection, but the number of NF-κB positive bystander cells per infection site (5.2 ± 1.11) was significantly reduced (Figure II.5, panel D and E). Given that NF-κB controls IL-8 expression, a reduced number of IL-8 positive bystander cells was expected. This assumption was confirmed and a reduced number of IL-8 positive bystander cells per infected cell in HEK/null cells (8.3 ± 1.4) compared to HEK/hNOD1 cells (14.8 ± 1.6) (Figure II.5, panel F and G) was observed. These findings are in line with the RIPK2 data in HeLa cells, and suggest the existence of a NOD1 independent signaling pathway that contributes to bystander IL-8 expression.
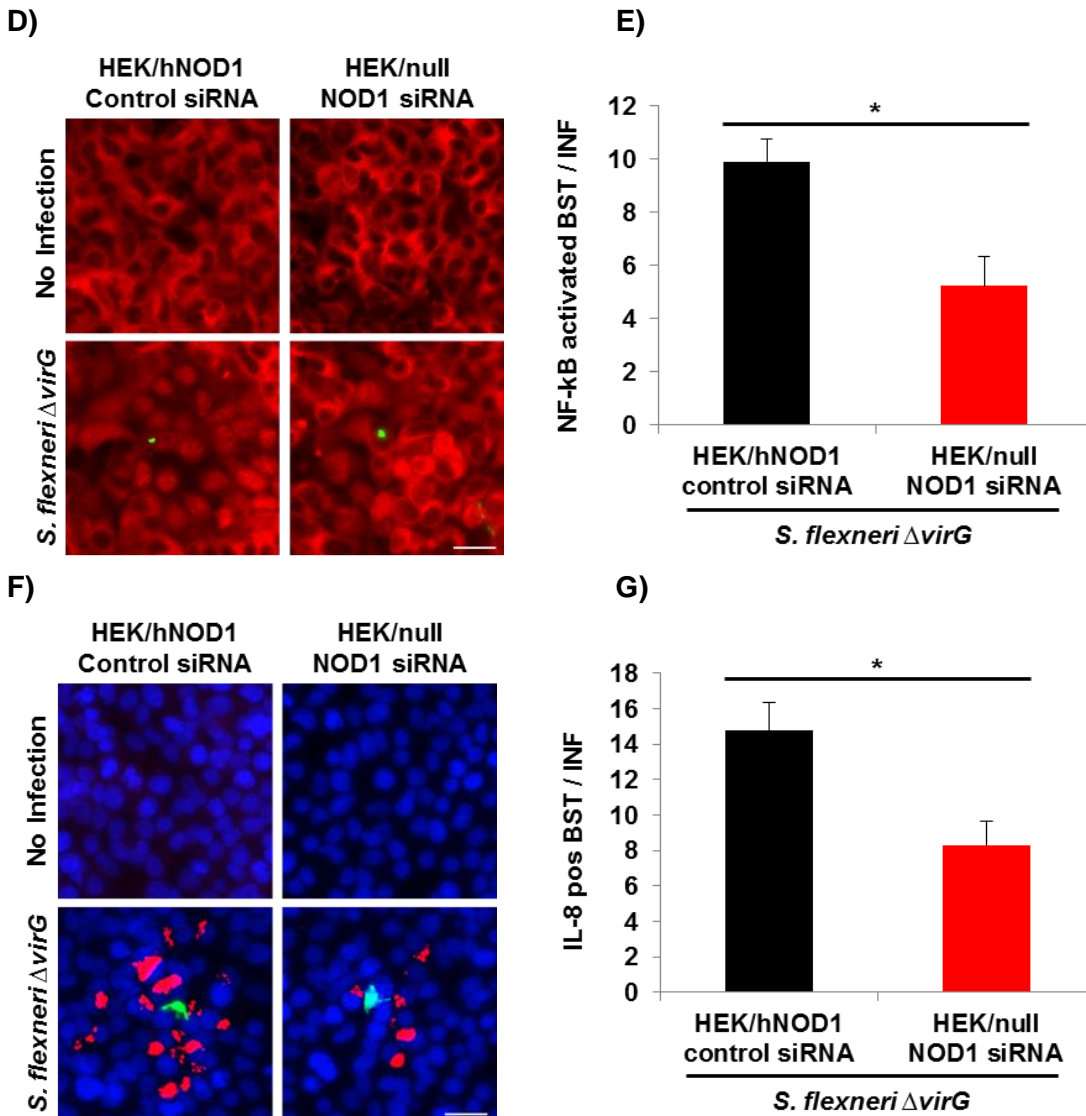
Figure II.5

Figure II.5 Continued. (**D**) NOD1 dependent bystander NF-κB activation in HEK cells infected with *S. flexneri*. HEK/hNOD1 cells and HEK/null treated for 72 hours with control or NOD1 siRNA, respectively, were infected with *S. flexneri* (MOI=0.1) for 50 minutes, stained with p65 antibody (NF-κB in red, *S. flexneri* in green). Scale bar represents 25 µm (**E**) Quantification of NOD1 dependent NF-κB activation in bystander cells of *S. flexneri* infection, the number of NF-κB positive bystander cells per infection site was determined by automated image analysis (means ± SD of 9 wells, graph representative of three independent experiments; *p = 2.6E-08). (**F**) NOD1 dependent bystander IL-8 expression of HEK cells infected with *S. flexneri*. HEK hNOD1 cells and HEK/null cells treated for 72 hours with control or NOD1 siRNA, respectively, were infected with *S. flexneri* (MOI=0.1) for 3.5 hours and stained with an IL-8 antibody and Hoechst (IL-8 in red, *S. flexneri* in green, Hoechst in blue). Scale bar represents 25 µm. (**G**) Quantification of NOD1 dependent IL-8 expression in bystander cells of *S. flexneri* infection. The number of IL-8 positive bystander cells per infection site was determined by automate image analysis (means ± SD of 9 wells, graph representative of three independent experiments; *p = 8.2E-08).

In order to perform a mixed cell population assay a HEK 293 cell line stably expressing GFP was generated. Control experiments were performed to select a HEK/null-GFP cell line that responded similarly to *S. flexneri* infection as the parental HEK 293 cell line used in the previous experiments. These cells were used in a mixed cell population assay to assess the requirement of NOD1 signaling in infected cells for the production of a signaling molecule that mediates bystander activation and to assess the role of NOD1 in bystander cells for IL-8 expression. By means of immunofluorescence microscopy, mixed cell layers consisting of few NOD1 depleted cells (HEK/null-GFP) surrounded by a majority of NOD1 overexpressing bystander cells (HEK/hNOD1) were analyzed. Unexpectedly, *S. flexneri* infected HEK/null-GFP cells induced in HEK/hNOD1 bystander cells the same IL-8 response (red curve) as an infected HEK/hNOD1 cell (black curve), indicating that NOD1 signaling in infected cells was not required to trigger the signals that lead to bystander activation (Figure II.6, panel A top, IF image; bottom, quantification). Analysis of infected cell layers consisting of few HEK/hNOD1 cells surrounded by a majority of HEK/null-GFP cells revealed that NOD1 contributes in bystander cells to IL-8 expression (FigureII.6, panel B top, IF image; bottom, quantification). Of note, in two mixed cell population assays the IL-8 response of HEK/null-GFP bystander cells was stronger decreased as compared to the IL-8 response of parental HEK/null cells, whereas in one mixed cell population experiment the IL-8 response of HEK/null-GFP bystander cells was not significantly reduced. I assume that by repeating the mixed cell population experiment the data of the parental HEK/null cell line can be reproduced.

Figure II.6
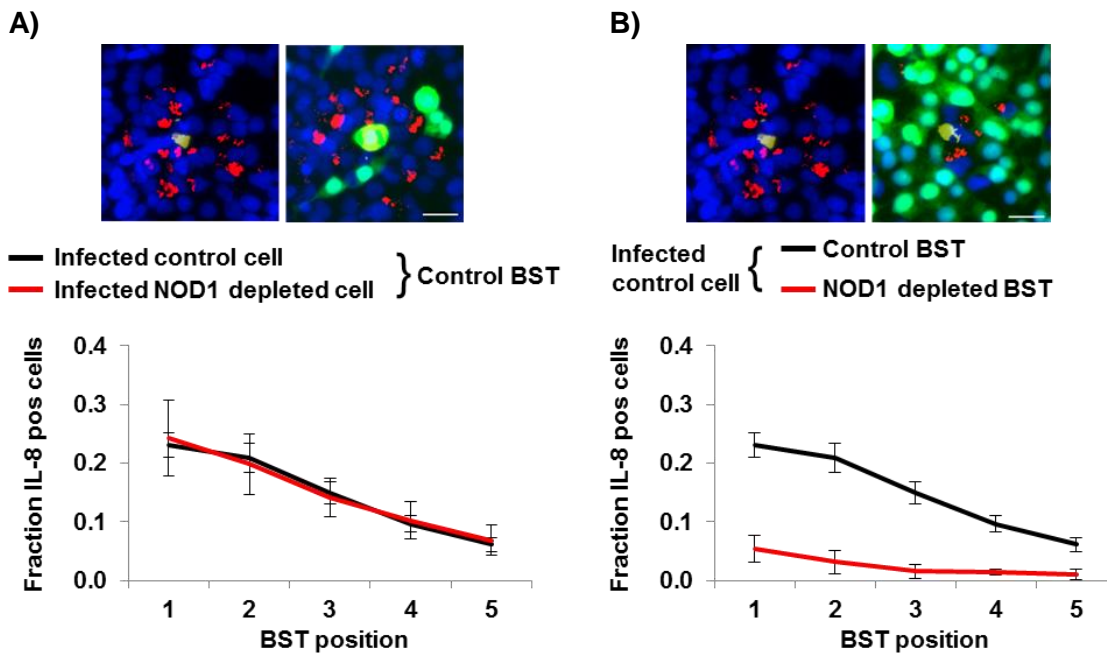
Figure II.6 NOD1 is not required to trigger bystander activation but contributes to IL-8 expression in bystander cells of *S. flexneri* infection. (**A+B, top**) One representative IF image (HEK/hNOD1 in blue, HEK/null in green, *S. flexneri* in yellow, IL-8 in red), scale bar represents 25 µm. (**A, bottom**) Spatial propagation of IL-8 expression triggered from either a *S. flexneri* infected HEK/hNOD1 cell or a HEK/null-GFP cell depleted for NOD1 into HEK/hNOD1 bystander cells. Infection of mixed cell layers at MOI=0.02. Each number corresponds to the fraction of IL-8 producing cells for a given bystander cell position. Quantification was performed by automated image analysis as described previously [39] (means ± SD of 18 wells, graph representative of 3 independent experiments; p > 0.24 at any given position). (**B, bottom**) Spatial propagation of IL-8 production from a *S .flexneri* infected HEK/hNOD1 cell into either HEK/hNOD1 bystander cells or HEK/null-GFP bystander cells depleted for NOD1. Each number corresponds to the fraction of IL-8 producing cells for a given bystander cell position. Quantification was performed by automated image analysis as described previously [39] (means ± SD of 18 wells, graph representative of 3 independent experiments; p < 1.1E-16). (IF = immunofluorescence microscopy, INF = infected cells; BST = bystander cells)

Taken together, these results showed that NOD1 contributes in bystander cells of *S. flexneri* infection to IL-8 expression, while in infected cells the activation of the NOD1 dependent signaling pathway is not required to trigger bystander activation. In line with the data gained on RIPK2 in HeLa cells, these data imply the existence of a NOD1 independent signaling pathway in bystander cells, which contributes to bystander IL-8 expression.

2.4 TIFA and TRAF6 are required exclusively in bystander cells for IL-8 expression

In the frame of the InfectX project, a genome-wide RNAi screen was performed in order to study various aspects of *Shigella* virulence, including bystander IL-8 production (performed by C.A. Kasper). Primary hits from the genome-wide screen were validated in a secondary screen resulting in a list of candidate proteins that could be involved in bystander IL-8 expression. Among these the Na^+/K^+-ATPase (ATP1A1), the TRAF-interacting protein with a FHA domain (TIFA) and the TNF receptor-associated factor 6 (TRAF6) were investigated in more detail. The ion pump Na^+/K^+-ATPase is an ubiquitous enzyme located at the plasma membrane, which is involved in maintaining the cell membrane potential. TRAF6 is an E3 ubiquitin ligase that is known to activate TAK1 and subsequently NF-κB and the MAPKs downstream of various receptors including TNF and Toll-like receptors [170]. Finally, TIFA was shown to interact with TRAF6 in TNFα-stimulated cells leading to NF-κB activation [171]. *S. flexneri* infected HeLa cell layers depleted either for TRAF6 or for TIFA were not able to activate NF-κB in bystander cells and consequently no IL-8 production was observed (C.A. Kasper, unpublished data). In contrast, HeLa cells depleted for ATP1A1 were still able to activate NF-κB in bystander cells, while at the same time no bystander IL-8 production was observed (C. Kasper, unpublished data). We hypothesized that depletion of ATP1A1 could interfere with the osmoregulation of the cell and thereby could inhibit protein synthesis in general [172]. Thus, we did not follow up on ATP1A1 but instead focused on the other two hits.

First, I controlled the knock down efficiency of TRAF6 and TIFA by means of qRT-PCR. The mRNA levels for both TRAF6 and TIFA were reduced by 92 ± 2% (Figure II.7, panel A and B). Next, we controlled the specificity of the siRNA mediated depletion of TRAF6 and TIFA, with a rescue experiment, in which TRAF6 or TIFA, respectively, were rescued by transient transfection of a siRNA resistant variant (2 to 3 silent mutations in the siRNA seed region). This experiment confirmed that IL-8 expression during *S. flexneri* infection in cells depleted for TRAF6 or TIFA, respectively, could be rescued (C.A. Kasper, unpublished data, not shown).
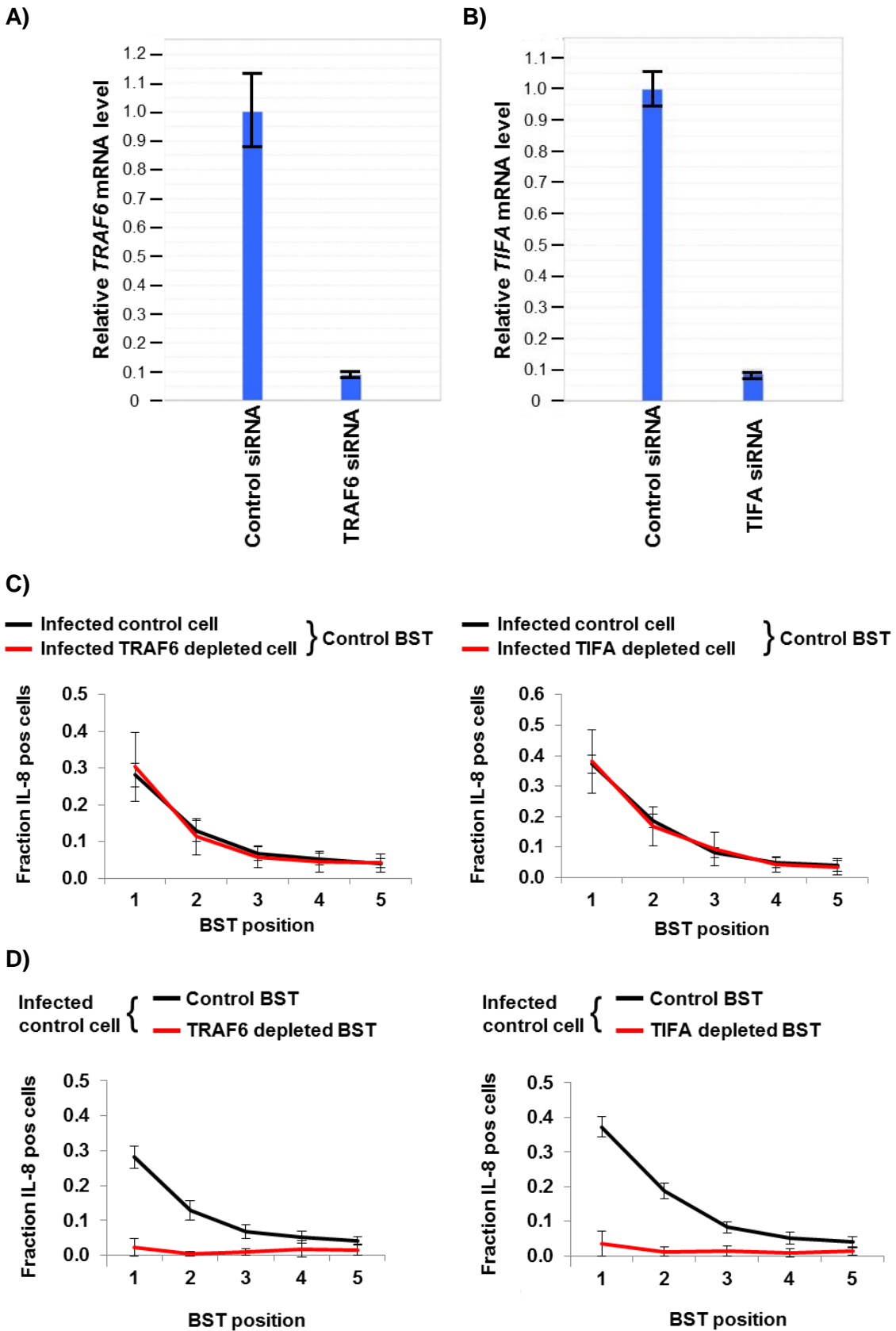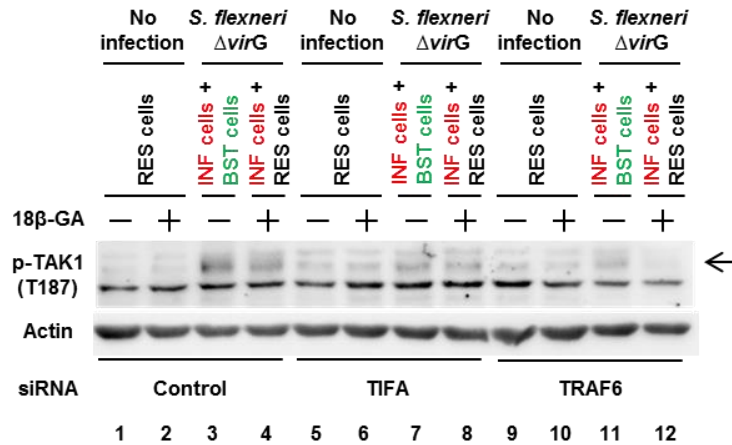
Figure II.7

A)

B)

C)

D)

Figure II.7 TIFA and TRAF6 are essential for bystander IL-8 expression. (**A + B**) Control of siRNA mediated TRAF6 and TIFA knock down. HeLa cells were transfected for 72 hours with the respective siRNA. *TRAF6* or *TIFA* mRNA levels were measured by quantitative real-time PCR. Values represent relative quantities (RQ) ± RQ max and RQ min of triplicate samples and indicate the *TRAF6* or *TIFA* mRNA level of HeLa cells depleted for TRAF6 or TIFA, respectively, relative to HeLa control cells after normalization to *GAPDH* mRNA; graph representative of 1 experiment. (**C**) Spatial propagation of IL-8 expression triggered from either a *S. flexneri* infected control cell or HeLa-GFP cell depleted for TRAF6 (left) or TIFA (right) into control bystander cells. Mixed cell layers were infected at MOI=0.02. Quantification was performed by automated image analysis as described previously [39]. Each number corresponds to the fraction of IL-8 producing cells for a given bystander cell position (means ± SD of 18 wells, graph representative of 3 independent experiments; TRAF6: p > 0.18 at any given position; TIFA: p > 0.25 at any given position). (**D**) Spatial propagation of IL-8 production from an infected control cell into either control bystander cells or HeLa-GFP bystander cells depleted for TRAF6 (left) or TIFA (right). Mixed cell layers were infected at MOI=0.02. Each number corresponds to the fraction of IL-8 producing cells for a given bystander cell position. Quantification was performed by automated image analysis as described previously [39] (means ± SD of 18 wells, graph representative of 3 independent experiments; TRAF6: p < 1.4E-05 at any given position; TIFA: p < 1.6E-05 at any given position).

To discriminate between signaling events taking place in infected and in bystander cells a mixed cell population assay was performed. Automated analysis of immunofluorescence images revealed that infected cells depleted for TRAF6 or TIFA, triggered the same bystander IL-8 response in control bystander cells (red curve) as an infected control cell (black curve) (Figure II.7, panel C). In contrast, TRAF6 or TIFA depleted bystander cells, of infected control cells were not able to express IL-8 (Figure II.7, panel D). These data point to a role for TRAF6 and TIFA exclusively in bystander cells of *S. flexneri* infection, while signals that trigger bystander activation in infected cells are generated independently of TIFA and TRAF6.

As TRAF6 is a known activator of TAK1 [170] and TIFA is known to activate TRAF6 [171], I tested, whether TAK1 activation in infected and in bystander cells of *S. flexneri* infection was TRAF6 and/or TIFA dependent. This was done by means of immunoblotting with the phospho-specific antibody described previously. Upon knock down of TRAF6 or TIFA, HeLa cells were left untreated or treated with the gap junction inhibitor 18β-GA prior to infection. Analysis of lysates of HeLa cells depleted for TRAF6 revealed that TAK1 activation in *S. flexneri* infected cells and in bystander cells was completely TRAF6 dependent (Figure II.7, panel E and F, lanes 11 and 12). HeLa cells depleted for TIFA showed in infected and in bystander cells a reduced TAK1 activation (Figure II.7, panel E and F, lanes 7 and 8).

Figure II.7

E)

F)
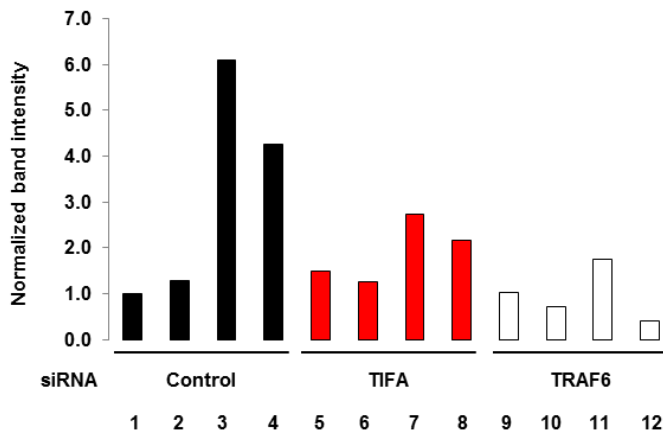
Figure II.7 Continued. (E) TRAF6 and TIFA dependent activation of TAK1 in *S. flexneri* infected HeLa cells and bystander cells. HeLa cells were transfected with control, TIFA or TRAF6 siRNA for 72 hours, 1 hour prior infection with *S. flexneri* at MOI=4, cells were treated or not with the gap junction inhibitor 18β-GA. After 45 minutes of infection cells were lysed and analyzed by immunoblotting using a p-TAK1 (T187) antibody. Actin was used as loading control. **(F)** Densitometric quantification of phosphorylated TAK1 in control cells and TIFA or TRAF6 depleted HeLa cells. Graph representative of 2 independent experiments. (RES = resting cells; INF = infected cells; BST = bystander cells)

Altogether, these data indicate that the signals underlying cell-cell communication are produced independently of TIFA or TRAF6 activation in infected cells, while in bystander cells, TIFA and TRAF6 are essential for IL-8 expression. Furthermore, the data indicates that in bystander cells TAK1 activation is partially TIFA dependent and completely TRAF6 dependent.

2.5 NOD1 signals partially in a TIFA/TRAF6-dependent manner to TAK1 in bystander cells

The E3 Ub ligase TRAF6 gets activated downstream of various receptors, such as IL-1Rs, TLRs or TNFRs, and signals then to TAK1 [170]. Furthermore, it is known to be activated by TIFA upon TNFα stimulation. Therefore, we examined whether TIFA/TRAF6 were activated downstream of NOD1 or whether they formed part of a second signaling pathway contributing to IL-8 expression in bystander cells of *S. flexneri* infection. To address this question, I used the HEK/hNOD1 cell line that can be stimulated selectively with the NOD1 ligand iE-DAP. First, TRAF6, TIFA or TAK1, respectively, were depleted by means of RNA interference in HEK/hNOD1 cells, and the knock down efficiency was confirmed by qRT-PCR. Indeed, a significant reduction of mRNA levels compared to control cells of 91 ± 2%, 93 ± 1% and 94 ± 3%, could be found for all three knock downs (Figure II.8, panel A). Thereafter, HEK/hNOD1 cells depleted for TIFA, TRAF6 or TAK1, were either infected with *S. flex*neri or were stimulated with the NOD1 ligand C_{12}-iE-DAP and the proinflammatory responses elicited by the differently stimulated cells was compared. Automated image analysis of immunofluorescence images was used to determine the fraction of NF-κB positive and the fraction of IL-8 positive cells during S*. flexneri* infection or in C_{12}-iE-DAP treated cells. In line with our HeLa data, TAK1 depletion in HEK/hNOD1 cells severely impaired proinflammatory signals in bystander cells of infection with a reduction of the fraction of NF-κB p65 positive bystander cells by 87% (Figure II.8, panel B left) and a reduction of IL-8 positive bystander cells by 76% (Figure II.8, panel B right) compared to control cells. Selective stimulation of the NOD1 signaling pathway with C_{12}-iE-DAP of HEK/hNOD1 cells depleted for TAK1, revealed a reduction of NF-κB positive bystander cells by 85% (FigureII.8, panel B left) and subsequently a reduction of IL-8 positive bystander cells by 82% compared to control cells (FigureII.8, panel B right). In summary, these data show that the majority of proinflammatory signals in bystander cells of *S. flexneri* infection converge on TAK1.
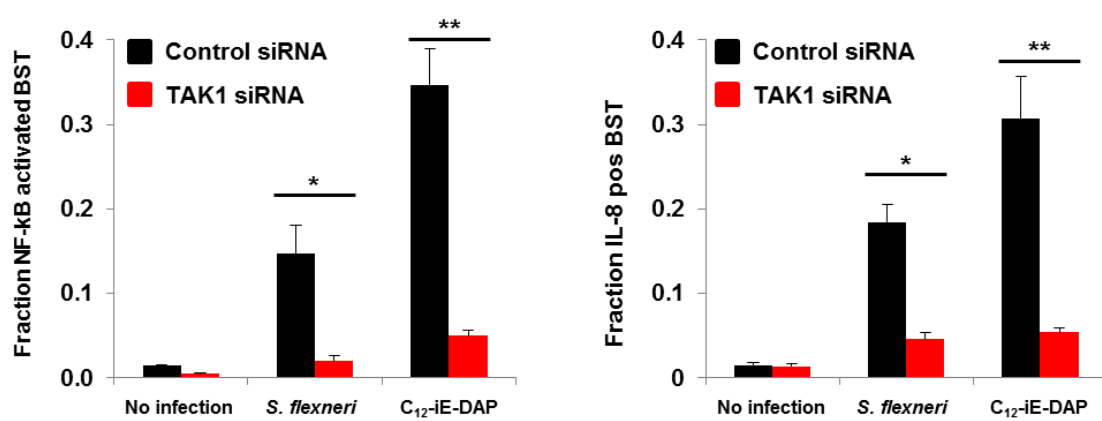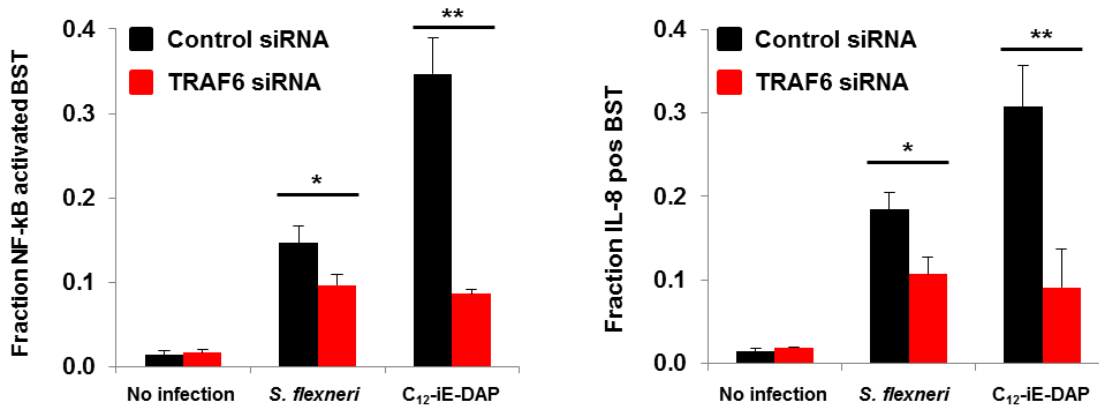
Figure II.8

A)
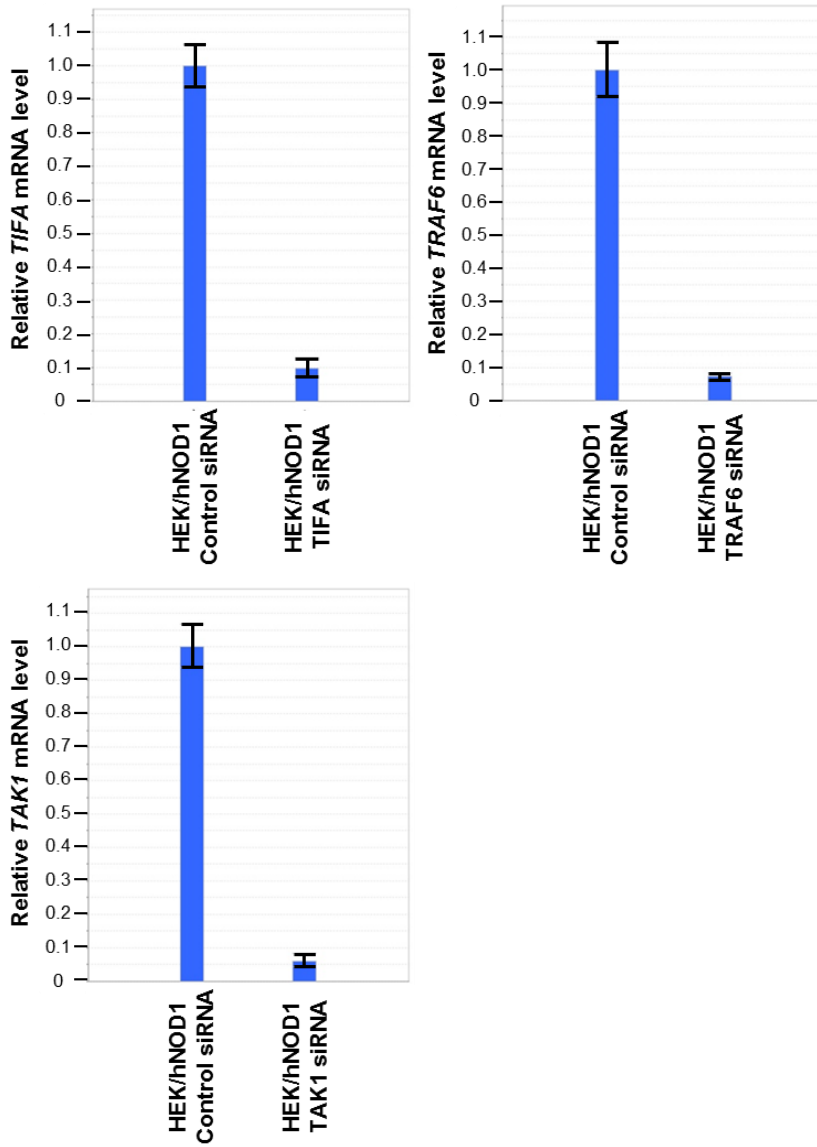
B)

Figure II.8 NOD1 signals partially in a TIFA/TRAF6 dependent manner to TAK1 in bystander cells. (**A**) Control of siRNA mediated TIFA, TRAF6 and TAK1 knock down in HEK/hNOD1 cells. HEK/hNOD1 cells were transfected for 72 hours with the respective siRNA. *TIFA, TRAF6* or *TAK1* mRNA levels were measured by qRT-PCR. Values represent relative quantities (RQ) ± RQ max and RQ min of triplicate samples and indicate the mRNA level of HEK/hNOD1 cells depleted for TIFA, TRAF6 or TAK1 relative to HEK/hNOD1 control cells after normalization to *GAPDH* mRNA; graph representative of 1 experiment for RIPK2 and TIFA and 2 experiments for TRAF6 and TAK1. (**B**) *S. flexneri* and C_{12}-iE-DAP stimulated HEK/NOD1 cells require TAK1 for NF-κB activation and IL-8 expression. HEK/hNOD1 cells treated for 72 hours with control or TAK1 siRNA were infected with *S. flexneri* at MOI=0.1 or stimulated with C_{12}-iE-DAP (500 ng/ml). Cells were either fixed after 50 minutes and stained with a p65 antibody, or fixed after 3.5 hours and stained with an IL-8 antibody. The fraction of NF-κB positive BST (left) or IL-8 positive BST (right) was determined by automated image analysis [39] (means ± SD of 9 wells, graph representative of three independent experiments; NF-κB: *p = 6.5E-09; **p = 2.9E-04; IL-8: *p = 1.9E-12, **p = 8.9E-04).

Bystander cells of *S. flexneri* infection of HEK/hNOD1 cells depleted for TRAF6 showed upon infection a reduction of the fraction of NF-κB p65 positive bystander cells by 34% (Figure II.8, panel C left) and a reduction of IL-8 positive bystander cells by 41% compared to control cells (Figure II.8, panel C right). Noteworthy, the loss in NF-κB activation and IL-8 production in HEK/hNOD1 cells is, in contrast to the knock down in HeLa cells, not complete. This can be explained by the fact that NOD1 is over-expressed in HEK/hNOD1 cells compared to HeLa cells and proinflammatory signals are mediated via the classical NOD1-RIPK2 signaling pathway. Interestingly, stimulation of the NOD1 signaling pathway with C_{12}-iE-DAP in HEK/hNOD1 cells depleted for TRAF6, revealed a strong reduction of NF-κB positive bystander cells by 75% (Figure II.8, panel C left) and subsequent reduction of IL-8 positive bystander cells by 71% compared to control cells (Figure II.8, panel C right). This data suggest that NOD1 signals in a TRAF6 dependent manner to TAK1.

Next, we analyzed TIFA depleted HEK/hNOD1 bystander cells of *S. flexneri* infection and found a reduction of the fraction of NF-κB p65 positive bystander cells by 35% (FigureII.8, panel D left) and a reduction of IL-8 positive bystander cells by 46% compared to control cells (FigureII.8, panel D right). Similar to the TRAF6 knock down, the discrepancy of TIFA data gained in HeLa and HEK/hNOD1 cells might be explained by the over expression of NOD1 in HEK cells. Stimulation of the NOD1 signaling pathway with C_{12}-iE-DAP of HEK/hNOD1 cells depleted for TIFA revealed a reduction of NF-κB positive bystander cells compared to control cells by 64% (FigureII.8, panel D left) and a reduction of IL-8 positive bystander cells compared to control cells by 48% (Figure II.8, panel D right). These results suggest that NOD1 signaling is partially TIFA dependent.

Figure II.8

C)

D)
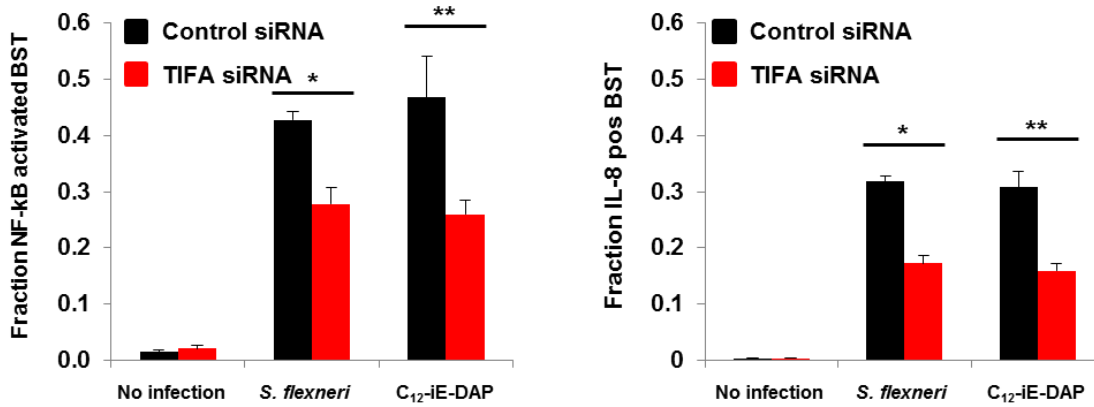
Figure II.8 Continued. (**C**) NOD1 signaling in response to *S. flexneri* infection is partially TRAF6 dependent. HEK/hNOD1 cells were treated for 72 hours with control or TRAF6 siRNA and infected with *S. flexneri* at MOI=0.1 or stimulated with C_{12}-iE-DAP (500 ng/ml). Cells were either fixed after 50 minutes and stained with a p65 antibody, or fixed after 3.5 hours and stained with an IL-8 antibody. The fraction of NF-κB positive BST (left) or IL-8 positive BST (right) was determined by automated image analysis [39] (means ± SD of 9 wells, graph representative of three independent experiments; NF-κB: *p = 5.9E-03; **p = 4.7E-04; IL-8: *p = 4.3E-07; **p = 5.2E-03). (**D**) TIFA contributes to NOD1 signaling in *S. flexneri* infected HEK/hNOD1 cells. HEK/hNOD1 cells treated for 72 hours with control or TIFA siRNA respectively, infected with *S. flexneri* at MOI=1 or stimulated with C_{12}-iE-DAP (100 ng/ml). Cells were either fixed after 50 minutes and stained with a p65 antibody, or fixed after 3.5 hours and stained with an IL-8 antibody. The fraction of NF-κB positive BST (left) or IL-8 positive BST (right) was determined by automated image analysis (means ± SD of 3 wells, graph representative of two independent experiments for NF-κB and five independent experiments for IL-8; NF-κB: *p = 1.5E-03; **p = 1.0E-02; IL-8: *p = 1.3E-04; **p = 1.3E-03). (**E**) Model describing signaling taking place in bystander cells upon *S. flexneri* infection or C_{12}-iE-DAP stimulation of epithelial cells.

Figure II.8

E)
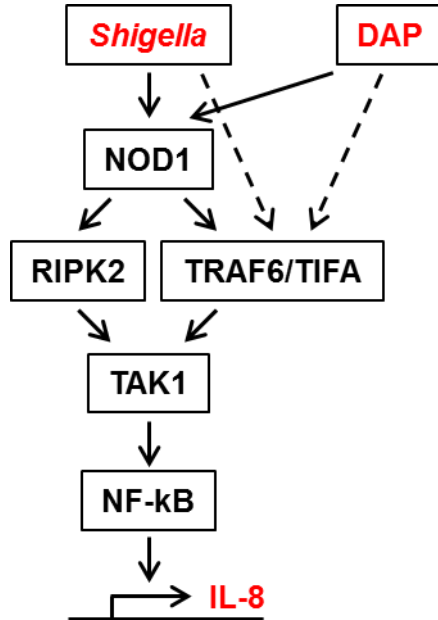
In summary, these data indicate that NOD1 signals in bystander cells of *S. flexneri* infection partially in a TIFA and TRAF6 dependent manner to TAK1, which in turn is essential for NF-κB activation and subsequent IL-8 expression (Figure II.8, panel E).

2.6 *S. flexneri* induced intercellular calcium signaling contributes to bystander IL-8 production, but does not affect NF-κB activation

Cell–cell communication between adjacent cells during *S. flexneri* infection is mediated via gap junctions and depends on the diffusion of small molecules (< 1 – 2 kDa) such as ions, second messengers, nucleotides amino acids and metabolites. In order to identify the small diffusing molecules responsible for bystander activation during *S. flexneri* infection, we started a collaboration with the group of J.A. Vorholt (ETHZ) who had developed different methods to identify and quantify metabolites and small molecules using LC-HRMS. The idea was to compare the levels of small molecules in resting and infected cells within the first 30 minutes of *S. flexneri* infection. The results from the 2 first LC-HRMS experiments revealed an increase of cAMP and cGMP after infection, suggesting that these two second messengers could be important for cell-cell communication. As these data were also accompanied by an increase in inositol 1,4,5-trisphosphate (IP_3) and hepoxilin A3, molecules known to be produced upon *S. flexneri* infection, we pursued this hypothesis and determined the level of cAMP and cGMP

after infection. Yet, measurements by ELISA indicated no increase in the concentration for cAMP and cGMP (data not shown). In addition, reanalysis of the two first LC-HRMS datasets with newly developed analysis tools had in the meantime disproved an increase of cAMP and cGMP after *S. flexneri* infection. As the method itself turned out not to be sensitive and robust enough to measure significant concentration differences of small molecules such as cAMP and cGMP, we went on with the hypothesis driven approach.

It is reported that *Shigella* induces calcium waves involving IP_3-dependent opening of internal calcium stores [173]. In the field of cell physiology, it is suggested that IP_3-induced gap junction mediated intercellular calcium ion waves may represent a general mechanism, by which cells do communicate and coordinate multicellular responses [158]. Furthermore, we found that the NOD1 receptor contributed in bystander cells of *S. flexneri* infection to IL-8 expression. Thus, we combined this knowledge, and hypothesized that the IP_3-induced calcium waves together with the NOD1 ligand iE-DAP could trigger bystander IL-8 expression. To test this hypothesis we performed co-stimulation experiments in HeLa and HEK NOD1 overexpressing cells. We stimulated the cells with C_{12}-iE-DAP and challenged them in addition with ionomycin, which triggers calcium. HeLa or HEK/hNOD1 cells, respectively, stimulated with ionomycin alone did not produce IL-8, while stimulation with C_{12}-iE-DAP induced IL-8 production in HeLa and in HEK/hNOD1 cells. Upon co-stimulation of HeLa or HEK/hNOD1 cells with C_{12}-iE-DAP and ionomycin the IL-8 response was potentiated (Figure II.9, panel A). Based on these data we hypothesized that IP_3-induced calcium waves together with iE-DAP released from replicating *S. flexneri* could be the trigger for bystander IL-8 expression.

Figure II.9

A)
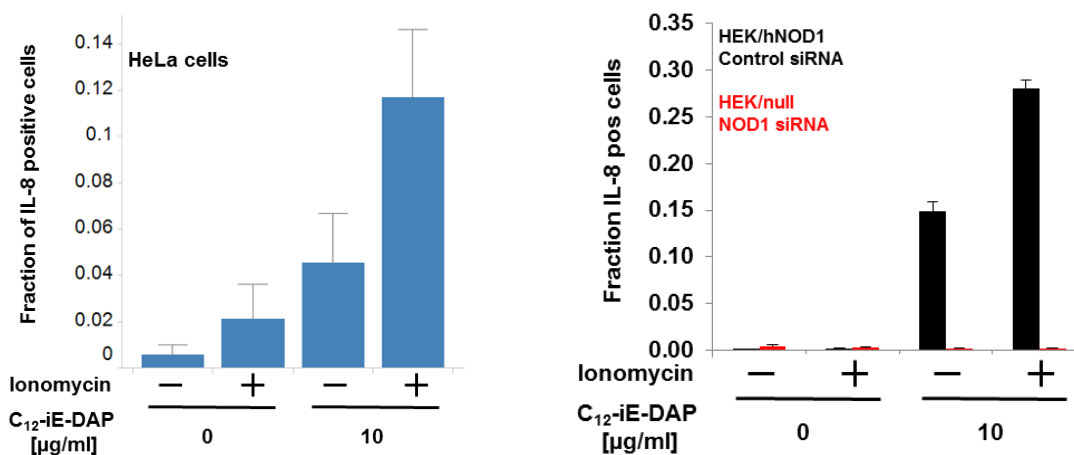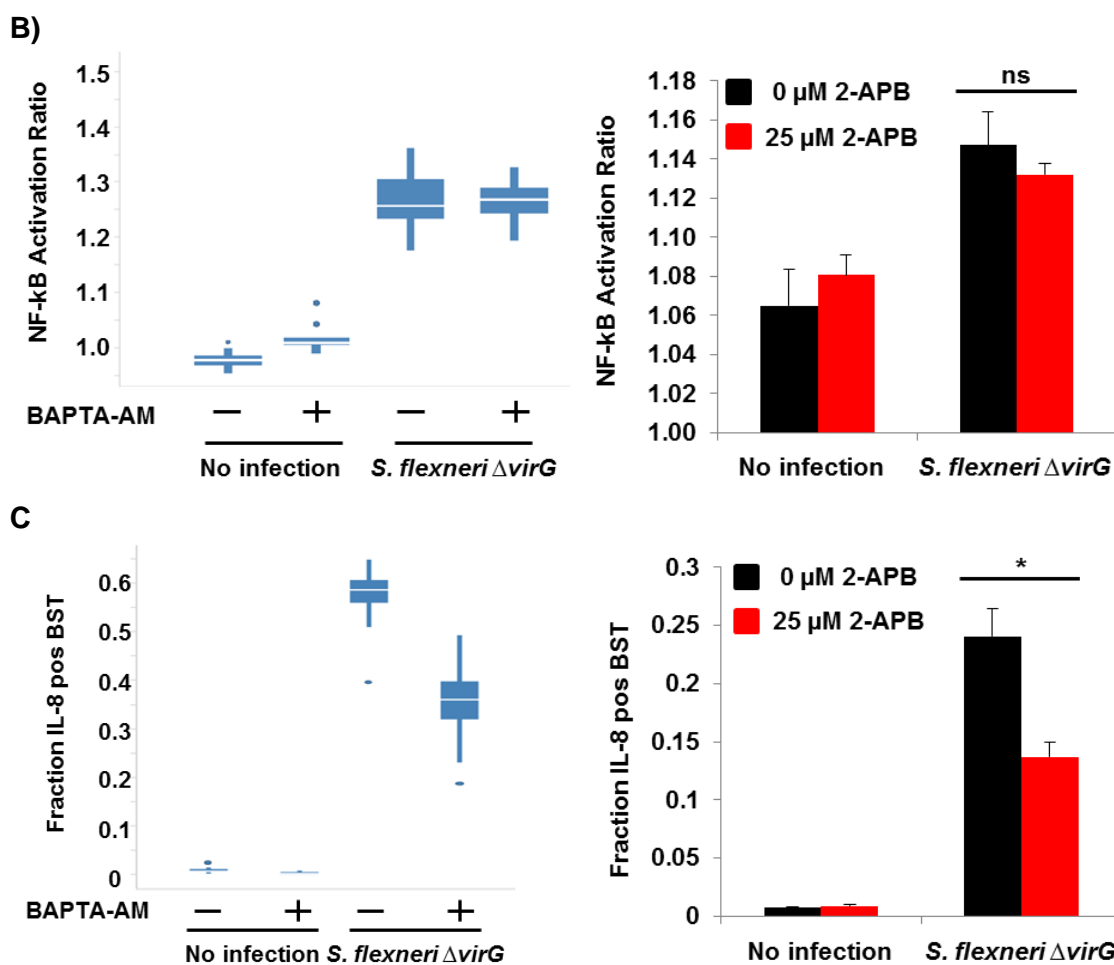
Figure II.9 *Shigella flexneri* **induced increase in the intracellular [Ca^{++}] seems to contribute to bystander IL-8 secretion, but does not affect NF-κB activation.** (**A**) Intracellular calcium increase potentiates DAP dependent IL-8 production. HeLa (left) and HEK/hNOD1 cells (right) were stimulated with C$_{12}$-iE-DAP (10 µg/ml) for 5 hours, after 2 hours ionomycin (1µM) was added for the remaining three hours. Immunofluorescence images were analyzed by automated image analysis and the fraction of IL-8 producing cells was determined. (means ± SD of 3 wells, graph representative of one experiment (**B**) NF-κB activation is independent of calcium signaling. HeLa cells were pretreated with the calcium chelator BAPTA-AM (left) at 20 µM or the IP$_3$ receptor inhibitor 2-APB (right) at 50 µM for 30 minutes, and infected with *S. flexneri* at MOI=1, after infecting cells inhibitor concentrations were as follows:10 µM and 25 µM, respectively. 30 minutes p.i. BAPTA-AM was removed 1 hour p.i. due to avoid toxicity. Cells were fixed and stained with a p65 antibody. The nuclear translocation of NF-κB p65 was analyzed by automated image analysis and the nuclear/cytoplasmic p65 intensity ratio was calculated as described in [39]. The data shown are mean values +/- SD of triplicate wells per condition; graph representative of 2 independent experiments. (**C**) IL-8 expression in bystander cells of *S. flexneri* infection depends on calcium release from internal stores. HeLa cells treated with BAPTA-AM at 20 µM (left) or with 2-APB at 50 µM (right) 30 minutes prior to infection, were infected with *S. flexneri* (MOI=1), p.i. inhibitor concentrations were divided into halve: 10 µM and 25 µM, respectively. BAPTA-AM was removed 1 hour p.i. in order to avoid toxicity. After 3.5 hours cells were fixed and stained with an IL-8 antibody. The fraction of IL-8 positive BST was determined by automated image analysis (means ± SD of 3 wells, graph representative of two independent experiments; *p = 2.7E-03).

Results

To further investigate the impact of calcium signaling, we did live cell imaging. HeLa cells that were loaded with the calcium indicator Fluo4-AM were challenged with *S. flexneri.* Calcium waves were monitored over the first 15 minutes of infection. *S. flexneri* indeed induced calcium waves that were BAPTA-AM (BAPTA-AM, a chelater of intracellular calcium ions) sensitive and could in addition be blocked by inhibition of the IP_3 receptor with 2-APB (I. Sorg, data not shown). Next, we treated HeLa cells with either BAPTA-AM or the IP_3 receptor inhibitor 2-APB and infected them with *S. flexneri* for 50 minutes or 3.5 hours and stained for NF-κB or IL-8, respectively. Inhibition of calcium waves by BAPTA-AM treatment (Figure II.9, panel B left) or IP_3 receptor inhibition with 2-APB (Figure II.9, panel B right) did not affect NF-κB activation in bystander cells. The finding that NF-κB activation in bystander cells was not calcium signaling dependent additionally indicated that the BAPTA-AM and 2-APB had no inhibitory effect on gap junction mediated cell–cell communication. Yet, we observed a significantly reduced bystander IL-8 response upon BABTA-AM treatment (Figure II.9, panel C left) as well as upon IP_3 receptor inhibition with 2-APB (Figure II.9, panel C right). These data indicate that *S. flexneri* induced calcium waves contribute to bystander IL-8 expression.

S. flexneri is known to mediate the phosphatidylinositol 5-phosphate (PI5P) dependent activation of the epidermal growth factor receptor (EGFR) signaling pathway [174]. One branch of signaling downstream of EGFR leads to PI3-kinase and AKT activation, whereas the second branch leads to PLCγ1 activation, which catalysis the cleavage of phosphatidylinositol 4,5-bisphosphate (PIP_2) into inositol trisphosphate (IP_3) and diacylglycerol (DAG). To test the possibility that PLCγ1 was involved in the process of bystander IL-8 expression, we treated HeLa cells prior to infection with the PLCγ1 inhibitor U73122 and monitored the NF-κB activation and IL-8 expression in bystander cells of infection. Because U73122 treatment affected the infection rate, C.A. Kasper determined the fraction of NF-κB positive and IL-8 positive cells at bystander positions 1 to 5, when infecting cells at very low MOI. As expected, we observed no impact of PLCγ1 inhibition at the level of NF-κB activation in bystander cells of *S. flexneri* infection (Figure II.10, panel A), whereas the fraction of IL-8 producing bystander cells was significantly reduced (Figure II.10, panel B), suggesting a role for PLCγ1 in the process of bystander IL-8 production.

Taken together, our data indicate a role for calcium signaling in the process of bystander IL-8 expression, which might be mediated via the activation of PLCγ1 in infected cells.

Figure II.10
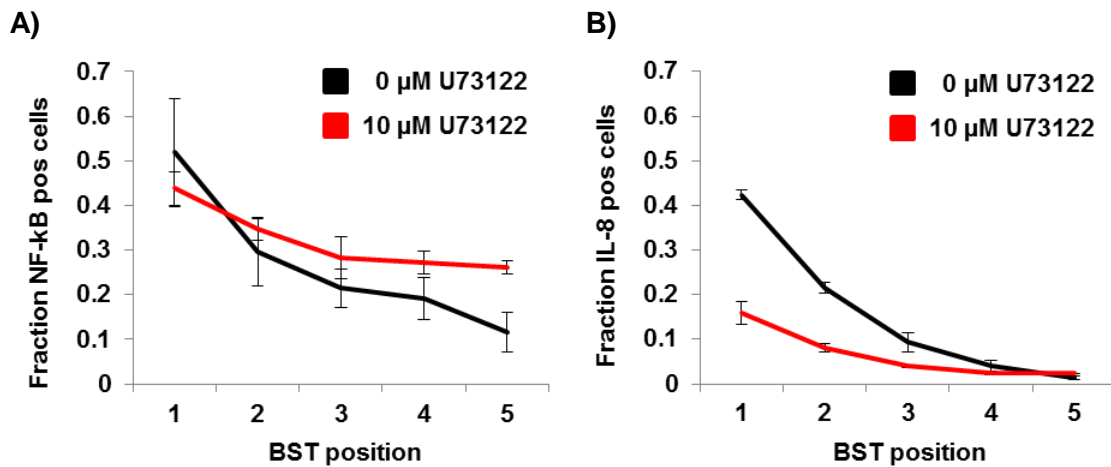
Figure II.10 PLCγ1 signaling contributes to bystander IL-8 expression. (**A**) NF-κB activation during *S. flexneri* infection is PLCγ1 independent. HeLa cells were treated with U73122 at 10 µM 30 min prior infection up to 1 p.i. Cells were infected with *S. flexneri* at MOI=0.02. After 1 hour of infection cells were fixed and stained for NF-κB p65 subunit. The nuclear translocation of NF-κB p65 was monitored by immunofluorescence and quantified by automated image analysis. The nuclear/cytoplasmic p65 intensity ratio was calculated as described in [39] (means ± SD of 3 wells, graph representative for one experiment). (**B**) IL-8 expression is PLC γ1 dependent. HeLa cells were treated with U73122 at 10 µM 30 min prior infection up to 1 hour p.i. and at 5 µM until fixation. Cells were infected with *S. flexneri* at MOI=0.02 for 3.5 hours, fixed and stained with an IL-8 antibody. IL-8 accumulation was monitored by automated imaging. The fraction of IL-8 positive BST at position 1 to 5 was determined by automated image analysis (means ± SD of 3 wells, graph representative for two independent experiments).

III Materials and Methods

1   Cell lines

HeLa cells were purchased from ATCC. HEK293/null and HEK293/hNOD1 cells were obtained from Invivogen (San Diego, USA). All cell lines were cultivated in DMEM, supplemented with 10% FCS, antibiotics and 2 mM L-glutamine. HeLa and HEK293/null cells stably expressing GFP were kindly provided by Dr. R. Okujava (Biozentrum, University of Basel, Switzerland).

2   Antibodies and Reagents

Antibody against NF-κB p65 was purchased from Santa Cruz Biotechnology (Santa Cruz, USA). Anti human IL-8 antibody was obtained from BD Pharmingen (San Jose, USA). Phospho-TAK1 antibody was purchased from Cell Signaling (Danvers, USA), Alexa Fluor 647-coupled anti-mouse IgG antibody and Hoechst 33342 were obtained from Invitrogen (Carlsbad, USA). DY-495-Phalloidin was purchased from Dyomics (Jena, Germany). C_{12}-iE-DAP was purchased from Invivogen (San Diego USA).The antibody against actin was purchased from Millipore (Billerica, USA). Monensin, 18β glycyrrethinic acid (18β-GA), Poly-D-lysine, 2-APB and U73122 were obtained from Sigma-Aldrich (St. Louis, USA). BABTA-AM was purchased from Fluka/Sigma-Aldrich (St. Louis, USA).

3   Bacterial strains

The *icsA* (*virG*) deletion mutant (Δ*virG)* generated in the M90T *S. flexneri 2a* strain was generously provided by Dr. P. Sansonetti (Institut Pasteur, Paris, France). The Δ*virG* Δ*ospF* mutant was generated as previously described [175] In addition, all *S. flexneri* strains were transformed with the pMW211 plasmid to express the DsRed protein under control of a constitutive promoter. The pMW211 plasmid was a generous gift from Dr. D. Bumann (Biozentrum, University of Basel, Switzerland).

4   Small interfering RNA (siRNA) reverse transfection protocol

NOD1 siRNA was purchased from Santa Cruz Biotechnology (Santa Cruz, USA). RIPK2, TIFA and TRAF6 siRNAs were obtained from Ambion (Carlsbad, USA). p65

human RELA (NF-κB subunit), TAK1 and scrambled siRNAs were purchased from Dharmacon (Dallas, USA). Transfection of siRNAs was carried out using RNAimax (Invitrogen, Carlsbad, USA). Cells, seeded in a 6-well plate (200'000 HEK or 250'000 HeLa cells/well), were reversely transfected with 40 nM siRNA according to the manufacturer's instruction. Cells were harvested after 48 hours and seeded into 96 well plates (3.65E5 HEK/null, 4.35E5 HEK/hNOD1 and 1.35E5 HeLa cells/ml) and used 24 hours later. For HEK cell experiments 96 well plates were coated with poly-D-lysin before use. Briefly, 96 well plates were incubated for 1 hour with 10 µg/ml poly-D-lysin in PBS. Then the poly-D-lysine solution was removed and the plates were washed 4 times with PBS, dried for 1 hour at room temperature, and finally were stored at 4°C until use.

5 Mixed cell population assay

For the mixed HeLa cell population experiments, HeLa-GFP cells were transfected with specific siRNAs and HeLa cells with control siRNA for 48 hours. After harvesting of the two cell populations the cell number was adjusted to 1.35E5 cells/ml for both cell populations. Next, HeLa-GFP depleted for a protein of interest and HeLa control cells were mixed at ratios 1 to 5 and 5 to 1 and seeded into a 96 well plate, per well 150 µl cell suspension were added. Per condition 21 wells were seeded, 18 wells for infections at MOI=0.02 and 3 wells served as uninfected controls. After another 24 hours of incubation, the experiment was performed.

For the mixed HEK cell assay, HEK-GFP cells were treated with NOD1 siRNA and HEK/hNOD1 cells with control siRNA for 48 hours. The two cell populations were harvested and the cell number was adjusted to 3.65E5 cells /ml cells for HEK-GFP cells and to 4.35E5 cells/ml for HEK/hNOD1 cells. Next, the two cell populations were mixed at ratios1 to 5 and 5 to 1 and seeded into a poly-D-lysin coated 96 well plate, per well 150 µl cell suspension were added. Per condition 21 wells were seeded, 18 wells for infections at MOI=0.02 and 3 wells served as uninfected controls. After another 24 hours of incubation, the experiment was performed.

6 Infection assay

S. flexneri strains were grown in tryptic soy broth (TSB) to exponential log phase at 37°C and coated with poly-L-lysine before infection. 30 minutes before infection,

complete growth medium was replaced by DMEM supplemented with 10 mM Hepes and 2 mM L-glutamine (assay medium). In the case of inhibitor treatment, 60 minutes prior infection the medium was replaced and 18β-GA was added at 2x concentration (10 μM). BAPTA-AM, 2-APB and U73122 were added 30 minutes prior infection at the indicated concentrations. Bacteria were added to cells at the indicated MOI. Infection was initiated by centrifuging the plates for 5 minutes and incubating at 37°C for the indicated time periods. Extracellular bacteria were killed by adding gentamycin (50 μg/ml) 30 minutes after infection and IL-8 secretion was prevented by adding monensin (50 μM) 30 minutes p.i.

7   SDS-PAGE and immunoblotting

Cells were washed twice in ice cold PBS, lysed in PhosphoSafeTM extraction reagent Novagen (Darmstadt, Germany) supplemented with 1x protease inhibitor cocktail Calbiochem (Darmstadt, Germany), incubated on ice for 10 minutes, and subsequently centrifuged at 4°C for 20 minutes at 16'000g. The protein concentration was determined by the use of the Protein Assay kit Pierce (Rockford, USA). 10-15 μg of protein were resolved on SDS-polyacrylamide gels and electroblotted onto Hybond C-Extra nitrocellulose membrane from Amersham Bioscience (Pittsburgh, USA). Immunoblotting was performed using primary antibodies diluted in phosphate buffered saline containing 0.1% tween and 5% bovine serum albumin. For detection of primary antibodies HRP-conjugated secondary antibodies from GE Healthcare (Chalfont St Giles, United Kingdom) or Cell signaling technology (Danvers, USA) were used. The blots were developed with an enhanced chemiluminescence method from Pierce (Rockford, USA) using an ImageQuant LAS4000 digital imaging system from GE Healthcare (Chalfont St Giles, United Kingdom). Finally, images were analyzed by densitometry.

8   Immunofluorescence

Cells were fixed with 4% paraformaldehyde in PBS. For the visualization of NF-κB localization, cells were first incubated for 1 hour in blocking buffer (1xPBS/ 5% goat serum/ 0.3% Triton X-100) followed by the incubation with a monoclonal mouse anti-p65 antibody in antibody dilution buffer (1xPBS/ 1% BSA/ 0.3% Triton X-100; 1:250) overnight at 4°C. After washing with PBS, cells were stained with Alexa Fluor 647-coupled goat anti-mouse IgG in antibody dilution buffer (1:500). Cell nuclei were stained with Hoechst (HeLa 1:2500, HEK 1:1000). IL-8 was visualized by adding a monoclonal

mouse anti human IL-8 antibody in saponin buffer (1xPBS/ 0.2% saponin; 1:300) for 2 hours at room temperature. After washing with PBS, cells were incubated with Alexa Fluor 647-coupled goat anti-mouse IgG diluted in saponin buffer (1:500). Nuclei and F-actin were stained with Hoechst (HeLa 1:2500, HEK 1:1000) and DY-495-Phalloidin (1:400), respectively.

9   Automated microscopy and image analysis

Images were automatically acquired with an ImageXpress Micro (Molecular devices, Sunnyvale, USA). At each site, images at 360nm, 480nm, 594nm and 640nm were acquired to visualize Hoechst, GFP expression or phalloidin F-actin, DsRed expressing *S. flexneri* and Alexa Fluor 647-coupled secondary antibodies. Image analysis was performed with CellProfiler and MATLAB (The MathWorks, Inc, Natick, USA) as described previously [39, 176] (see V Appendix).

10   Quantitative real-time PCR

The level of various mRNAs was measured by quantitative real-time PCR (qRT-PCR) as follows. Total RNA was isolated from cells treated with control or target specific siRNA for 72 hours using the RNeasy Mini Kit and RNase-Free DNase Set (Quiagen, Hilden, Germany). Total RNA was reverse transcribed using oligo(dT)15 primer (Promega) with Superscript III reverse transcriptase (Invitrogen). qRT-PCR was performed on StepOne Real time PCR system (Applied Biosystems) using the SYBR green PCR Master Mix (Applied Biosystems). GAPDH was used as an internal control to normalize mRNA expression. Each sample was analyzed in triplicate. The primer sequences used are summarized below:

NOD1-forward: 5'-CCTGACAAGGTCCGCAAA
NOD1-reverse: 5'-CACGTAGGCATCTGCGAGT
RIPK2-forward: 5-CCATTGAGATTTCGCATCCT
RIPK2-reverse: 5-ATGCGCCACTTTGATAAACC
TRAF6-forward: 5'-AGCACAGCAGTGCAATGGAAT
TRAF6-reverse: 5'- CCGGGTTTGCCAGTGTAGAAT
TAK1-forward: 5'-AGTGATAACGCGTCGGAAAC
TAK1-reverse: 5'-CAGGCTCTCAATGGGCTTAG
TIFA-forward: 5'- GTGCATGGTCAGATTCGGAGA

TIFA-reverse: 5'-TGGTGGCCAGTTGTTTTCTTG

GAPDH-forward: 5'-GAAGGT GAAGGTCGGAGTC

GAPDH-reverse: 5'-GAAGATGGTGATGGGATTTC

11   Statistical analysis

Data presented are representative of at least three independent experiments if not stated otherwise. Data are expressed as mean ± standard deviation of triplicate samples or as indicated in the figure legends. p-values were calculated with a two-tailed two-sample equal variance t-test.

IV Discussion and Outlook

1. Discussion

Upon bacterial infection host cells sense various bacterial products present at the surface of bacteria or released during infection (PAMPs) as well as the presence of miss localized endogenous components (DAMPs). This leads to the activation of signaling cascades, which induce the expression of proinflammatory cytokines. Many bacterial pathogens interfere with these signaling cascades by injecting effector proteins into the host cell cytosol. *Shigella flexneri* for example injects several effectors that suppress pronflammatory signals and thereby block the expression of cytokines such as IL-8 in the infected cell. Nevertheless, IL-8 was detected in *Shigella* infected tissues [38]. This suggested that there is a host strategy to counteract the immune-suppressive activity of bacterial effectors. We recently provided evidence for such a strategy. We reported a mechanism of cell–cell communication between consecutive epithelial cells that allows *S. flexneri* infected cells to propagate NF-κB and MAP kinase activation to uninfected bystander cells in a gap junction dependent manner. Bystander cells subsequently express proinflammatory genes and secrete massive amounts of cytokines [39]. Furthermore, we found that triggering of the NOD1 signaling pathway with TriDAP was sufficient to induce bystander IL-8 expression, suggesting that the recognition of Nod1 ligands in infected cells may be sufficient to generate the underlying signals that mediate IL-8 expression in bystander cells of *S. flexneri* infection.

The goal of this study was to elucidate the molecular mechanism of cell-cell communication during *S. flexneri* infection. In particular, we aimed at finding signaling events required in infected cells that trigger bystander IL-8 expression. Furthermore, we dissected signaling events taking place in bystander cells of infection that culminate in IL-8 production and finally, we aimed at identifying the signaling molecule(s) responsible for bystander IL-8 expression. To our surprise, we found that signals underlying cell-cell communication during *S. flexneri* infection were generated independently of the activation of the NOD1 signaling pathway and of the activation of the two newly identified candidate proteins for bystander activation, TIFA and TRAF6, in infected cells. In contrast, in bystander cells of infection the NOD1 signaling pathway contributes together with a NOD1 independent signaling pathway to the expression of proinflammatory genes. We identified TIFA and TRAF6 as members of this NOD1 independent pathway. Moreover, C_{12}-iE-DAP stimulation experiments revealed first, that NOD1 signaling in bystander cells of infection was not exclusively mediated via the

adaptor protein RIPK2 but was partially TIFA and TRAF6 dependent and the signaling in bystander cells converge on TAK1. Finally, we show that IP_3 induced intercellular calcium waves contribute to bystander IL-8 expression.

1.1   Signaling in infected cells

Cellular stresses such as bacterial invasion lead to the activation of NF-κB. NF-κB is an ubiquitous transcription factor that controls the expression of proinflammatory genes including cytokines, acute phase response proteins, and cell adhesion molecules and promotes cell survival. Small interfering RNA mediated depletion of NF-κB revealed the essential function of this transcription factor during *S. flexneri* infection. Epithelial cells depleted for NF-κB were no longer able to produce IL-8 in response to bacterial challenge. A detailed analysis of NF-κB activation in *S. flexneri* infected and in uninfected bystander cells indicated that NF-κB activation was essential in bystander cells to control IL-8 expression but was dispensable in infected cells to trigger bystander activation. These data suggest that early signaling events in infected cells are responsible for bystander activation and not gene expression downstream of NF-κB. This was expected due to the observation that NF-κB activation propagated within the first 15 minutes of infection to neighboring cells [39].

The MAP3 kinase TAK1 is a key element in many signaling pathways that are activated in response to environmental stresses [170], including *S. flexneri* infection. Once activated TAK1 in turn activates the IKK complex that mediates NF-κB translocation. Moreover, TAK1 activates the MAP kinases p38 and JNK. While p38 acts on histone phosphorylation and thereby promotes DNA accessibility for transcription factors, JNK activates AP-1 another transcription factor that contributes to proinflammatory gene expression. Dissecting the role of TAK1 activation in the process of bystander activation during *S. flexneri* infection pointed to an essential role for this protein complex exclusively in bystander cells. Although TAK1 is activated not only in bystander cells but also in infected cells, our data clearly showed that TAK1 activation in infected cells was dispensable for the production of a signaling molecule that triggers bystander activation. This finding excludes a role for the MAP kinases p38 or JNK in infected cells in the process of bystander activation.

Since microinjection of the NOD1 ligand TriDAP was sufficient to trigger bystander IL-8 expression, we hypothesized that signals underlying bystander activation are generated in infected cells in a NOD1 signaling pathway dependent manner. Unexpectedly,

depletion of RIPK2 in HeLa cells or depletion of NOD1 in HEK cells resulted not in a complete block of IL-8 expression during *S. flexneri* infection, implying the existence of a NOD1 independent signaling pathway that contributes to bystander IL-8 expression. Next, by performing the mixed cell population assay, it became evident that signals in infected cells that trigger bystander activation are generated independently of RIPK2 or NOD1 signaling. These data indicate that signals that are required for bystander activation are produced independent of pathogen recognition by NOD1 or alternatively, result from the activation of the NOD1 independent signaling pathway.

In the genome wide RNAi screen performed by C.A. Kasper, TRAF6 was identified as a protein involved in the process of bystander IL-8 expression. TRAF6 turned out to be a candidate protein that could be part of a NOD1 independent signaling pathway that triggers bystander activation. TRAF6 is an E3 ubiquitin ligase known to activate TAK1 and NF-κB downstream of various receptors including TLRs and IL-1R [177]. Moreover, TRAF6 was shown to be recruited to membrane fragments produced by invading *S. flexneri* [178], which are sensed as DAMPs and induce inflammatory responses. On the other hand, Sanada and colleagues showed that TRAF6 activation in *S. flexneri* infected cells was suppressed by the effector protein OspI leading to impaired NF-κB activation [140]. We found that TRAF6 was essential for IL-8 expression during *S. flexneri* infection in HeLa cells. In HEK cells over-expressing NOD1 we could not observe this strong impact of TRAF6 depletion on NF-κB activation and IL-8 expression during infection. This might be due to the over expression of NOD1 in this cell line, leading to RIPK2 dependent activation of NF-κB and subsequent IL-8 production. Since the NOD1 mRNA level in HeLa cells is comparable to the one of freshly isolated human colon epithelial cells [139], data gained in HeLa cells might better reflect the role of TRAF6 signaling during *S. flexneri* infection. Finally, our detailed analysis of TRAF6 signaling in infected HeLa cells revealed that signals required to trigger bystander IL-8 expression are generated independently of TRAF6, which is not surprising when considering the fact that TRAF6 activation is inhibited by *S. flexneri* in infected cells.

TIFA another candidate protein found in the genome wide RNAi screen was as well found to be essential for bystander IL-8 expression during *S. flexneri* infection. So far, TIFA was desribed as a TRAF6 interacting protein [179]. TIFA was shown to mediate NF-κB and JNK activation, most likely by linking TRAF6 to IRAK1 in the IL-1 signaling pathway. In *in vitro* reconstitution experiments TIFA was found to induce the oligomerization and ubiquitination of TRAF6 resulting in the activation of the TAK1 and

IKK protein complexes [180]. As for TRAF6 we found that TIFA was not required in infected cells to trigger signals underlying bystander activation.

As the signals, that trigger bystander activation, are apparently produced independently of the signaling pathways tested, we addressed the question whether *S. flexneri* uptake into epithelial cells was required for the induction of bystander IL-8 expression or whether already the insertion of the T3SS needle and injection of effector proteins was sufficient to induce a proinflammatory response. For this purpose HeLa cells were treated with cytochalasin D, an inhibitor of actin polymerization thereby preventing the dynamic cytoskeletal rearrangements that are necessary for *S. flexneri* invasion into epithelial cells. The IL-8 response of treated cells compared to the IL-8 response of untreated control cells was completely abolished, indicating that *S. flexneri* uptake into epithelial cells is essential for the induction of a proinflammatory response (data not shown), which raises the question whether actin cytoskeletal rearrangements or phagosomal membrane remnants, that act as signaling platforms, might be required to trigger bystander IL-8 expression.

1.2   Signaling in bystander cells

In this work, signaling events taking place in bystander cells of *S. flexneri* infected epithelial cells were investigated, in order to determine the signaling network that mediates the proinflammatory response. Our detailed analysis of signaling events taking place in bystander cells of *S. flexneri* infection indicated, to our surprise, that NOD1 and RIPK2 contribute to IL-8 expression exclusively in bystander cells. This was unexpected and raises the question how the classical NOD1-RIPK2 pathway is activated in bystander cells. The most obvious hypothesis would be that NOD1 ligands diffuse from infected to bystander cells and trigger the NOD1 pathway. An alternative hypothesis could be that NOD1 detects the activation of small RHO GTPases. It was shown that constitutively active RHO GTPases such as RAC1, CDC42 and RHOA were sufficient to activate the NOD1-RIPK2 signaling pathway [119]. During *S. flexneri* infection activated ARGEF2, a known activator of RHOA, has been found to potentiate NOD1 signaling in infected cells, and the authors of this report observed an increased ARGEF2 expression in the cytoplasm of uninfected neighboring cells [120], pointing to the possibility that RHOA gets activated in bystander cells and activates the NOD1 signaling pathway. Preliminary data suggest that RHOA indeed could be activated in bystander cells, because inhibition of the RHOA downstream target RHOA kinase (ROCK) in bystander cells of *S. flexneri* infected cells, resulted in an abolished IL-8

response. We also tested whether ERK1/2 could be involved in ARHGEF2 activation in bystander cells. ERK1/2 is activated in bystander cells of *S. flexneri* infection and recently, ERK1/2 was shown to activate the guanine exchange factor ARHGEF2 thereby mediating RHOA activation [181]. siRNA mediated depletion of ERK1/2 did not result in a decreased number of IL-8 producing bystander cells/infection site (data not shown). Since cells depleted for ERK1/2 and stimulated with PMA, an activator of the ERK pathway, showed a reduction of IL-8 positive cells of 82% (± 2%) compared to control cells, we assumed that siRNA mediated depletion of ERK1/2 worked in this experiment. In addition, the impact of MEK1/2 inhibition on IL-8 production in bystander cells of *S. flexneri* infection was tested. MEK1/2 are the MAP2 kinases that activate ERK1/2. A slightly reduced IL-8 response was observed, when MEK1/2 was inhibited (data not shown). As ERK1/2 is - together with p38 - also involved in histone H3 phosphorylation, the effect observed might not be attributed to a triggering of NOD1 signaling in bystander cells.

The newly identified proteins, TIFA and TRAF6 were as well found to be exclusively required in bystander cells for the production of IL-8. To put them into a signaling network we monitored TAK1 phosphorylation in bystander cells. It turned out that TAK1 indeed is activated in bystander cells. Moreover, analysis of TAK1 phosphorylation in TIFA or TRAF6 depleted cells revealed that TAK1 activation was strongly TIFA and completely TRAF6 dependent, indicating that TIFA and TRAF6 are upstream of TAK1 and contribute together with NOD1-RIPK2 signaling to TAK1 activation.

Further analysis of the signaling network in bystander cells by stimulation of TRAF6 depleted HEK NOD1 over expressing cells with the NOD1 ligand, revealed that NOD1 signaling to NF-κB in bystander cells was partially TRAF6 dependent, linking TRAF6 to the NOD1 signaling pathway in bystander cells of *S. flexneri* infection. This observation is in line with data gained in human periodontal ligament fibroblasts (HPDLFs). HPDLFs belong to the peridontal ligament, a tissue that is located at the root end of a tooth. Besides connecting the root with the alveolar bone, these cells upon encountering bacteria produce several pro-inflammatory cytokines, such as IL-1β, IL-6, and IL-8. iE-DAP stimulation of HPDLFs depleted for TRAF6 by means of RNA interference, resulted in an impaired IL-1β, IL-6, and IL-8 response, indicating as well that NOD1 signaling involves TRAF6 activity [182]. The TRAF6 interacting protein TIFA was also found to contribute to NOD1 signaling in bystander cells of *S. flexneri* infected cells, but to a lesser extent than TRAF6, suggesting that signals activating the NOD1 independent pathway lead to TIFA dependent TRAF6 activation, which in turn

potentiates NOD1 signaling. Finally, because TAK1 depleted cells are no longer able to respond to *S. flexneri* infection or to iE-DAP stimulation, signals apparently converge on TAK1 in bystander cells.

Recently, Huang and colleagues unraveled the molecular mechanism of the TIFA dependent activation of TRAF6 upon TNFα stimulation. They identified a threonine phosphorylation site (T9) on TIFA that, when phosphorylated, is recognized by the TIFA FHA domain [171]. This interaction provokes the self oligomerization of TIFA leading to TRAF6 recruitment and activation and subsequent activation of NF-κB. We tested whether during *S. flexneri* TIFA phosphorylation at T9 was required for signaling events that lead to IL-8 expression in bystander cells and found that it was indeed the case (C.A. Kasper unpublished data). TIFA has so far been linked to signaling pathways including IL-1R, TNFR and TLR signaling [171, 179, 183]. We show for the first time, that TIFA contributes to NOD1 signaling in bystander cells of *S. flexneri* infection and that TIFA phosphorylation is required for the activation of NF-κB.

1.3 Signaling molecules

In our previous study we showed that cell-cell communication during *S.flexneri* infection is not mediated by secretion of signaling molecules, but is strictly dependent on cell-cell contact and mediated via gap junctions. Gap junctions are channels formed between adjacent cells. Only small and hydrophilic molecules (< 1- 2 kDa) are able to diffuse through these channels from cell to cell. The finding that NOD1 signaling was exclusively required in bystander cells for IL-8 expression was surprising and implicates hat the NOD1 ligand itself might be one of the signaling molecules that induce bystander IL-8 expression. The NOD1 minimal ligand iE-DAP is a dipeptide small enough to diffuse via gap junctions. Dividing bacteria cleave their peptidoglycan chains into smaller monomers or fragments of peptidoglycan. It is estimated that gram-negative bacteria recycle only 30 – 60% of this peptidoglycan, indicating that during replication considerable amounts of peptidoglycan are constantly released into the cytosol of host cells [184]. Moreover, analysis of the culture supernatant of *Escherichia coli* K12 strains (which share more than 98% sequence identity with *S. flexneri*) revealed that these bacteria released various NOD1-activating peptidoglycan moieties [185] amongst which many are small enough to diffuse via gap junctions. In our previous study, bystander activation turned out to be a general mechanism observed in response to other enteropathogens such as *S. enterica* ser. Typhimurium and *Listeria monocytogenes*. Even though *L. monocytogenes* is a gram-positive pathogen its

peptidoglycan contains iE-DAP and was shown to activate NOD1 [90, 186]. Taken together these observations support the idea that diffusion of the NOD1 ligand iE-DAP, which is released by all kind of pathogens that possess iE-DAP in their peptidoglycan, might well be one of the signals that trigger bystander IL-8 expression during bacterial infection.

Interestingly, we observed that *S. flexneri* infected cells depleted for NOD1 were still able to produce IL-8, indicating that a NOD1 independent signaling pathway contributes to the induction of the inflammatory response elicited by host cells. In search for such a pathway, we decided to investigate whether calcium signaling contributed to bystander IL-8 expression for several reasons: First, invading *S. flexneri* induce intercellular calcium signaling that include IP_3 dependent calcium release from internal stores [173]. Second, calcium and IP_3 are two second messengers that are able to diffuse through gap junctions. Third, in the field of cell physiology, it is suggested that IP_3-induced intercellular calcium signaling mediated via gap junctions may represent a general mechanism by which cells do communicate over short distances to coordinate their activity in physiological and in pathological conditions [158]. And finally, the fact that an IL-8 response in epithelial cells induced by the NOD1 ligand iE-DAP could be potentiated when calcium signaling was triggered, further supported this idea. Our studies confirmed a role for intercellular calcium signaling and for IP_3 in the process of bystander IL-8 expression. Interestingly, inhibition of intercellular calcium signaling with the calcium chelator BABTA-AM or the inhibition of the IP_3 receptor with 2-APB, exclusively led to a reduced IL-8 response in bystander cells but did not affect NF-κB activation indicating that calcium signaling might trigger MAP kinase signaling downstream of TAK1, thereby mediating histone phosphorylation and consequently DNA accessibility for transcription factors required for proper gene expression. Moreover our preliminary data, suggest that PLCγ1 might be responsible for the production of IP_3 during *Shigella* infection. Inhibition of this enzyme did again not affect NF-κB activation but the IL-8 response in bystander cells was significantly reduced. Strikingly, ATP1A1 depleted HeLa cells infected with *S. flexneri*, showed a similar pattern i.e. NF-κB activation not affected combined with a reduced, yet abolished IL-8 response. The Na^+/K^+-ATPase is a sodium pump located at plasma membranes. However, it was found to act not only as a pump for ions across the plasma membrane but also as signal transducing receptor for cardiotonic steroids such as ouabain [187]. Activation of the signaling function of ATP1A1 resulted in tyrosin phosphorylation of multiple proteins including SRC and EGFR. Furthermore, in co-immunoprecipitation

experiments ATP1A1 was shown to bind to PLCγ1 and to the IP3 receptor leading to calcium release from internal stores [188]. Further investigation is required to establish the novel role for ATP1A1 in calcium signaling that contributes to a proinflammatory response during bacterial infection.

In our previous study, bystander activation turned out to be a general mechanism observed in response to other enteropathogens such as *S. enterica* ser. Typhimurium and *Listeria monocytogenes.* In a parallel work to ours, bystander activation during *L. monocytogenes* has been studied in an infection model using murine mIC_{12} cells (small intestinal epithelial cells) [163]. Detection of *L. monocytogenes* was NOD2 dependent. Cell-cell propagation of proinflammatory signals was gap junction independent, instead it required the production of ROI by the NADPH oxidase NOX4. ROI was detected in bystander cells and inhibition of ROI production resulted in abolished bystander CXCL2 and CXCL5 production. The differences in the mechanisms identified might origin from the different cell lines and the different pathogens used as model systems. However, the observed differences in the mechanisms of bystander activation between *Shigella* and *Listeria* could as well indicate that there exist diverse host signaling pathways that upon activation mediate bystander activation.

A mechanism of cell-cell communication based on the diffusion of peptidoglycan moieties and IP_3 molecules via gap junctions could very well explain the observations made during bacterial infection of epithelial cells. Dividing bacteria produce iE-DAP, which diffuses to bystander cells and induces the inflammatory response. IP_3 induced intercellular calcium signaling contribute to the porinflammatory response. Infected cells by sensing the bacteria as a stress close their gap junctions thereby terminating cell-cell communication. DAP is no longer released from infected cells and by diffusing dilutes out until at some point the critical concentration required for NOD1 activation is below the limits. IP_3 has a short half live and thereby its activity is limited. Thus, a defined group of healthy neighboring cells gets signals from a single infected cell and allows the host to induce an effective inflammation response resulting in the clearance of infection. Further investigation is required to completely elucidate the mechanism of bystander activation (Figure IV.1).

Taken together, we have shown that signals underlying cell-cell communication during *S. flexneri* infection are generated independently of the NOD1 signaling pathway and of the newly identified candidate proteins for bystander activation, TIFA and TRAF6. Our detailed analysis of signaling events taking place in bystander cells of *S. flexneri* infection indicate that the NOD1 signaling pathway and a NOD1 independent pathway contribute to the induction of proinflammatory gene expression. The newly identified signaling proteins TIFA and TRAF6 could be assigned to the NOD1 independent pathway and were in addition found to contribute to NOD1 signaling upstream of TAK1 activation. Furthermore, there is evidence that intercellular calcium signaling induced by invasive *S. flexneri* contribute to the propagation and amplification of the proinflammatory response observed during *S. flexneri* infection.
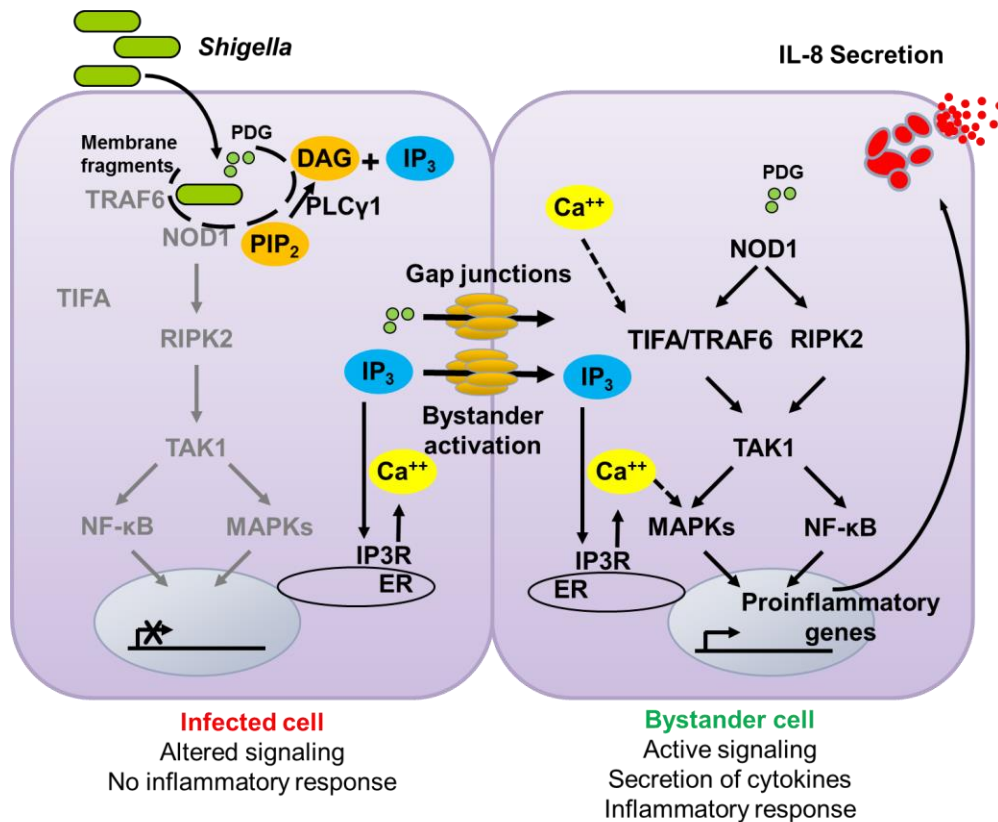
Figure IV.1 Proposed model of Bystander activation. Intracellular *S. flexneri* release PDG moieties by replicating in the cytosol. PDG might diffuse to bystander cells and activate the NOD1 signaling pathway resulting in the expression of proinflammatory genes. In addition, at vacuolar membrane remnants, produced by invading *S. flexneri*, inter cellular calcium signaling is triggered, that contributes to proinflammatory gene expression in bystander cells, eventually by activating TIFA that signals via TRAF6 to TAK1. (DAG, diacylglycerol; ER, endoplasmatic reticulum; IP$_3$, inositol triphosphate; IP3R, IP$_3$ receptor; MAPKs, MAP kinases; PDG, peptidoglycan; PIP$_2$, phosphatidylinositol 4,5-bisphosphate; PLCγ1, phospholipase Cγ1)

2 Outlook

2.1 Identification of the signaling molecules required for bystander activation

We identified a NOD1-dependent and a NOD1-independent signaling pathway in bystander cells that control the expression of proinflammatory genes during *S. flexneri* infection. The NOD1-dependent pathway in bystander cells most likely gets activated by peptidoglycan derived from replicating bacteria representing signal 1, whereas intercellular calcium signaling could be the second signal that might trigger the NOD1-independent pathway in bystander cells. To test this hypothesis, control cells and cells depleted for NOD1 should be left untreated or treated with a calcium inhibitor and then infected with *Shigella*, subsequently the activation of NF-κB and the production of IL-8 should be monitored by immunofluorescence microscopy. In case that calcium signaling and stimulation of the NOD pathway together are responsible for bystander IL-8 expression, inhibitor treated cells depleted for NOD1 would not be able to activate NF-κB and subsequently no IL-8 could be detected.

Next, it should be investigated, whether peptidoglycan moieties derived from replicating bacteria indeed are able to diffuse via gap junctions to neighboring cells. By microinjecting fluorescently labeled iE-DAP, in presence or absence of the gap junction inhibitor 18β-GA, the diffusion of the NOD1 ligand from cell to cell, could be monitored by fluorescence microscopy.

If this is the case, the next question would be, whether the amount of diffusible NOD1 ligands, released by replicating bacteria, is sufficient to trigger NOD1 signaling in bystander cells. To test this hypothesis, A431 connexin43 overexpressing cells, which allow optimal diffusion via gap junctions, should be infected with wild-type *Shigella* and *Shigella* Δ*mppA*, a mutant strain, which is impaired in peptidoglycan recycling [189], and the areas covered with IL-8 around infected cells should be monitored by immunofluorescence microscopy. If peptidoglycan is signal 1, which diffuses to bystander cells to activate the NOD1-dependent pathway, the mutant strain releasing bigger amounts of peptidoglycan, should cause significantly bigger areas covered with IL-8 compared to wild-type *Shigella*.

2.2 Is NOD1 a sensor for PAMPs and/or DAMPs in bystander cells?

The NOD1 pathway gets activated by sensing of the PAMP iE-DAP and by sensing of DAMPs, such as activated RHO GTPases, including RHOA, CDC42 and RAC1 [119]. Experiments on iE-DAP diffusion will be one part of the answer how NOD1 might get activated in bystander cells. Furthermore, the use of NOD1 mutants, that harbor point mutations in the LRR domain, which have been shown to drastically impair iE-DAP dependent NOD1 activation [190], might provide a tool to discriminate between iE-DAP dependent NOD1 activation and/or DAMP dependent activation of NOD1, given that NOD1 acts as scaffolding protein in the latter case, and a functional LRR domain is not required for DAMP dependent activation of NOD1. Cells, overexpressing NOD1 mutants impaired in iE-DAP sensing, should be infected with *Shigella* and NF-κB activation and IL-8 production in bystander cells should be monitored by immunofluorescence microscopy. An impaired inflammation response could then point to iE-DAP diffusion dependent NOD1 activation in bystander cells.

It could as well be that NOD1 acts as a DAMP sensor in bystander cells. One possible DAMP, which might be present in bystander cells of *S. flexneri* infected cells, is RHOA, because we observed that inhibition of the RHOA downstream target ROCK in bystander cells abolishes IL-8 expression. By means of a pull down assay for activated RHOA it should be tested, whether RHOA is activated in bystander cells. If this is the case, by inhibiting RHOA with pharmacological tools or by RNAi mediated depletion, its possible impact on NF-κB activation and IL-8 production in bystander cells should be evaluated by immunofluorescence microscopy.

2.3 What is upstream of TIFA in bystander cells?

The observation that TIFA phosphorylation of threonine 9 is required during *S. flexneri* infection implies that a serine/threonine kinase is upstream of TIFA. In co-immunoprecipitation experiments AKT and aurora kinase were identified as candidate proteins for TIFA phosphorylation upon TNFα stimulation (Huang, unpublished data) and in *in vitro* kinase assays TIFA phosphorylation was PKC inhibitor sensitive [171]. Since we could show, that AKT is exclusively activated in infected cells, AKT cannot be the kinase phosphorylating TIFA in bystander cells. Furthermore, no reduction in bystander IL-8 expression of *S. flexneri* infected HeLa cells depleted for aurora kinase was observed (C.A. Kasper unpublished data). In contrast, PKC might be a promising

candidate protein for TIFA activation in bystander cells, because PKC is activated downstream of calcium signaling [191]. In addition, this would link calcium to the NOD1-independent signaling pathway in bystander cells. Therefore, the effect of PKC inhibitors as well as siRNA mediated depletion of PKC on NF-κB activation and on bystander IL-8 expression during *S. flexneri* infection should be tested.

2.4   What is the role of ATP1A1 (Na$^+$/K$^+$-ATPase)?

To further characterize the role of ATP1A1 in the process of bystander activation, first a possible general defect in protein synthesis should be excluded by monitoring of IL-8 mRNA in *Shigella* infected HeLa cells depleted for ATP1A1. If also IL-8 mRNA is reduced, the requirement of ATP1A1 in infected and/or in bystander cells should be tested in a mixed cell population assay. Furthermore, by means of live cell imaging one could test, whether in ATP1A1 depleted cells intercellular calcium signaling is blocked. Moreover, ATP1A1 has been found to function as scaffolding protein, bringing PLCγ1 and the IP$_3$ receptor together to form a signaling complex [188]. The *N*-terminal tail of the catalytic α-subunit (αNT-t) of ATP1A1 was found to mediate this interaction, which results in calcium dependent NF-κB activation [192]. To study, whether this interaction is required during *Shigella* infection, small peptides corresponding to αNT-t could be overexpressed that are known to interfere with the interaction between ATP1A1 and the IP$_3$ receptor, and subsequently abolish calcium dependent NF-κB activation [192]. If ATP1A1 acts as a scaffolding protein during *Shigella* infection, one can expect that NF-κB activation would not be affected but the IL-8 response would be abolished.

2.5   What is the role of ROCK during *S. flexneri* infection?

During *Shigella* infection ROCK activation was associated with NF-κB phosphorylation and activation in infected cells [120]. As mentioned before, we observed an abolished IL-8 response upon inhibition of ROCK with Y-27632 in bystander cells of *S. flexneri* infected cells (data not shown). By depletion of ROCK by RNAi and performing of mixed cell population assays the role of ROCK activation in infected and in bystander cells could be addressed in more detail.

2.6 What is the contribution of the NOD1-dependent and the NOD1–independent pathway in bystander cells in controlling gene expression?

To further characterize the complex signaling events taking place in bystander cells during S. *flexneri* infection, it will be of interest to dissect the contribution of the NOD1-dependent and the NOD1-independent signaling pathways to the expression of proinflammatory genes. Proteins of interest can either be depleted by RNAi or inhibited by pharmacological tools. Cells will be infected with *Shigella* or selectively stimulated with the NOD1 ligand or with calcium (ionomycin). Then the activation of TAK1, NF-κB, p38, JNK and ERK will be monitored by immunoblotting. The signaling patterns of each protein, should then allow assigning them to the different signaling pathways.

V   Appendix

1 Statement of contribution

I contributed the in situ hybridization, Fig. 4B; infections in Tnfr-/- MEF, Fig. 6A and S6A/B; TNFα and GM-CSF in bystander cells, Fig. S4E-G.

Cell-Cell Propagation of NF-κB Transcription Factor and MAP Kinase Activation Amplifies Innate Immunity against Bacterial Infection

Christoph Alexander Kasper,[1] Isabel Sorg,[1] Christoph Schmutz,[1] Therese Tschon,[1] Harry Wischnewski,[1] Man Lyang Kim,[1] and Cécile Arrieumerlou[1,*]
[1]Biozentrum, University of Basel, Klingelbergstrasse 50-70, CH-4056, Basel, Switzerland
*Correspondence: cecile.arrieumerlou@unibas.ch
DOI 10.1016/j.immuni.2010.10.015

SUMMARY

The enteroinvasive bacterium *Shigella flexneri* uses multiple secreted effector proteins to downregulate interleukin-8 (IL-8) expression in infected epithelial cells. Yet, massive IL-8 secretion is observed in Shigellosis. Here we report a host mechanism of cell-cell communication that circumvents the effector proteins and strongly amplifies IL-8 expression during bacterial infection. By monitoring proinflammatory signals at the single-cell level, we found that the activation of the transcription factor NF-κB and the MAP kinases JNK, ERK, and p38 rapidly propagated from infected to uninfected adjacent cells, leading to IL-8 production by uninfected bystander cells. Bystander IL-8 production was also observed during *Listeria monocytogenes* and *Salmonella typhimurium* infection. This response could be triggered by recognition of peptidoglycan and is mediated by gap junctions. Thus, we have identified a mechanism of cell-cell communication that amplifies innate immunity against bacterial infection by rapidly spreading proinflammatory signals via gap junctions to yet uninfected cells.

INTRODUCTION

The ability of a host organism to mount an innate immune response after pathogen infection is critical for survival. The epithelial cells, which represent the first physical barrier to invasive pathogens, play a critical role in this process. They act as sentinels of the immune system and largely contribute to the secretion of factors that orchestrate inflammation in infected tissues. Infection by *Shigella* bacteria is a well-suited model to analyze the complex host-pathogen interactions that shape the immune response of intestinal epithelial cells (IECs) to invasive bacteria (Phalipon and Sansonetti, 2007). *Shigella* are Gram-negative foodborne bacteria that invade the colonic and rectal epithelium of humans, causing an acute mucosal inflammation called Shigellosis, responsible for 1.1 million deaths annually (Schroeder and Hilbi, 2008).

Shigella flexneri, the etiological agent of the most endemic form of Shigellosis, translocates across the intestinal epithelial barrier by transcytosis through M cells. In the submucosal area, *S. flexneri* makes use of a type III secretion (T3S) apparatus to trigger apoptosis in macrophages and to actively invade IECs via their basolateral surface. The T3S apparatus is a syringe-like nanomachine enabling the translocation of bacterial effector proteins (Cornelis, 2006) that subvert various host cellular pathways in order to promote bacterial entry, modulate cell cycle, and dampen inflammation signaling (Iwai et al., 2007; Parsot, 2009; Phalipon and Sansonetti, 2007). Once internalized, *S. flexneri* multiplies in the cytoplasm and uses actin-based motility to spread to adjacent IECs. During infection, massive mucosal inflammation is observed in the intestine of infected patients (Islam et al., 1997). IECs are critical in this process. They sense pathogenic invasion and respond by inducing a transcriptional program whose major function is to stimulate innate immune defense mechanisms. *Shigella* recognition by IECs occurs essentially intracellularly via the pattern recognition receptor Nod1 that recognizes the core dipeptide structure, γ-D-glutamyl-meso-diaminopimelic acid (Girardin et al., 2003), found in the peptidoglycan of all Gram-negative and certain Gram-positive bacteria (Kufer et al., 2006). Upon ligand recognition, Nod1 homodimerizes and recruits the kinase RIPK2 (Strober et al., 2006). This leads to the sequential recruitment and activation of the TAK1-TAB1-TAB2 and IKKα-IKKβ-IKKγ complexes and the phosphorylation of inhibitor of NF-κB alpha (IκBα). Once phosphorylated, IκBα undergoes polyubiquitination and proteasomal degradation. NF-κB, released from IκBα, translocates to the nucleus and upregulates expression of proinflammatory genes. TAK1 activation also leads to activation of the MAP kinases c-Jun-N-terminal kinase (JNK) and p38 (Lee et al., 2000; Ninomiya-Tsuji et al., 1999; Wang et al., 2001). The MAP kinase ERK is also activated during *S. flexneri* infection of IECs (Köhler et al., 2002). NF-κB, JNK, ERK, and p38 contribute collectively to the initiation of a proinflammatory program. JNK and p38 regulate the activity of the transcription factor AP-1 (Holtmann et al., 1999). p38 and ERK control the access of chromatin to transcription factors via phosphorylation of histone H3 by the kinases MSK1 and MSK2 (Saccani et al., 2002). Among the genes upregulated during infection of IECs, the chemokine interleukin-8 (IL-8) plays a central role (Sansonetti et al., 1999) by attracting polymorphonuclear cells (PMNs) from the peripheral circulation to the infected area to limit the spread of *S. flexneri* invasion.

Appendix

S. flexneri uses multiple strategies to downregulate inflammation. For example, T3 secreted effector proteins OspG and OspF attenuate IL-8 expression by preventing IκBα degradation and dephosphorylating nuclear p38 and ERK, respectively (Arbibe et al., 2007; Kim et al., 2005; Li et al., 2007).

Despite the immunosuppressive activity of multiple bacterial effector proteins, massive IL-8 expression is observed in IECs during Shigellosis, suggesting that the secreted molecules may partially block IL-8 expression or that a host mechanism compensates for their effect. Here, we report the discovery of a host cell-cell communication mechanism that circumvents the bacterial effector proteins and amplifies IL-8 expression. By monitoring proinflammatory signals at the single-cell level, we found that, within minutes of infection, the activation of NF-κB and the MAP kinases JNK, ERK, and p38, propagates from infected to uninfected bystander cells. These cells, in which signaling is not altered by bacterial effector proteins, represent the main source of IL-8 secretion during *S. flexneri* infection. Bystander IL-8 expression can be triggered by recognition of peptidoglycan via Nod1 and is mediated by gap junctions. Thus, we have identified a gap junction-mediated cell-cell communication mechanism that strongly amplifies innate immunity during bacterial infection by rapidly spreading proinflammatory signals to yet-uninfected cells.

RESULTS

NF-κB Is Activated in Bystander Cells of *S. flexneri* Infection

To better characterize the molecular mechanisms that control inflammation during bacterial infection, we analyzed NF-κB activation at the single-cell level during *S. flexneri* infection of epithelial cells. The nuclear translocation of the NF-κB p65 subunit, which follows IKK-mediated IκBα degradation, was used as readout for NF-κB activation and was visualized by immunofluorescence microscopy. HeLa cells were infected with noninvasive BS176 or wild-type invasive M90T *S. flexneri* strains at low and high multiplicity of infection (MOI). As expected, extracellular bacteria failed to activate NF-κB in HeLa cells as shown by the fact that p65 remained exclusively cytosolic after infection with BS176 *S. flexneri* (Figure 1A, top left). In contrast, cells infected with M90T at MOI 20 showed massive nuclear localization of p65, reflecting the detection of intracellular bacteria and activation of NF-κB (Figure 1A, top right). Surprisingly, when cells were challenged with M90T at low MOI, a strong p65 nuclear translocation was also observed in some cells that were not infected (Figure 1A, bottom left). Single-cell measurements of *S. flexneri* invasion and p65 nuclear/cytoplasmic ratio (NF-κB activation ratio) confirmed that, at low MOI, more cells were NF-κB activated than infected (Figure 1A, bottom right). False color representations of the NF-κB activation ratio clearly showed that uninfected NF-κB-activated cells were not randomly distributed in the field of view but located in close proximity with infected cells forming NF-κB activation foci around them (Figure 1B). A similar pattern of NF-κB activation was observed during *S. flexneri* infection of the colonic epithelial cell line Caco-2, the lung epithelial cell line A549, and the human umbilical vein endothelial cells (HUVECs) derived from umbilical cord (Figure S1 available

online), suggesting that bystander activation of NF-κB represents a broad response to *S. flexneri* infection.

During infection, *S. flexneri* uses actin-based motility to spread to adjacent IECs. To control that bystander NF-κB activation was not due to bacterial intercellular motility, we examined NF-κB activation in cells infected with the nonmotile *virG* deletion mutant (ΔvirG) (Makino et al., 1986). As expected, ΔvirG bacteria efficiently invaded HeLa cells (Figure 1C, right). However, unlike wild-type (Figure 1C, left), they failed to form actin comet tails and accumulated overtime in the perinuclear region (Figure 1C, right). Interestingly, infection with the ΔvirG mutant induced p65 nuclear translocation in infected and in bystander cells (Figure 1D) similarly to infection with wild-type *S. flexneri* (Figure 1A), suggesting that bystander NF-κB activation was not caused by intercellular motility, but reflected instead a novel host response to bacterial infection. Because the intracellular microcolonies formed by the ΔvirG mutant were easily detected by automated image analysis, this mutant was used hereafter in our studies.

In order to further characterize bystander NF-κB activation, we analyzed its kinetic during *S. flexneri* infection in HeLa cells. Representative examples of bystander activation at different time points were chosen for illustration (Figure 1E). Within 15 min of infection, NF-κB was almost exclusively activated in infected cells. Then, at 30 min and up to 120 min, NF-κB activation was observed in infected and bystander cells, suggesting that the signals underlying bystander NF-κB activation were generated very early during infection (within 30 min) and propagated from infected to bystander cells. Considering that each infected cell was surrounded by approximately 2–6 NF-κB-activated cells, our results demonstrate that this mechanism of cell-cell communication strongly amplifies the total NF-κB response to *S. flexneri* infection.

JNK and ERK Are Also Activated in Bystander Cells of *S. flexneri* Infection

The activation of the JNK signaling pathway is required to mount an inflammatory response, and in particular, to induce IL-8 expression. We therefore tested, whether in addition to NF-κB, the JNK pathway was also activated in bystander cells of *S. flexneri* infection in HeLa and Caco-2 cells. JNK activation was analyzed by immunofluorescence microscopy via a phospho-specific antibody that detects p46 and p54 JNKs phosphorylated at residues threonine 183 and tyrosine 185 (p-JNK). Cytosolic p65 localization and basal p-JNK staining indicated that both pathways were inactive in control cells (Figure 2A). As expected, a clear nuclear translocation of p65 and a significant increase of p-JNK were observed in *S. flexneri*-infected cells. Interestingly, bystander cells of infection also showed an increase of p-JNK, indicating that the JNK pathway was turned on in these cells as well (Figure 2A and Figure S2A). This observation was confirmed by measuring with automated image processing the degree of nuclear p-JNK in control, infected, and bystander cell populations (Figure 2B, see Supplemental Experimental Procedures).

In addition to JNK, the activation of ERK was analyzed by immunofluorescence microscopy by means of an antibody that recognizes p22 and p44 ERKs phosphorylated at residues threonine 202 and tyrosine 204 (p-ERK). Representative images of NF-κB and p-ERK at different time points were chosen for

88
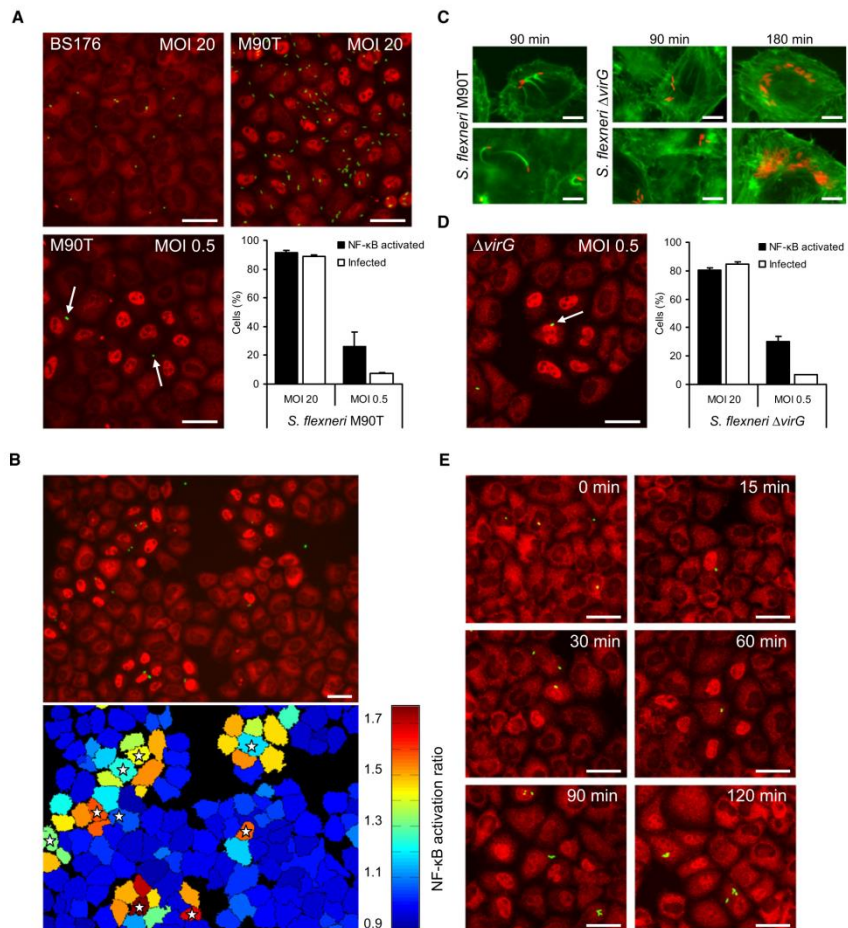
Figure 1. NF-κB Is Activated in Bystander Cells of *S. flexneri* Infection

(A) Nuclear localization of NF-κB p65 during *S. flexneri* infection. HeLa cells were infected for 1 hr with BS176 (MOI = 20, top left) and M90T (MOI = 20, top right; MOI = 0.5, bottom left), stained with a p65 antibody, and visualized by fluorescence microscopy (p65 in red, *S. flexneri* in green). Arrows indicate *S. flexneri*. Percent of NF-κB activated and infected cells at high and low MOI (bottom right, means ± SD of triplicate wells, graph representative of two independent experiments). Scale bars represent 40 μm.

(B) False color representation of NF-κB activation ratio during *S. flexneri* M90T infection of HeLa cells. Stars indicate infected cells. Scale bar represents 40 μm.

(C) Actin-based motility of *S. flexneri* M90T (left) and Δ*virG* mutant (right). After infection, cells were stained for F-actin with phalloidin (F-actin in green, *S. flexneri* in red). Scale bars represent 10 μm.

(D) Bystander NF-κB activation during infection with *S. flexneri* Δ*virG* (left). p65 in red, *S. flexneri* in green. Arrow indicates *S. flexneri*. Percent of NF-κB activated and infected cells at high and low MOI (right, means ± SD of triplicate wells, graph representative of two independent experiments). Scale bar represents 40 μm.

(E) Time course of p65 translocation during infection with *S. flexneri* Δ*virG*. Representative images were selected for illustration. Scale bars represent 40 μm.

Figure 2. JNK and ERK Are Activated in Bystander Cells of *S. flexneri* Infection

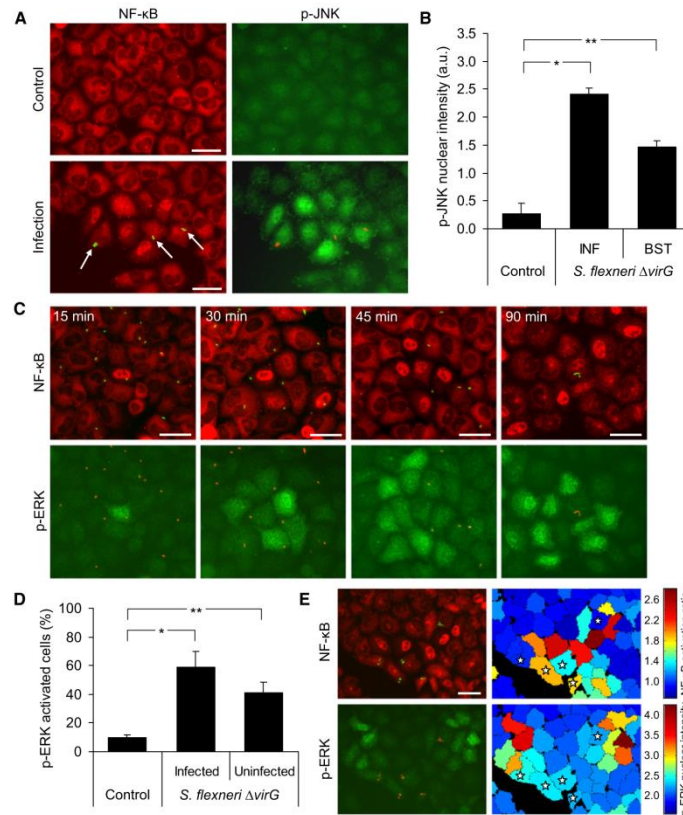(A) Analysis of JNK and NF-κB activation by immunofluorescence microscopy. HeLa cells were left untreated or infected with *S. flexneri* ΔvirG at MOI = 0.5 for 90 min and costained with p65 and p-JNK antibodies. Arrows indicate *S. flexneri*. Scale bars represent 40 μm.

(B) Quantification of nuclear p-JNK intensity in control, infected (INF), and bystander (BST) cell populations by automated image processing (a.u., arbitrary units, means ± SD of triplicate wells, graph representative of five independent experiments, *p = 7.2E-5, **p = 7.6E-4).

(C) Time course of ERK and NF-κB activation during infection with *S. flexneri*. HeLa cells were infected with *S. flexneri* ΔvirG at MOI = 0.5 for indicated time periods and costained with p65 and p-ERK antibodies. Scale bars represent 40 μm.

(D) Percent of ERK-activated cells during *S. flexneri* infection. Cells were infected for 1 hr at MOI = 5. Quantification was performed by automated image processing as described in Supplemental Experimental Procedures (means ± SD of triplicate wells, graph representative of three independent experiments, *p = 1.9E-3, **p = 4.7E-3).

(E) False color representations of NF-κB activation ratio and nuclear p-ERK 1 hr after infection with *S. flexneri* ΔvirG. Stars indicate infected cells. Scale bar represents 40 μm.

illustration (Figure 2C). Within 15 min of infection, ERK activation was observed in only a fraction of infected cells. At 30 min and up to 90 min, ERK was also activated in bystander cells of infection (Figures 2C and 2D and Figure S2B). NF-κB and ERK activation did not strictly correlate at the single-cell level. Indeed, after 45 min of infection, ERK activation was no longer visible in a fraction of infected or proximal bystander cells, suggesting that this pathway was only transiently induced. Furthermore, ERK activation was observed in cells located outside the NF-κB activation foci, suggesting that ERK activation preceded NF-κB activation (Figures 2C and 2E). Altogether, these results suggested that besides the activation of NF-κB, the activation of JNK and ERK also propagates from infected to bystander cells during *S. flexneri* infection of HeLa and Caco-2 cells.
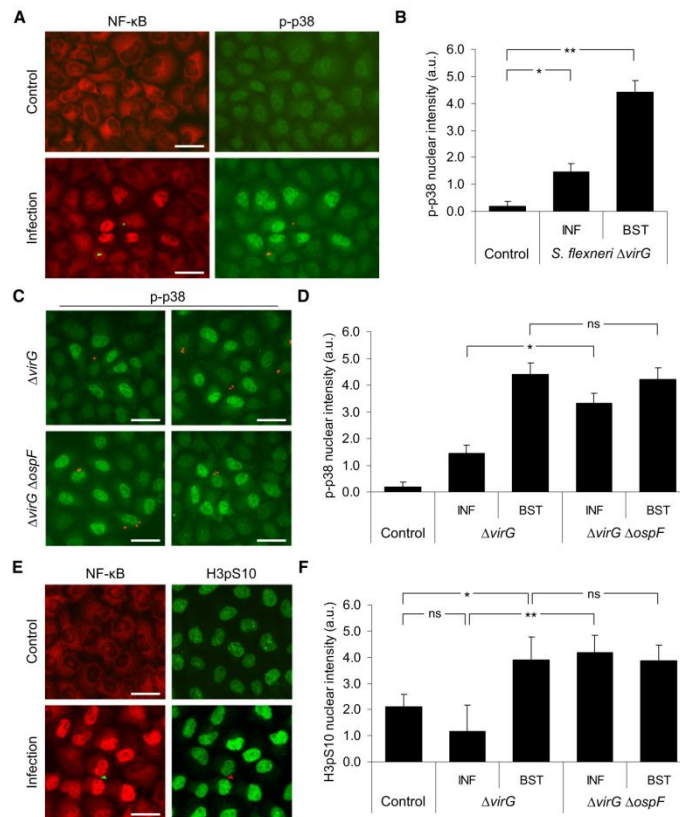
Figure 3. p38 Activation and Histone H3 Phosphorylation Occur Mainly in Bystander Cells

(A) Analysis of p38 and NF-κB activation by immunofluorescence microscopy. HeLa cells were left untreated or infected with *S. flexneri* Δ*virG* at MOI = 0.5 for 90 min and costained with p65 and p-p38 antibodies. Scale bars represent 40 μm.

(B) Quantification of nuclear p-p38 intensity in control, infected (INF), and bystander (BST) cell populations (a.u., arbitrary units, means ± SD of triplicate wells, graph representative of five independent experiments, *p = 4.1E-3, **p = 1.0E-4).

(C) Phosphorylation of p38 in cells infected with Δ*virG* or Δ*virG* Δ*ospF S. flexneri* visualized by immunofluorescence microscopy. Scale bars represent 40 μm.

(D) Quantification of nuclear p-p38 intensity by automated image processing in control, infected, and bystander cell populations during infection with Δ*virG* or Δ*virG* Δ*ospF S. flexneri* (means ± SD of triplicate wells, graph representative of five independent experiments, *p = 4.2E-3).

(E) Analysis of histone H3 phosphorylation by immunofluorescence microscopy. HeLa cells were left untreated or infected with *S. flexneri* Δ*virG* at MOI = 0.5 for 90 min and costained with p65 and H3pS10 antibodies. Scale bars represent 40 μm.

(F) Quantification of nuclear H3pS10 intensity in control, infected, and bystander cell populations (means ± SD of triplicate wells, graph representative of five independent experiments, *p = 4.9E-2, **p = 1.1E-3).

p38 Activation and Histone H3 Phosphorylation Mainly Occur in Bystander Cells of Infection

Because p38 activation is also critical for IL-8 expression, we examined whether p38 was activated in bystander cells of *S. flexneri* infection in HeLa and Caco-2 cells. p38 activation was analyzed by immunofluorescence microscopy by means of an antibody that detects p38 phosphorylated at residues thre-

onine 180 and tyrosine 182 (p-p38). As reported previously (Arbibe et al., 2007), a very modest increase of p38 activation was observed in infected cells (Figures 3A and 3B and Figure S3). In contrast, a strong increase was found in bystander cells of infection indicating that, in addition to NF-κB, JNK, and ERK, p38 was also activated in these cells (Figures 3A and 3B and Figure S3). Signal transduction in infected cells is altered by multiple

effectors that translocate into the host cytoplasm via the T3S apparatus. In particular, p38 is dephosphorylated in the nucleus of infected cells by the phosphothreonine-lyase activity of OspF (Li et al., 2007). Given that bystander cells showed massive p38 activation, we hypothesized that the activation of p38 in bystander cells was not affected by OspF. To test this assumption, HeLa cells were infected with ΔvirG and ΔvirG ΔospF S. flexneri mutants. As previously reported (Arbibe et al., 2007), p38 activation was restored in cells infected with ΔospF bacteria, confirming the role of OspF in p38 dephosphorylation (Figures 3C and 3D). In contrast, the amount of p38 activation in bystander cells remained unchanged (Figure 3D), indicating that OspF failed to impair the ability of the host to spread p38 activation to neighboring cells. Taken together, our data showed that the mechanism of bystander p38 activation circumvents the suppressive activity of OspF in infected cells and amplifies p38 activation during S. flexneri infection.

In addition to its role in AP-1 phosphorylation, p38 controls IL-8 expression by regulating chromatin accessibility to transcription factors such as NF-κB via the phosphorylation of histone H3 by MSK1 and MSK2 (Saccani et al., 2002). To assess whether bystander p38 activation led to histone H3 phosphorylation in bystander cells, phosphorylation at serine 10 (H3pS10) was analyzed by immunofluorescence microscopy via a phospho-specific antibody. To minimize H3pS10 staining from mitotic cells, HeLa cells were arrested in S phase by a double-thymidine block. Consistent with the pattern of p38 activation during S. flexneri infection, H3pS10 was higher in bystander than infected cells (Figures 3E and 3F). Furthermore, the deletion of ospF restored H3pS10 in infected cells but had no effect in bystander cells (Figure 3F). Collectively, these results demonstrate that p38 activation and the subsequent phosphorylation of histone H3, which are both impaired in infected cells because of the activity of OspF, are fully operating in bystander cells of S. flexneri infection.

Cell-Cell Propagation of Proinflammatory Signals Amplifies Cytokine Expression

The NF-κB, JNK, ERK, and p38 signaling pathways were turned on in bystander cells of S. flexneri infection. Given that these pathways control the expression of proinflammatory genes including IL-8, we tested whether bystander cells of S. flexneri infection secreted IL-8. IL-8 secretion was first measured by an enzyme-linked immunosorbent assay (ELISA) in the supernatant of HeLa cells infected by S. flexneri at different MOIs. We observed that the amount of secreted IL-8 decreased as the MOI was raised (Figure 4A). Because low and high MOIs corresponded to low and high infected to bystander cell ratios, respectively (Figure S4A), this result suggested that IL-8 was most probably secreted by bystander cells of infection. This hypothesis was tested by in situ mRNA hybridization to visualize at the single-cell level the amount of IL-8 mRNA produced during S. flexneri infection. As shown in Figure 4B, IL-8 mRNAs were almost exclusively present in bystander cells of infection. To confirm that bystander cells were the main IL-8-producing cells during S. flexneri infection, we performed an intracellular IL-8 immunofluorescence microscopy assay in cells treated with monensin, a protein transport inhibitor that blocks secretion and enables intracellular IL-8 accumulation in the Golgi appa-

ratus (Mollenhauer et al., 1990). In line with the ELISA and the mRNA data, almost no IL-8 was visible in infected cells, but massive intracellular IL-8 accumulation was found in bystander cells (Figures 4C and 4D). An average of 2.8 ± 1.6, 4.2 ± 2.5, 6.5 ± 4.7, and 29.3 ± 13.5 bystander IL-8-producing cells per infected one was measured in HeLa, Caco-2, A549, and HUVEC cells, respectively (Figures S4B–S4D). Interestingly, tumor necrosis factor α (TNF-α) and granulocyte macrophage colony-stimulating factor (GM-CSF), two other inflammatory cytokines upregulated during S. flexneri infection of epithelial cells (Pédron et al., 2003), were also found in bystander cells (Figures S4E–S4G), suggesting that the mechanism of bystander activation contributes to different facets of inflammation during infection.

Strong cytokine expression in bystander cells indicated that cell-cell communication was not affected by S. flexneri effector proteins. This was tested by investigating the effect of OspF on IL-8 expression in infected and bystander cell populations. As previously reported (Arbibe et al., 2007), an increase of IL-8 production was observed in cells infected with ΔospF S. flexneri (Figure 4E). In contrast, the number of bystander cells producing IL-8 was independent of OspF (Figure 4F) indicating that, in line with our p38 activation and H3pS10 results, OspF failed to affect IL-8 expression in bystander cells.

To further characterize the mechanism of bystander activation, we tested whether it also occurred after infection with Listeria monocytogenes or Salmonella typhimurium, two enteroinvasive bacteria that induce IL-8 expression during invasion of IECs (Eckmann et al., 1993). Consistent with data on S. flexneri infection, IL-8 accumulation was also observed in bystander cells of L. monocytogenes and S. typhimurium infection (Figure 4G) but at a lower frequency. In conditions where bystander IL-8 expression was observed for nearly 100% of S. flexneri-infected cells, it occurred for approximately 40% and 70% of Listeria- and Salmonella-infected cells, respectively. In contrast to S. flexneri infection, IL-8 accumulation was also detected in a fraction of cells infected with L. monocytogenes or S. typhimurium (approximately 20% and 40%, respectively), indicating that these bacteria do not manipulate their host to the same extent as S. flexneri, for which low levels of IL-8 were detected in less than 5% of infected cells (Figure 4E). Altogether these results show that cell-cell communication between infected and uninfected bystander cells leads to the potentiation of inflammatory cytokine expression during bacterial infection. They also establish that this is a general host response to invasive bacteria that occurs with an amplitude and a frequency that vary between cell types and pathogens.

Nod1-Mediated Peptidoglycan Sensing Is Sufficient to Induce Bystander IL-8 Expression

During S. flexneri infection, the presence of intracellular bacteria is sensed through peptidoglycan recognition by the intracellular receptor Nod1 (Girardin et al., 2003). To determine whether pathogen sensing via Nod1 was sufficient to induce bystander IL-8 production, we monitored IL-8 accumulation after microinjection of the synthetic Nod1 ligand L-Ala-D-γ-Glu-meso-diaminopimelic acid (TriDAP) into the cytoplasm of A549 cells. An Alexa 488-labeled IgG antibody (IgG A488) was used as fluorescent marker to identify microinjected cells. In response to IgG A488 microinjection, no IL-8 was detected (Figure 5A, left, and
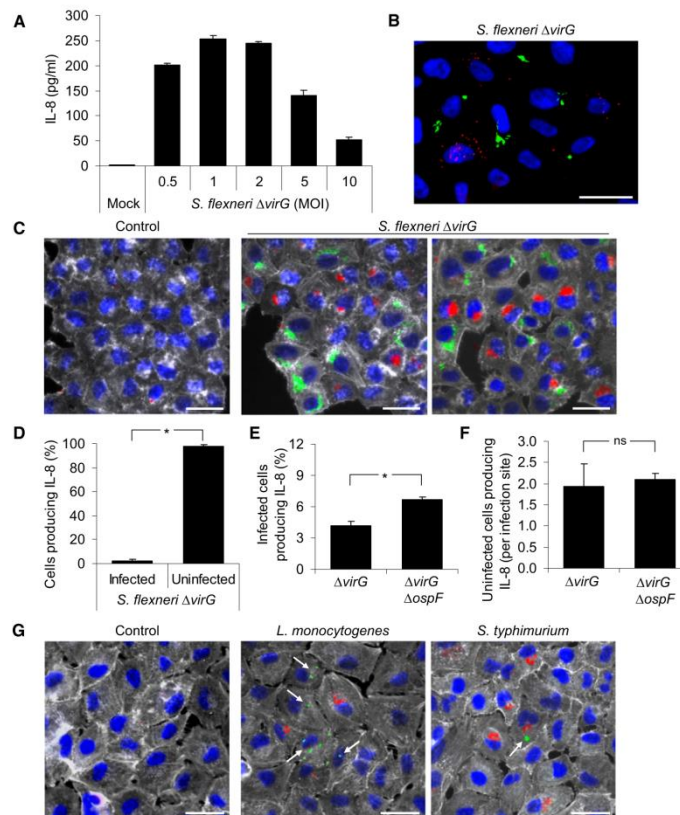
Figure 4. IL-8 Production by Bystander Cells Is a General Response to Bacterial Infection

(A) Measurements of IL-8 secretion by ELISA 6 hr after infection (means ± SD of triplicate wells, graph representative of two independent experiments).

(B) Visualization of IL-8 mRNA 2 hr after infection by in situ hybridization (IL-8 mRNAs in red, *S. flexneri* in green, Hoechst in blue, MOI = 2). Scale bar represents 40 μm.

(C) IL-8 accumulation in bystander cells of infection. IL-8 staining of monensin-treated HeLa cells 3 hr after infection (IL-8 in red, *S. flexneri* in green, Hoechst in blue, F-actin in gray, MOI = 2). Scale bars represent 40 μm.

(D) Percent of infected and uninfected cells among all IL-8-producing cells (MOI = 1). Quantification was performed by automated image processing based on the use of threshold intensity values for bacterial and IL-8 detection (means ± SD of triplicate wells, graph representative of three independent experiments, *p = 3.9E-16).

(E) Percent of infected cells producing IL-8 during infection with Δ*virG* and Δ*virG* Δ*ospF S. flexneri* (MOI = 5). Quantification was performed as described in (D) (means ± SD of triplicate wells, graph representative of two independent experiments, *p = 4.5E-4).

(F) Number of uninfected cells producing IL-8 per site of infection during infection with Δ*virG* and Δ*virG* Δ*ospF S. flexneri* (MOI = 1). Quantification was performed as described in (D) (means ± SD of triplicate wells, graph representative of two independent experiments).

(G) IL-8 production (in red) in bystander cells during *L. monocytogenes* (MOI = 0.25, green) and *S. typhimurium* (MOI = 0.5, green) infection of A549 cells. F-actin in gray, arrows indicate bacteria. Scale bars represent 40 μm.

Figure 5B). In contrast, when TriDAP was combined with IgG A488, both microinjected and bystander cells showed massive intracellular IL-8 accumulation (Figure 5A, right, and Figure 5B). To verify that IL-8 production was not caused by extracellular TriDAP leaking during microinjection, the concentration of TriDAP used in the microcapillary was uniformly applied to the extracellular medium. In contrast to TNF-α, extracellular TriDAP failed to induce IL-8 expression (Figure 5C and Figure S5).
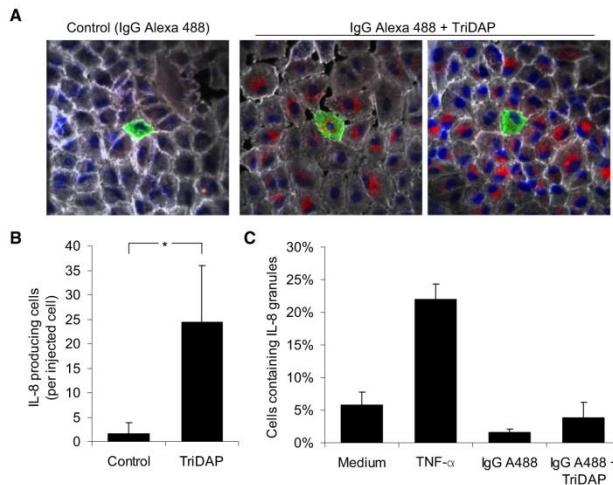
Figure 5. Intracellular Recognition of a Nod1 Ligand Is Sufficient to Induce IL-8 Expression in Bystander Cells

(A) IL-8 accumulation in bystanders of microinjected A549 cells. After injection of IgG Alexa 488 alone (left) or combined with TriDAP (right), cells were stained for IL-8, F-actin, and DNA (IgG A488 in green, IL-8 in red, F-actin in gray, Hoechst in blue).

(B) Number of IL-8-producing cells per injected cell. Quantification was performed by counting all IL-8-expressing cells located in contact with microinjected cells or other bystander cells (control, n = 20; TriDAP, n = 21; *p = 1.0E-9).

(C) Percent of cells containing IL-8 after extracellular treatment with TNF-α, IgG A488 alone, or combined with TriDAP. Cells were stained for IL-8 and DNA and analyzed by automated image processing (means ± SD of triplicate wells, graph representative of two independent experiments).

Together, these results suggested that Nod1-mediated recognition of intracellular TriDAP was necessary and sufficient to induce IL-8 expression by bystander cells of microinjection. Because Nod1-mediated recognition of peptidoglycan also takes place in *S. flexneri*-infected cells, this result suggested that pathogen sensing may be sufficient to trigger IL-8 expression in bystander cells of *S. flexneri* infection.

Bystander Activation Is Not Mediated by Paracrine Signaling but Requires Cell-Cell Contact

Reports indicating that TNF-α is upregulated during *S. flexneri* infection and that NF-κB, p38, ERK, and JNK are activated by TNF-α suggested that this cytokine may induce bystander activation via paracrine signaling (Dong et al., 2002; Pédron et al., 2003). This hypothesis was tested by examining bystander activation in tumor necrosis factor receptor 1 (TNFR1)-deficient mouse embryonic fibroblasts ($Tnfr1^{-/-}$ MEFs). Because mice are deficient for the *IL8* gene, the chemokine macrophage inflammatory protein-2 (MIP-2) was chosen as readout of inflammation. Whereas $Tnfr1^{-/-}$ cells did not respond to TNF-α stimulation, massive MIP-2 expression was observed in bystander cells of *S. flexneri* infection (Figure 6A; Figures S6A and S6B), indicating that TNF-α was not the mediator of bystander activation. To investigate the role of protein secretion more broadly, we tested whether this process was impaired when protein secretion was abolished by the protein transport inhibitor brefeldin A (BFA). For conditions of drug treatment that blocked phorbol 12-myristate 13-acetate (PMA)-induced IL-8 secretion (Figure S6C), BFA had no effect on bystander activation during *S. flexneri* infection of Caco-2 cells (Figures 6B and 6C), suggesting that cell-cell propagation of proinflammatory signals was not mediated by secreted proteins.

To further explore the hypothesis of paracrine signaling, experiments of *S. flexneri* infection were performed in a flow chamber where fresh medium was perfused to wash away any potential secreted factors. A flow rate corresponding to the replacement of the entire volume of the chamber every second was used. IL-8 accumulation was still visible in bystander cells of infection located along an axis perpendicular or opposite to the direction of the flow (Figure S6D). Quantification of IL-8 (Figure 6D) showed no effect of perfusion, indicating that bystander activation was very improbably mediated by a long-ranged diffusing soluble factor.

To characterize the mechanism of bystander activation, we investigated whether it was cell-cell contact dependent. Infection was performed at subconfluent cell density to evaluate IL-8 expression in Caco-2 cells that had no physical interactions with infected cells. Inspection of images and manual quantification indicated that IL-8 was exclusively found in cells having direct or indirect contacts with infected cells and defined as class 1 (Figures 6E and 6F). Class 2 cells present in the vicinity of the infected cell (Experimental Procedures) but, separated by a gap, did not exhibit markedly more IL-8 than class 3 cells distant from any infection foci (Figure 6F). Collectively, these results demonstrated that the expression of IL-8 in bystander cells depends on cell-cell contact and is most probably not mediated by paracrine signaling.

Cell-Cell Propagation of Inflammatory Signals Is Mediated by Connexin Gap Junctions

An alternative hypothesis to paracrine signaling is direct communication via gap junction channels formed by connexin proteins. This hypothesis was directly tested by evaluating the effect of the gap junction blocker 18β-glycyrrhetinic acid (18β-GA) on IL-8 expression in bystander cells during *S. flexneri* infection of Caco-2 cells. In conditions of drug treatment that blocked Lucifer Yellow transfer through gap junctions of adjacent Caco-2 cells (Figure S7A), IL-8 expression in bystander
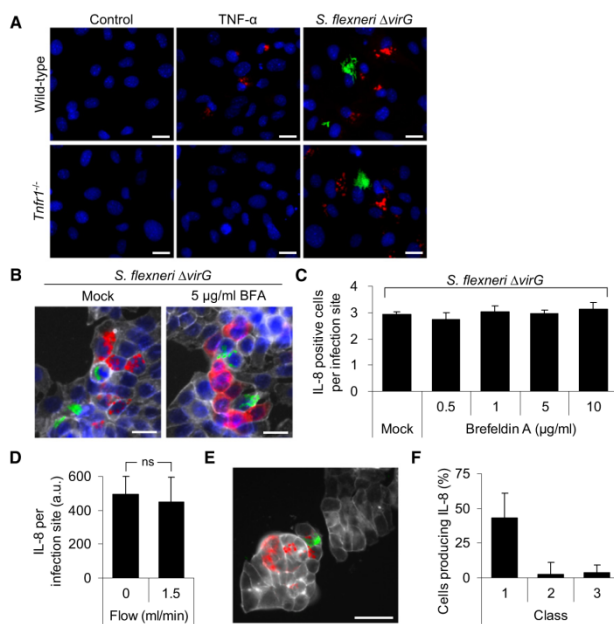
Figure 6. Bystander Activation Is Not Mediated by Paracrine Signaling but Is Cell-Cell Contact Dependent

(A) MIP-2 expression in wild-type and *Tnfr1*$^{-/-}$ MEF cells after TNF-α stimulation or *S. flexneri* infection visualized by fluorescence microscopy. After infection, cells were stained for MIP-2 and DNA with a MIP-2 antibody and Hoechst, respectively (MIP-2 in red, *S. flexneri* in green, Hoechst in blue). Scale bars represent 20 μm.
(B) Bystander IL-8 expression in Caco-2 cells pretreated with BFA and infected with *S. flexneri*. After infection (*S. flexneri* in green), cells were stained for IL-8, DNA, and F-actin with an IL-8 antibody (in red), Hoechst (in blue), and phalloidin (in gray), respectively. Scale bars represent 20 μm.
(C) Quantification of bystander IL-8 expression upon BFA treatment by automated image analysis (means ± SD of triplicate wells, graph representative of two independent experiments).
(D) Quantification of bystander IL-8 expression under flow conditions. IL-8 was quantified by measuring for each infected cell the area of IL-8 staining (a.u., arbitrary units, means ± SD, n = 10, graph representative of two independent experiments).
(E) Cell-cell contact analysis of bystander IL-8 expression. Caco-2 cells, seeded at subconfluent density and infected with *S. flexneri* (in green), were stained for IL-8 (in red) and F-actin (in gray). Scale bar represents 50 μm.
(F) Fractions of IL-8-producing cells in class 1, 2, 3 cell populations as defined in Experimental Procedures (means ± SD, n > 38, graph representative of two independent experiments).

cells of infection was strongly reduced (Figures 7A and 7B). In contrast, TNF-α-induced IL-8 secretion, used as control, was not affected (Figures S7B and S7C). A similar result was obtained with the gap junction inhibitor carbenoxolone (Figures S7D and S7E). Furthermore, treatment with glycyrrhizic acid, a compound structurally related to 18β-GA but which fails to block gap junction communication at concentrations below 100 μM (Davidson et al., 1986), had no effect on *S. flexneri*-induced IL-8 expression by bystander cells (Figure 7B). Taken together, these results suggested that IL-8 expression by bystander cells of infection was mediated by communication through gap junctions.

Because gap junction inhibitors have unspecific effects, we further validated this finding by testing whether the propagation of inflammatory signals was connexin dependent. In A431 cells that are poorly coupled via gap junctions and express connexin43 (Cx43) below the level of detection with antibodies (Troyanovsky et al., 1994), very limited activation of NF-κB, JNK, p38, and ERK and residual IL-8 expression were found in bystander cells of *S. flexneri* infection (Figure 7C, left, and Figure 7D, top). In contrast, in Cx43-overexpressing A431 cells (A431-Cx43) that are effectively coupled via gap junctions (Neijssen et al., 2005), large foci of NF-κB, JNK, p38, and ERK activation and IL-8 expression were found around infected cells (Figure 7C, right, and Figure 7D, bottom). Quantification of IL-8 expression in consecutive A431 or A431-Cx43 bystander cells

by automated image processing, as described in Supplemental Experimental Procedures, confirmed that the propagation of IL-8 expression was Cx43 dependent (Figures 7D and 7E). As expected, bystander IL-8 expression was strongly reduced when A431-Cx43 cells were depleted of Cx43 by RNA interference (Figure 7F and Figure S7F) or treated with 18β-GA (Figure 7G and Figure S7G).

In contrast to typical hemichannel-based signaling, communication via gap junction channels requires connexin proteins in both donor and recipient cells. To confirm that this condition was fulfilled for bystander activation, the propagation of inflammatory signals from *S. flexneri*-infected A431-Cx43 cells to either A431-Cx43 or A431 bystander cells was analyzed in experiments where A431-Cx43 and A431 cells were mixed prior seeding. Cx43, used to discriminate A431 and A431-Cx43 cells, as well as IL-8 were detected by immunofluorescence. Whereas IL-8 expression robustly spread within consecutive A431-Cx43 cells, the propagation from infected A431-Cx43 to adjacent A431 cells was very limited (Figure S7H). This observation, quantified by automated image processing (Figure 7H and Figure S7I), indicated that Cx43 proteins were also required in uninfected bystander cells to efficiently potentiate inflammation. Taken together, these data convincingly showed that the propagation of inflammation during bacterial infection of epithelial cells depends on connexin gap junctions.
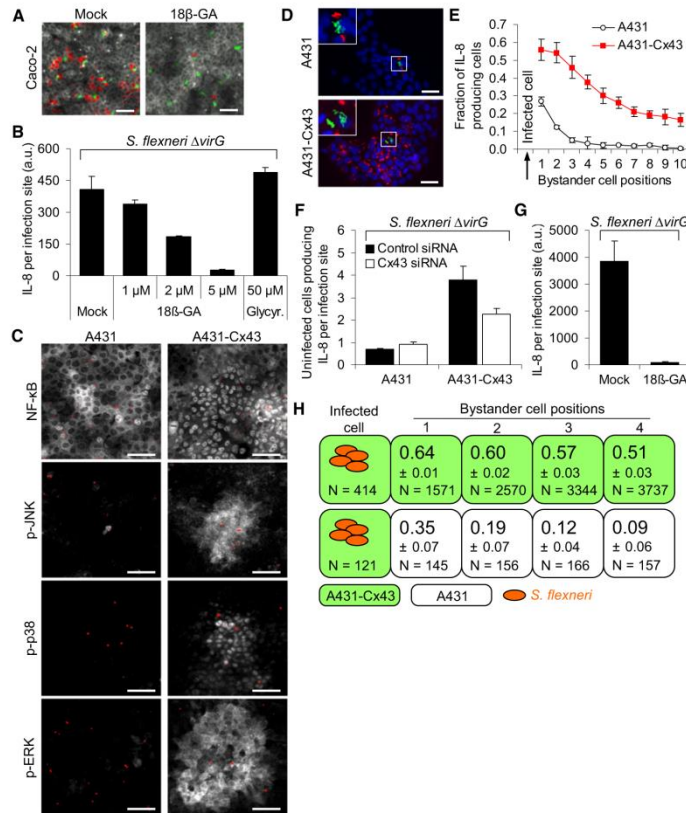
Figure 7. Propagation of Inflammation Is Mediated by Gap Junctions

(A) Effect of 18β-GA on IL-8 expression during infection of Caco-2 cells. Cells were pretreated with 18β-GA, infected with ΔvirG S. flexneri, and stained for IL-8 and F-actin with an IL-8 antibody and phalloidin, respectively (IL-8 in red, S. flexneri in green, F-actin in gray). Scale bars represent 50 μm.

(B) Quantification of IL-8 accumulation per site of infection in cells left untreated or pretreated with 18β-GA or glycyrrhizine. Quantification was performed by automated image processing as described in Supplemental Experimental Procedures (means ± SD of triplicate wells, graph representative of two independent experiments).

(C) Cell-cell propagation of proinflammatory signals in A431 and A431-Cx43 cells visualized by immunofluorescence. NF-κB p65, p-JNK, p-p38, and p-ERK immunofluorescence staining in A431 cells (left) and A431-Cx43 cells (right) after S. flexneri infection (NF-κB p65, p-JNK, p-p38, and p-ERK in gray, S. flexneri in red). Scale bars represent 40 μm.

(D) Propagation of IL-8 expression during S. flexneri infection of A431 and A431-Cx43 cells visualized by immunofluorescence. After infection, cells were stained for IL-8 and DNA with an IL-8 antibody and Hoechst, respectively (IL-8 in red, S. flexneri in green, Hoechst in blue). Inserts show the infection foci (magnification: ×2.5). Scale bars represent 40 μm.

(E) Spatial propagation of IL-8 expression in consecutive A431 or A431-Cx43 bystander cells during S. flexneri infection (means ± SD of six wells; graph representative of two independent experiments). Quantification was performed as described in Supplemental Experimental Procedures.

(F) Quantification of bystander IL-8 expression after siRNA-mediated Cx43 depletion. IL-8 was analyzed by immunofluorescence in A431 and A431-Cx43 cells transfected with control or Cx43 siRNAs and infected with S. flexneri and quantified by automated image analysis (means ± SD of triplicate wells, graph representative of two independent experiments, p = 3.9E-06).

(G) Quantification of bystander IL-8 expression in A431-Cx43 cells pretreated with 18β-GA and infected with S. flexneri (means ± SD of triplicate wells, graph representative of three independent experiments).

(H) Spatial propagation of IL-8 expression from S. flexneri-infected A431-Cx43 cells into either A431-Cx43 or A431 adjacent cells. Each number corresponds to the fraction of IL-8-producing cells for a given bystander cell position. Quantification was performed by automated image processing and is described in Supplemental Experimental Procedures (means ± SD of triplicate wells, graph representative of two independent experiments, p < 7.5E-04 at any given position).

DISCUSSION

In the present study, we provide evidence that during *S. flexneri* infection, the activation of the proinflammatory pathways NF-κB, JNK, ERK, and p38 propagates from infected to uninfected adjacent cells leading to IL-8 expression in bystander cells of infection. This mechanism, mediated by gap junction communication between infected and uninfected cells, circumvents the immunosuppressive activity of bacterial effectors and massively amplifies inflammation during bacterial infection.

Nod1 contributes to the detection of intracellular *S. flexneri* via the recognition of peptidoglycan-derived peptides (Girardin et al., 2003). In infected IECs, Nod1 ligation leads to NF-κB activation and upregulation of proinflammatory genes. By using an in vitro single-cell assay of *S. flexneri* infection, we found that NF-κB activation was not restricted to infected cells. Indeed, by performing infections at low MOIs, we observed within minutes of infection the propagation of NF-κB activation from infected to uninfected bystander cells. This cell-cell communication mechanism resulted in massive amplification of the total NF-κB response to *S. flexneri* infection. Because NF-κB controls the expression of proinflammatory genes, this result suggested that the mechanism of bystander activation may amplify the inflammatory response of an infected epithelial cell layer. This hypothesis was supported by the observation that JNK, ERK, and p38, three kinases involved in the control of inflammation, were also activated in bystander cells of *S. flexneri* infection. Noticeably, p38 activation was markedly higher in bystander than infected cells, suggesting that the effector OspF, which dephosphorylates p38 in the nucleus of infected cells via its phosphothreonine-lyase activity, did not affect p38 bystander activation. This hypothesis was validated by the observation that the deletion of *ospF* enhanced p38 activation in infected but not in bystander cells. Infection at low MOI reflects the early phase of Shigellosis, when the number of bacteria that have reached the basolateral surface of the IECs is limited. By rapidly propagating NF-κB and MAP kinase activation to uninfected cells, the mechanism of bystander activation may enable the host to fully activate these signaling pathways before their manipulation by future internalized bacteria, for instance via the effectors OspG and OspF (Arbibe et al., 2007; Kim et al., 2005).

The concept of bystander responses has been previously described in the context of ionizing radiation where nonirradiated cells receive signals from neighboring or distant irradiated ones (Hamada et al., 2007), in wound healing (Yang et al., 2004), or more recently after double-stranded DNA recognition (Patel et al., 2009). In all cases, the activation of signaling pathways emanates from cells exposed to local stress and propagates into the adjacent healthy tissue to amplify and orchestrate a multicellular response to an aggression. Here, we provide evidence for a similar mechanism in innate immunity against pathogenic bacteria.

By attracting neutrophils to the infected area, IL-8 has a central function in innate immunity against pathogens and in Shigellosis, in particular. It has been proposed that IL-8 is secreted by *S. flexneri*-infected cells after recognition of intracellular peptidoglycan-derived peptides via Nod1 (Girardin et al., 2003). Yet, the immunosuppressive activity of several effectors that alters signaling in infected cells challenges the ability of these cells to secrete large amounts of IL-8 as observed in Shigellosis. To directly address this question, we analyzed IL-8 expression during *S. flexneri* infection at the mRNA and protein level by in situ hybridization and intracellular immunofluorescence microscopy, respectively, two methods that combine single-cell resolution and spatial information at the site of infection. Here, we showed that the propagation of NF-κB, JNK, ERK, and p38 activation leads to IL-8 expression in bystander cells of infection. This mechanism efficiently amplifies the total IL-8 response of the infected cell monolayer by increasing the number of IL-8-producing cells per site of infection. Furthermore, our results clearly demonstrated that infected cells were inefficient at producing IL-8, confirming the immunosuppressive activities of secreted effectors on IL-8 expression. In line with the effect of OspF on p38 and histone H3 phosphorylation, IL-8 production was increased in cells infected with a ΔospF mutant. However, the deletion of *ospF* had only a limited effect on IL-8 expression, suggesting that the complete block observed in infected cells is mediated by multiple effectors. Additional effectors such as OspG, OspB, and IpaH$_{9.8}$ may also contribute to block IL-8 expression in infected cells (Kim et al., 2005; Okuda et al., 2005; Zurawski et al., 2009). Interestingly, we showed that OspF did not affect IL-8 expression in bystander cells, indicating that through cell-cell communication, the host appears to circumvent the activity of OspF in infected cells and amplifies the global IL-8 response to *S. flexneri* infection. In the rabbit intestinal loop model of Shigellosis, IL-8 expression was found in epithelial cells located beyond the zones of bacterial invasion, providing evidence for the physiological relevance of bystander IL-8 expression in vivo (Sansonetti et al., 1999).

IL-8 expression was also found in bystander cells of *S. typhimurium* and *L. monocytogenes* infection, showing that the potentiation of innate immunity by cell-cell communication corresponded to a broad host response to bacterial infection. However, the contribution of this mechanism to inflammation can vary for different pathogens. It depends on its frequency of occurrence but also on the ability of bacteria to alter signaling in infected cells. For *S. flexneri* that very efficiently blocks signaling in infected cells, bystander activation clearly constitutes the key pathway of IL-8 expression.

We addressed the role of peptidoglycan recognition in the mechanism of cell-cell communication leading to IL-8 expression in bystander cells and its underlying molecular basis. Interestingly, we found that the microinjection of the Nod1 ligand TriDAP was sufficient to induce IL-8 expression in bystander cells of microinjection, suggesting that the recognition of Nod1 ligands in infected cells may be sufficient to generate the underlying signals that mediate IL-8 expression in bystander cells of *S. flexneri* infection. Cell-cell communication can be mediated by different mechanisms: paracrine signaling, direct diffusion of small molecules through gap junctions, or membrane protein interactions. In Caco-2 cells, bystander IL-8 expression was not inhibited by BFA treatment or by perfusion, indicating that this process was most probably not mediated by paracrine signaling. Furthermore, it was cell-cell contact dependent, and therefore compatible with gap junction-mediated communication that enables direct diffusion of small molecules between adjacent

cells. This hypothesis was confirmed by showing that the mechanism of bystander IL-8 expression was blocked by gap junction inhibitors, limited in cells that are poorly coupled via gap junctions, and massively amplified by the overexpression of the gap junction protein Cx43. Finally, as required for the formation of connexins gap junction channels between adjacent cells, we showed that the presence of connexin proteins was necessary in both infected and bystander cells to efficiently propagate inflammation during bacterial infection.

Further studies are required to identify the small molecules (i.e., <2 kDa) diffusing from infected to bystander cells that control NF-κB, JNK, ERK, and p38 activation and lead to IL-8 expression during *S. flexneri* infection. Among potential candidates, the roles of known second messengers, which are involved in proinflammatory gene expression, including calcium, IP3, and cAMP, should be examined. An alternative hypothesis is the direct diffusion of small peptidoglycan-derived peptides through gap junctions.

In summary, we show that during *S. flexneri* infection, the activation of the proinflammatory pathways NF-κB, JNK, ERK, and p38 propagates from infected to uninfected adjacent cells leading to IL-8 expression in bystander cells of infection. This mechanism enables the host to circumvent the immunosuppressive activity of bacterial effectors and to massively amplify inflammation during bacterial infection. Moreover, by showing that this process is gap junction mediated, we provide evidence for a direct connection between gap junction communication and amplification of innate immunity during bacterial infection.

EXPERIMENTAL PROCEDURES

Cell Culture

HeLa, A549, Caco-2, A431, and MEF cells were cultured in Dulbecco's modified Eagle's medium (DMEM) supplemented with 10% FCS and 2 mM L-Glutamine. HUVECs were generously provided by C. Dehio (Biozentrum, University of Basel, Switzerland) and cultivated as previously described (Dehio et al., 1997).

Bacterial Strains

The *S. flexneri* strains M90T wild-type, its noninvasive derivative BS176, and the *icsA (virG)* deletion mutant were generously provided by P. Sansonetti (Bernardini et al., 1989). The ΔvirG ΔospF deletion mutant was generated as described in Supplemental Experimental Procedures (Table S1). The *Salmonella typhimurium* LT2 strain was provided by U. Jenal (Biozentrum, University of Basel, Switzerland) and the stably expressing GFP *Listeria monocytogenes* A21/B5 strain by M. Loessner (ETH Zurich, Switzerland).

Infection Assays

S. flexneri, S. typhimurium, and *L. monocytognes* were used in exponential growth phase. *S. flexneri* and *S. typhimurium* were coated with poly-L-lysine prior to infection. Cells seeded in 96-well plates were infected at indicated MOIs in DMEM supplemented with 10 mM HEPES and 2 mM L-glutamine. After adding bacteria, plates were centrifuged for 5 min and placed at 37°C for indicated time periods. Extracellular bacteria were killed by gentamicin (100 μg ml^{-1}). Infection assays were stopped by 4% PFA fixation.

Immunofluorescence and IL-8 Measurements

Immunofluorescence and IL-8 measurements were performed as described in Supplemental Experimental Procedures.

Automated Microscopy and Image Analysis

Images were automatically acquired with an ImageXpress Micro (Molecular devices, Sunnyvale, USA). Image analysis was performed via CellProfiler (Carpenter et al., 2006) and MATLAB (The MathWorks, Inc, Natick, USA) as described in Supplemental Experimental Procedures.

Microinjection and Flow Chamber Experiments

Microinjection and flow chamber experiments are described in Supplemental Experimental Procedures.

Analysis of Cell-Cell Contact

Infection was performed at subconfluent cell density. Cellular contacts and IL-8 were visualized by phalloidin and IL-8 staining, respectively. For each site of infection, the distance between the infected cell and the most distant bystander cell producing IL-8 was used as the radius of the "circle of bystander activation" centered on the infected cell. Within this circle, cells contacting directly the infected cell or indirectly by interacting with other bystander cells were classified as class 1. Cells making no direct or indirect contact with infected cells were defined as class 2. Cells located outside the circle and distant from any sites of infection were defined as class 3.

Statistical Analysis

Data are expressed as mean ± standard deviation of triplicate samples. p values were calculated with a two-tailed two-sample equal variance t test.

SUPPLEMENTAL INFORMATION

Supplemental Information includes Supplemental Experimental Procedures, seven figures, and one table and can be found with this article online at doi:10.1016/j.immuni.2010.10.015.

REFERENCES

Arbibe, L., Kim, D.W., Batsche, E., Pedron, T., Mateescu, B., Muchardt, C., Parsot, C., and Sansonetti, P.J. (2007). An injected bacterial effector targets chromatin access for transcription factor NF-kappaB to alter transcription of host genes involved in immune responses. Nat. Immunol. *8*, 47–56.

Bernardini, M.L., Mounier, J., d'Hauteville, H., Coquis-Rondon, M., and Sansonetti, P.J. (1989). Identification of icsA, a plasmid locus of Shigella flexneri that governs bacterial intra- and intercellular spread through interaction with F-actin. Proc. Natl. Acad. Sci. USA *86*, 3867–3871.

Carpenter, A.E., Jones, T.R., Lamprecht, M.R., Clarke, C., Kang, I.H., Friman, O., Guertin, D.A., Chang, J.H., Lindquist, R.A., Moffat, J., et al. (2006). CellProfiler: Image analysis software for identifying and quantifying cell phenotypes. Genome Biol. *7*, R100.

Cornelis, G.R. (2006). The type III secretion injectisome. Nat. Rev. Microbiol. *4*, 811–825.

Davidson, J.S., Baumgarten, I.M., and Harley, E.H. (1986). Reversible inhibition of intercellular junctional communication by glycyrrhetinic acid. Biochem. Biophys. Res. Commun. *134*, 29–36.

Dehio, C., Meyer, M., Berger, J., Schwarz, H., and Lanz, C. (1997). Interaction of *Bartonella henselae* with endothelial cells results in bacterial aggregation on the cell surface and the subsequent engulfment and internalisation of the bacterial aggregate by a unique structure, the invasome. J. Cell Sci. *110*, 2141–2154.

Dong, C., Davis, R.J., and Flavell, R.A. (2002). MAP kinases in the immune response. Annu. Rev. Immunol. *20*, 55–72.

Eckmann, L., Kagnoff, M.F., and Fierer, J. (1993). Epithelial cells secrete the chemokine interleukin-8 in response to bacterial entry. Infect. Immun. *61*, 4569–4574.

Girardin, S.E., Boneca, I.G., Carneiro, L.A., Antignac, A., Jéhanno, M., Viala, J., Tedin, K., Taha, M.K., Labigne, A., Zähringer, U., et al. (2003). Nod1 detects a unique muropeptide from gram-negative bacterial peptidoglycan. Science *300*, 1584–1587.

Hamada, N., Matsumoto, H., Hara, T., and Kobayashi, Y. (2007). Intercellular and intracellular signaling pathways mediating ionizing radiation-induced bystander effects. J. Radiat. Res. (Tokyo) *48*, 87–95.

Holtmann, H., Winzen, R., Holland, P., Eickemeier, S., Hoffmann, E., Wallach, D., Malinin, N.L., Cooper, J.A., Resch, K., and Kracht, M. (1999). Induction of interleukin-8 synthesis integrates effects on transcription and mRNA degradation from at least three different cytokine- or stress-activated signal transduction pathways. Mol. Cell. Biol. *19*, 6742–6753.

Islam, D., Veress, B., Bardhan, P.K., Lindberg, A.A., and Christensson, B. (1997). In situ characterization of inflammatory responses in the rectal mucosae of patients with shigellosis. Infect. Immun. *65*, 739–749.

Iwai, H., Kim, M., Yoshikawa, Y., Ashida, H., Ogawa, M., Fujita, Y., Muller, D., Kirikae, T., Jackson, P.K., Kotani, S., and Sasakawa, C. (2007). A bacterial effector targets Mad2L2, an APC inhibitor, to modulate host cell cycling. Cell *130*, 611–623.

Kim, D.W., Lenzen, G., Page, A.L., Legrain, P., Sansonetti, P.J., and Parsot, C. (2005). The *Shigella flexneri* effector OspG interferes with innate immune responses by targeting ubiquitin-conjugating enzymes. Proc. Natl. Acad. Sci. USA *102*, 14046–14051.

Köhler, H., Rodrigues, S.P., and McCormick, B.A. (2002). *Shigella flexneri* interactions with the basolateral membrane domain of polarized model intestinal epithelium: Role of lipopolysaccharide in cell invasion and in activation of the mitogen-activated protein kinase ERK. Infect. Immun. *70*, 1150–1158.

Kufer, T.A., Banks, D.J., and Philpott, D.J. (2006). Innate immune sensing of microbes by Nod proteins. Ann. N Y Acad. Sci. *1072*, 19–27.

Lee, J., Mira-Arbibe, L., and Ulevitch, R.J. (2000). TAK1 regulates multiple protein kinase cascades activated by bacterial lipopolysaccharide. J. Leukoc. Biol. *68*, 909–915.

Li, H., Xu, H., Zhou, Y., Zhang, J., Long, C., Li, S., Chen, S., Zhou, J.M., and Shao, F. (2007). The phosphothreonine lyase activity of a bacterial type III effector family. Science *315*, 1000–1003.

Makino, S., Sasakawa, C., Kamata, K., Kurata, T., and Yoshikawa, M. (1986). A genetic determinant required for continuous reinfection of adjacent cells on large plasmid in *S. flexneri* 2a. Cell *46*, 551–555.

Mollenhauer, H.H., Morré, D.J., and Rowe, L.D. (1990). Alteration of intracellular traffic by monensin; Mechanism, specificity and relationship to toxicity. Biochim. Biophys. Acta *1031*, 225–246.

Neijssen, J., Herberts, C., Drijfhout, J.W., Reits, E., Janssen, L., and Neefjes, J. (2005). Cross-presentation by intercellular peptide transfer through gap junctions. Nature *434*, 83–88.

Ninomiya-Tsuji, J., Kishimoto, K., Hiyama, A., Inoue, J., Cao, Z., and Matsumoto, K. (1999). The kinase TAK1 can activate the NIK-I kappaB as well as the MAP kinase cascade in the IL-1 signalling pathway. Nature *398*, 252–256.

Okuda, J., Toyotome, T., Kataoka, N., Ohno, M., Abe, H., Shimura, Y., Seyedarabi, A., Pickersgill, R., and Sasakawa, C. (2005). *Shigella* effector IpaH9.8 binds to a splicing factor U2AF(35) to modulate host immune responses. Biochem. Biophys. Res. Commun. *333*, 531–539.

Parsot, C. (2009). *Shigella* type III secretion effectors: How, where, when, for what purposes? Curr. Opin. Microbiol. *12*, 110–116.

Patel, S.J., King, K.R., Casali, M., and Yarmush, M.L. (2009). DNA-triggered innate immune responses are propagated by gap junction communication. Proc. Natl. Acad. Sci. USA *106*, 12867–12872.

Pédron, T., Thibault, C., and Sansonetti, P.J. (2003). The invasive phenotype of *Shigella flexneri* directs a distinct gene expression pattern in the human intestinal epithelial cell line Caco-2. J. Biol. Chem. *278*, 33878–33886.

Phalipon, A., and Sansonetti, P.J. (2007). *Shigella's* ways of manipulating the host intestinal innate and adaptive immune system: A tool box for survival? Immunol. Cell Biol. *85*, 119–129.

Saccani, S., Pantano, S., and Natoli, G. (2002). p38-dependent marking of inflammatory genes for increased NF-kappa B recruitment. Nat. Immunol. *3*, 69–75.

Sansonetti, P.J., Arondel, J., Huerre, M., Harada, A., and Matsushima, K. (1999). Interleukin-8 controls bacterial transepithelial translocation at the cost of epithelial destruction in experimental shigellosis. Infect. Immun. *67*, 1471–1480.

Schroeder, G.N., and Hilbi, H. (2008). Molecular pathogenesis of *Shigella* spp.: Controlling host cell signaling, invasion, and death by type III secretion. Clin. Microbiol. Rev. *21*, 134–156.

Strober, W., Murray, P.J., Kitani, A., and Watanabe, T. (2006). Signalling pathways and molecular interactions of NOD1 and NOD2. Nat. Rev. Immunol. *6*, 9–20.

Troyanovsky, S.M., Troyanovsky, R.B., Eshkind, L.G., Krutovskikh, V.A., Leube, R.E., and Franke, W.W. (1994). Identification of the plakoglobin-binding domain in desmoglein and its role in plaque assembly and intermediate filament anchorage. J. Cell Biol. *127*, 151–160.

Wang, C., Deng, L., Hong, M., Akkaraju, G.R., Inoue, J., and Chen, Z.J. (2001). TAK1 is a ubiquitin-dependent kinase of MKK and IKK. Nature *412*, 346–351.

Yang, L., Cranson, D., and Trinkaus-Randall, V. (2004). Cellular injury induces activation of MAPK via P2Y receptors. J. Cell. Biochem. *91*, 938–950.

Zurawski, D.V., Mumy, K.L., Faherty, C.S., McCormick, B.A., and Maurelli, A.T. (2009). *Shigella flexneri* type III secretion system effectors OspB and OspF target the nucleus to downregulate the host inflammatory response via interactions with retinoblastoma protein. Mol. Microbiol. *71*, 350–368.

Supplemental Information

Cell-Cell Propagation of NF-κB Transcription

Factor and MAP Kinase Activation Amplifies

Innate Immunity against Bacterial Infection

Christoph Alexander Kasper, Isabel Sorg, Christoph Schmutz, Therese Tschon, Harry Wischnewski, Man Lyang Kim, and Cécile Arrieumerlou

INVENTORY

Supplemental Figures and Legends

- **Figure S1, relates to Figure 1.** NF-κB is activated in bystander cells during *S. flexneri* infection of Caco-2, A549 and HUVEC cells.

- **Figure S2, relates to Figure 2.** JNK and ERK are activated in bystander cells of *S. flexneri* infection in Caco-2 cells.

- **Figure S3, relates to Figure 3.** p38 is activated in bystander cells of *S. flexneri* infection in Caco-2 cells.

- **Figure S4, relates to Figure 4.** Proinflammatory cytokines are expressed in bystander cells of *S. flexneri* infection.

- **Figure S5, relates to Figure 5.** Extracellular treatment with TriDAP failed to induce IL-8 expression.

- **Figure S6, relates to Figure 6.** *S. flexneri*-induced bystander IL-8 expression is not mediated by paracrine signaling but is cell-cell contact dependent.

- **Figure S7, relates to Figure 7.** *S. flexneri*-induced bystander IL-8 expression is mediated by gap junctions.

Supplemental Tables

- **Table S1.** Oligonucleotide primers used to generate the Δ*ospF* mutant.

Supplemental Experimental Procedures

- **Bacterial strains**
- **Double-thymidine block**

- **Immunofluorescence**
- **IL-8 and MIP-2 measurements**
- **Drug treatments**
- **siRNA transfection and western blot analysis**
- **Image acquisition and analysis**
- **Microinjection**
- **Flow chamber experiments**
- **Quantification of the propagation of IL-8 expression during** *Shigella* **infection of A431 and A431-Cx43 cells**
- **Quantification of the propagation of IL-8 expression in mixed A431 and A431-Cx43 cell populations**

Supplemental References
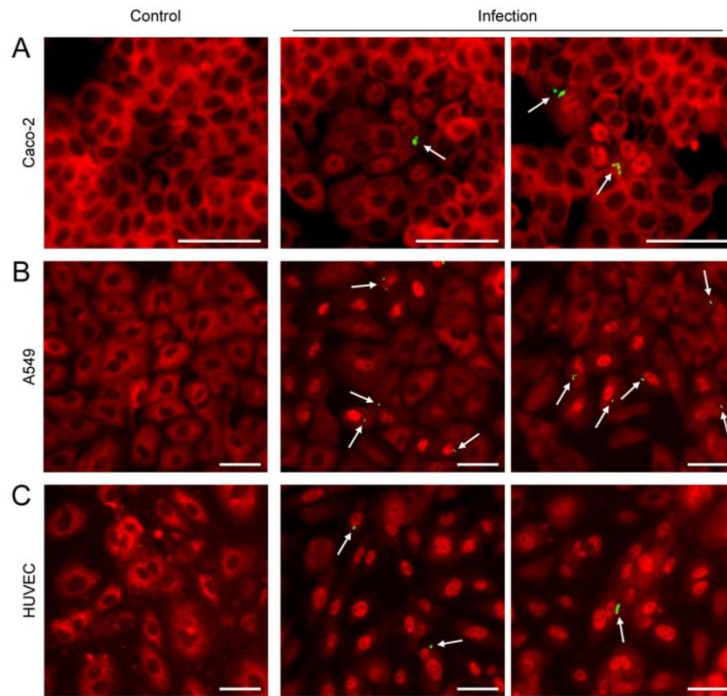
2

Figure S1, relates to Figure 1. NF-κB is activated in bystander cells during *S. flexneri* infection of Caco-2, A549 and HUVEC cells.
(A) Caco-2 cells
(B) A549 cells
(C) HUVEC cells
White arrows indicate bacteria. Bars, 50μm.
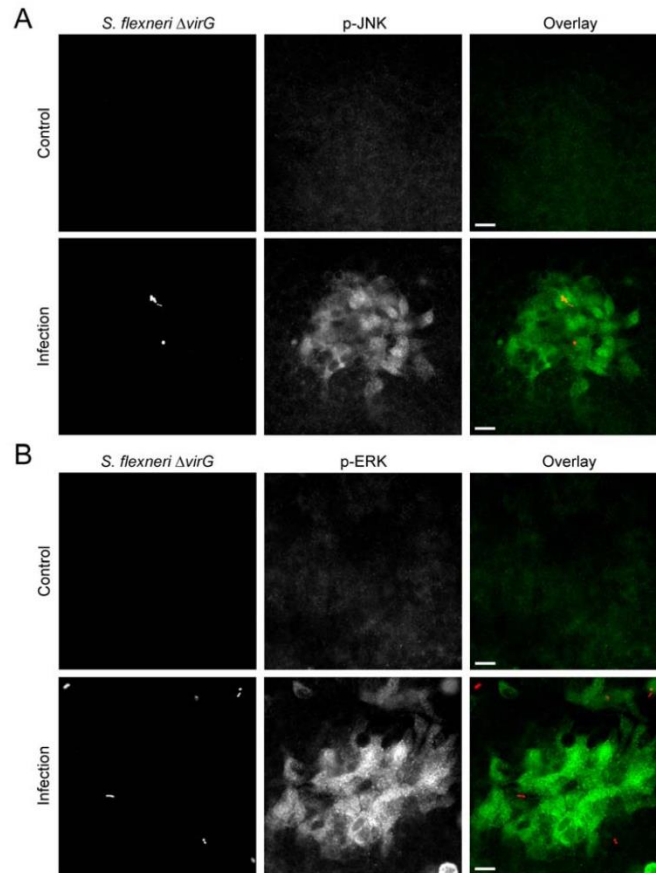
3

Figure S2, relates to Figure 2. JNK and ERK are activated in bystander cells of *S. flexneri* infection in Caco-2 cells
(A) JNK is activated in infected and bystander cells of *S. flexneri* infection in Caco-2 cells. Control or Δ*virG* infected cells (MOI=2, 90 minute infection) were stained for p-JNK (overlay: *S. flexneri* in red, p-JNK in green). Bars, 20 μm.
(B) ERK is mostly activated in bystander cells of *S. flexneri* infection in Caco-2 cells. Control or Δ*virG* infected cells (MOI=2, 90 minute infection) were stained for p-ERK (overlay: *S. flexneri* in red, p-ERK in green). Bars, 20 μm.
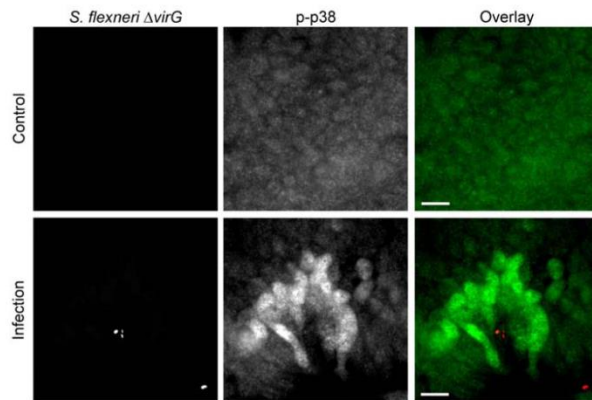
4

Figure S3, relates to Figure 3. p38 is activated in bystander cells of _S. flexneri_ infection in Caco-2 cells

p38 is activated in bystander cells of _S. flexneri_ infection in Caco-2 cells. Control or Δ*virG* infected cells (MOI=2, 90 minute infection) were stained for p-p38 (overlay: _S. flexneri_ in red, p-p38 in green). Bars, 20 μm.
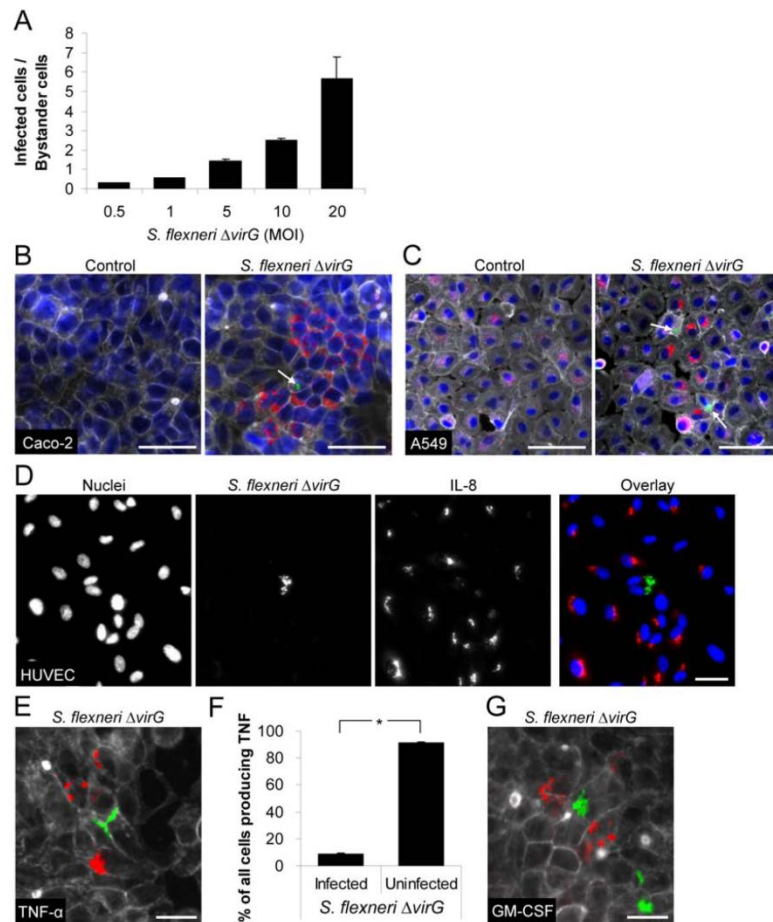
5

Figure S4, relates to Figure 4. Proinflammatory cytokines are expressed in bystander cells of *S. flexneri* infection.
(A) Infected to bystander cell ratios at different MOIs. HeLa cells were infected with the Δ*virG* mutant at indicated MOIs. The ratio between infected and bystander cells was determined by automated image processing. Results represent the mean +/- SD of triplicate wells. The graph shows a representative of 2 independent experiments.
(B) IL-8 production in bystander cells during *S. flexneri* infection of Caco-2 cells. Arrow indicates the infected cell (IL-8 in red, *S. flexneri* in green, Hoechst in blue, F-actin in grey). Bar, 40 μm.

(C) IL-8 production in bystander cells during *S. flexneri* infection of A549 cells Arrows indicate infected cells (IL-8 in red, *S. flexneri* in green, Hoechst in blue, F-actin in grey). Bar, 40 μm.

(D) HUVEC cells were infected for 3 hours with *S. flexneri* $\Delta virG$. Bar, 50 μm.

(E) TNF-α accumulation in bystander cells of *S. flexneri* infection in Caco-2 cells. TNF-α staining of monensin-treated Caco-2 cells during infection (TNF-α in red, *S. flexneri* in green, F-actin in grey). Bar, 20 μm.

(F) Quantification of TNF-α expression during *S. flexneri* infection of Caco-2 cells. The vast majority of cells producing TNF-α are uninfected cells. In conditions were 2% of cells were infected, around 1% of all cells exhibited TNF-α expression. Results represent the mean +/- SD of triplicate wells. The graph shows a representative of 2 independent experiments, *p = 2.16E-06.

(G) GM-CSF accumulation in bystander cells of *S. flexneri* infection in Caco-2 cells. GM-CSF staining of monensin-treated Caco-2 cells during infection (GM-CSF in red, *S. flexneri* in green, F-actin in grey). Bar, 20 μm.
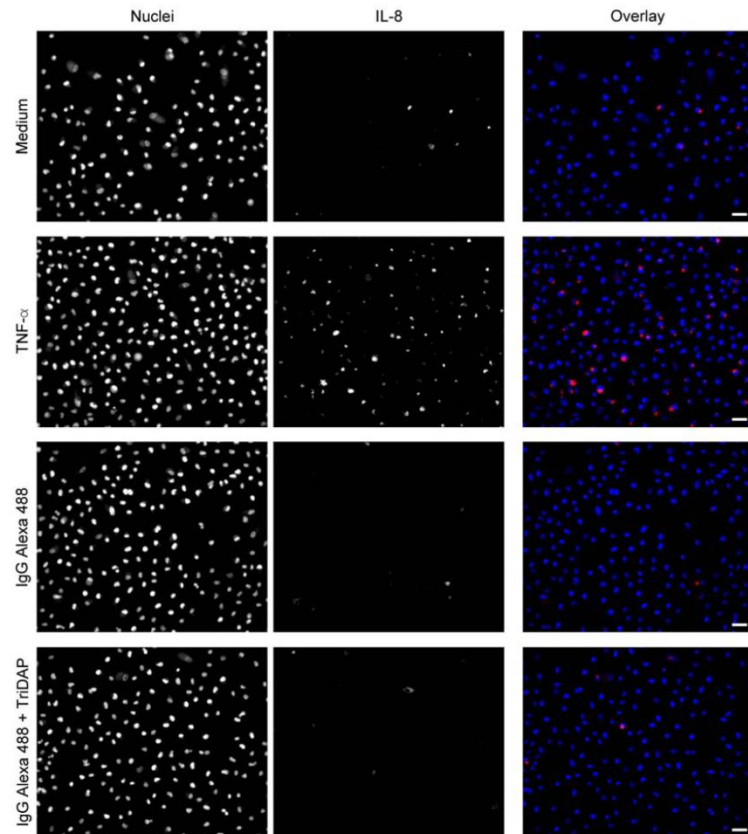
7

Figure S5, relates to Figure 5. Extracellular treatment with TriDAP failed to induce IL-8 expression.
IL-8 staining in A549 cells left untreated or treated extracellularly with TNF-α, IgG Alexa 488 alone or combined with TriDAP.
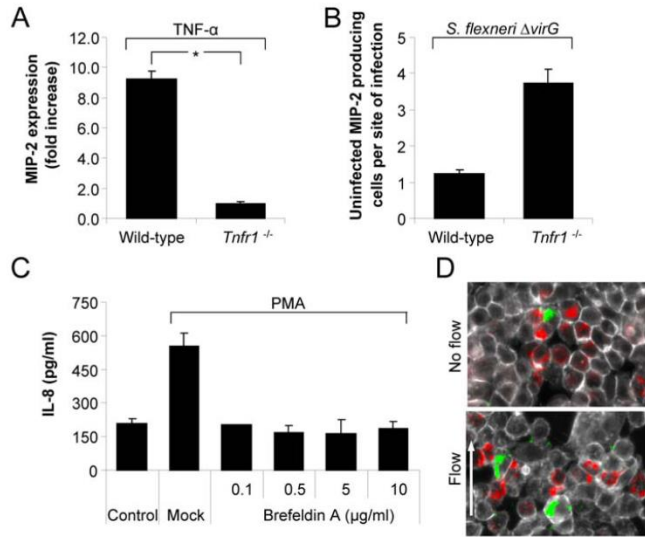
8

Figure S6, relates to Figure 6. *S. flexneri*-**induced bystander IL-8 expression is not mediated by paracrine signaling but is cell-cell contact dependent.**

(A) *Tnfr1*$^{-/-}$ MEF cells are TNF-α-irresponsive. MIP-2 expression was not induced in response to TNF-α stimulation in *Tnfr1*$^{-/-}$ MEF cells (mean +/- SD of triplicate wells, graph representative of 3 independent experiments, *p = 2.0E-03).

(B) Massive bystander MIP-2 expression was found during *S. flexneri* infection of *Tnfr1*$^{-/-}$ MEF cells (mean +/- SD of triplicate wells, graph representative of 3 independent experiments).

(C) BFA blocks PMA-induced IL-8 secretion. Effect of BFA pretreatment on IL-8 secretion measured by ELISA in the supernatant of resting or PMA-stimulated Caco-2 cells (mean +/- SD of triplicate wells, graph representative of 2 independent experiments).

(D) IL-8 expression in bystander cells of infection is not abolished under flow conditions. The direction of the flow is given by the white arrow (IL-8 in red, *S. flexneri* in green, F-actin in grey).
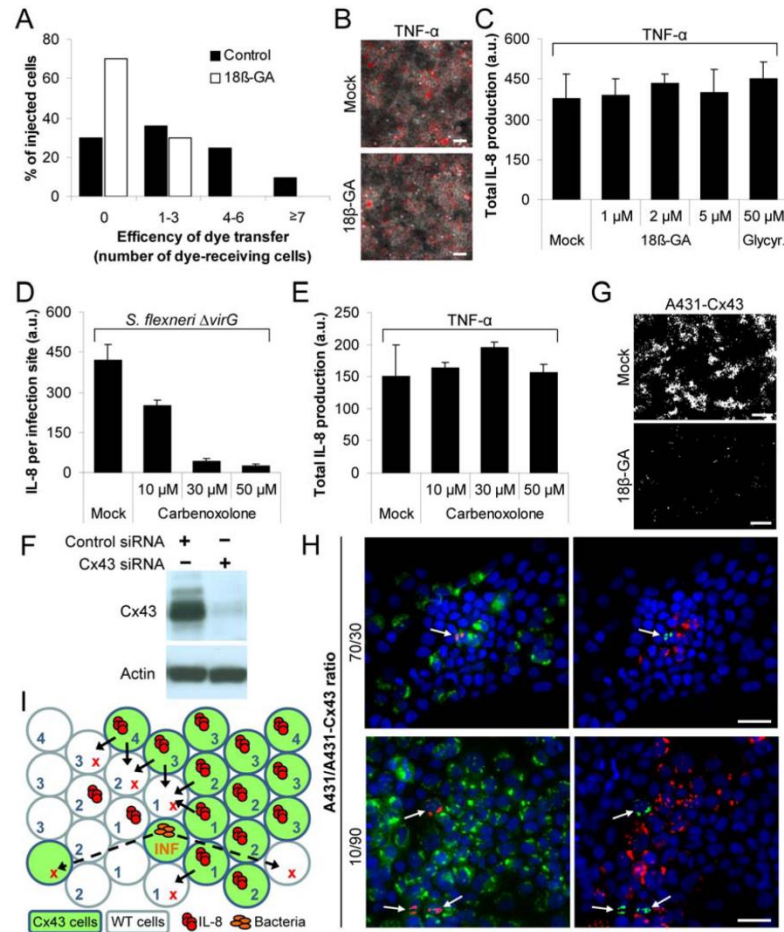
9

Figure S7, relates to Figure 7. *S. flexneri*-induced bystander IL-8 expression is mediated by gap junctions.

(A) Caco-2 cells have functional gap junctions that are sensitive to 18β-GA. Lucifer Yellow transfer from microinjected to neighboring cells in absence or in presence of 18β-GA (Control: n=334, 18β-GA: n=207).

(B) TNF-α-induced IL-8 accumulation is not affected by 18β-GA (5 μM) in Caco-2 cells. Bars, 50 μm.

(C) Effect of 18β-GA and glycyrrhizic acid on TNF-α-induced IL-8 accumulation quantified by automated image analysis (a.u., arbitrary unit;

10

mean +/- SD of triplicate wells, graph representative of 2 independent experiments).

(D) Quantification of intracellular IL-8 accumulation per site of *S. flexneri* infection in cells left untreated or pretreated with carbenoxolone (mean +/- SD of triplicate wells, graph representative of 2 independent experiments).

(E) Quantification of total IL-8 production in cells left untreated or pretreated with carbenoxolone following TNF-α stimulation (mean +/- SD of triplicate wells, graph representative of 2 independent experiments).

(F) siRNA-mediated depletion of Cx43 in A431-Cx43 cells. Cells were transfected with control or Cx43 siRNAs. Cx43 expression was analyzed 72 hours after transfection by a Cx43 immunoblot (top panel). Equal loading was verified with an actin immunoblot (bottom panel).

(G) *S. flexneri*-induced bystander IL-8 expression is inhibited by 18β-GA (5 μM) in A431-Cx43 cells. Bars, 300 μm.

(H) Images illustrating the spatial propagation of IL-8 expression from *S. flexneri* infected A431-Cx43 cells into either A431-Cx43 or A431 adjacent cells. Left panels: Cx43 in green, *S. flexneri* in red, Hoechst in blue. Right panels: IL-8 in red, *S. flexneri* in green, Hoechst in blue. Arrows indicate infected cells. Bars, 40 μm.

(I) Sketch representing the analysis algorithm used to quantify the propagation from *S. flexneri* infected A431-Cx43 cells into either A431-Cx43 or A431 adjacent cells. Numbers represent the position of the cell in the "path" from the infected cell. Cells at position 1-4 were exclusively considered for analysis. Cells containing an "X" were excluded from analysis. Black arrows indicate A431 cells in contact with A431-Cx43 producing IL-8. Dashed black arrows indicate invalid paths.

11

SUPPLEMENTAL TABLES

Mutant	Forward	Reverse
Δ*ospF*	ATTCTATTATATAGATAAAATATCT CCTGCAAAAGATACGGGTATTTT TGTGTAGGCTGGAGCTGCTTCG	TCAAAAGTTCGATGTTCCACCACAT CGACCGTAGAAGAGATGAGATAGTA CATATGAATATCCTCCTTAG

Table S1. Oligonucleotide primers used to generate the Δ*ospF* mutant.

The underlined sequences represent the priming sites used to amplify the *cat*

resistance cassette from pKD3.

12

SUPPLEMENTAL EXPERIMENTAL PROCEDURES

Bacterial strains

All *Shigella* and *Salmonella* strains were transformed with the pMW211 plasmid to express the DsRed protein under control of a constitutive promoter. The pMW211 plasmid was a generous gift from Dr. D. Bumann (Biozentrum, University of Basel, Switzerland).

The Δ*virG* Δ*ospF* deletion mutant was generated from the Δ*virG* mutant by allelic exchange using a modification of the lambda red-mediated gene deletion (Datsenko and Wanner, 2000). The genes for lambda red recombination were expressed from the pKM208 plasmid (Murphy and Campellone, 2003). The chloramphenicol resistance cassette (*cat*) of the pKD3 plasmid was amplified using the primers listed in Table S1. After *Dpn*I digestion, the PCR product was electroporated into the Δ*virG* mutant. Recombinants were selected on TSB plates containing 5 or 10 µg ml^{-1} chloramphenicol. The *cat* cassette was removed by transformation of pCP20 and incubation at 30°C on TSB plates containing 100 µg ml^{-1} ampicillin. Single colonies were screened by PCR.

Double-thymidine block

HeLa cells were seeded in a 96-well plate at 2750 cells per well. The next day, 2 mM thymidine was added. After 19 hours, cells were washed and incubated with fresh growth medium for 9 hours. Thymidine was, then, added again for a period of 16 to 18 hours. Cells were washed and infection performed as described above.

Immunofluorescence

After fixation, cells were permeabilized in 0.3-0.5% Triton X-100 for 10 minutes, incubated in PBS supplemented with 5% goat serum for 2 hours and then, overnight at 4°C, with different combinations of primary antibodies. NF-κB p65 localization was visualized by using a mouse monoclonal p65 antibody (Santa Cruz Biotechnology, Santa Cruz, USA). The phosphorylated forms of p38, JNK and ERK were stained with a rabbit monoclonal phospho(T180/Y182)-p38, a rabbit polyclonal phospho(T183/Y185)-SAPK/JNK and a rabbit monoclonal phospho(T202/Y204)-p44/p42 antibody (Cell signaling technology, Beverly, USA), respectively. The phosphorylated form of histone H3 was detected with a rabbit polyclonal phospho(S10)-Histone H3 (Upstate signaling solution, Billerica, USA). Intracellular TNF-α and GM-CSF were stained with a purified human TNF-α and a purified human GM-CSF antibody, respectively (BD Pharmingen, San Jose, USA). Cells were then stained with Cy5-, Alexa 647- or FITC-conjugated secondary antibodies accordingly (Invitrogen, Carlsbad, USA). DNA and F-actin were stained with Hoechst and FITC-phalloidin, respectively.

IL-8 and MIP-2 measurements

IL-8 secretion was measured by ELISA in the supernatant of HeLa cells infected with *S. flexneri* for 6 hours. The cell-free supernatant from triplicate wells was analyzed for its IL-8 content using the commercial ELISA kit (BD Pharmingen, San Jose, USA). *In situ* hybridization of *IL-8* mRNA was performed with the QuantiGene ViewRNA Plate-Based Assay kit (Panomics, Fremont, USA) 2 hours after infection. Alternatively, the production of IL-8 and

14

MIP-2 was measured by immunofluorescence using an IL-8 antibody (BD Pharmingen, San Jose, USA) and a MIP-2 antibody (BD Pharmingen, San Jose, USA) 3 hours after infection. Monensin (50 μM) was used in the infection assay to trap IL-8 and MIP-2 in intracellular compartments.

Drug treatments

When specified, cells were pretreated 30-60 minutes before infection with drugs at the concentration indicated on the figures. Brefeldin A, 18β-glycyrrhetinic acid, glycyrrhizine and carbenoxolone were from Sigma-Aldrich (Saint Louis, USA).

siRNA transfection and western blot analysis

A431-Cx43 cells were transfected with ON-TARGETplus SMARTpool siRNAs targeting Cx43 or ON-TARGETplus siCONTROL (Dharmacon, Dallas, USA). 72 hours after transfection, cells were lysed in Phosphosafe Extraction Buffer (Novagen, Darmstadt, Germany) supplemented with 1x protease inhibitor cocktail (Calbiochem, Darmstadt, Germany). Protein concentration was measured using the bicinchoninic acid (BCA) kit (Pierce, Rockford, USA). Equal amounts of proteins were resolved by SDS-PAGE and transferred to Hybond C-Extra membrane (Amersham Bioscience, Pittsburgh, USA) for immunoblotting with a Cx43 antibody or an actin antibody (Invitrogen, Carlsbad, USA). Primary antibody was detected using a horseradish peroxidase-conjugated rabbit IgG antibody and visualized with the ECL system (Pierce).

Image acquisition and analysis

At each site, images were acquired at 360 nm, 480 nm, 594 nm and 640 nm to visualize Hoechst, FITC-phalloidin or FITC-conjugated secondary antibodies, DsRed expressing *S. flexneri* and Cy5- or Alexa 647-conjugated secondary antibodies, respectively. For image analysis, the Hoechst staining was used as a mask to automatically identify cell nuclei. Cellular area was defined by extension of the nuclear mask. Subtraction of the nuclear area from the cellular area was used to define the cytoplasm.

For each cell, the ratio of p65 intensity in the nucleus and in the cytoplasm, defined as the NF-κB activation ratio, was calculated. In order to automatically quantify the fraction of NF-κB activated cells, a threshold of activation (T) was automatically calculated as such that 90% of control cells remained below this value. In parallel, the presence of bacteria within the area of each cell was also quantified. *S. flexneri* bacteria express DsRed at high levels and are therefore very effectively detected by automated image analysis. For automated detection, the "Robust Background Adaptive" algorithm described by Carpenter et al. was used (Carpenter et al., 2006). Briefly, the "Robust Background" method trims the brightest and dimmest 5% of pixel intensities off first, in a way that the remaining pixels represent a gaussian of intensity values that are mostly background pixels. It then calculates the mean and standard deviation of the remaining pixels and calculates the threshold as the mean + 2 times the standard deviation. As this is a dynamic method, the threshold value was calculated for each image. Performance of bacterial detection was checked by visual inspection of several images prior to

16

automated processing. In control images (no infection), the algorithm generally classified less then 1% of cells as infected.

Based on these measurements, cells containing bacteria and showing a NF-κB activation ratio > T were defined as infected cells. Cells, which did not contain bacteria, but had a ratio > T were classified as bystanders. The nuclear mask was used to measure activation of MAP kinases or histone H3 for infected and bystander cell populations. To automatically quantify the fraction of ERK activated cells, a threshold based on p-ERK nuclear intensity was defined as described above. For Caco-2 cells, the intracellular accumulation of IL-8 was quantified by measuring the area of IL-8 granules in uninfected cells using threshold intensity and size exclusion values. In the experiment performed to test the effect of BFA, we used a lower threshold intensity value for IL-8 detection combined to a higher threshold value for size exclusion.

Microinjection

For microinjection, A549 cells were seeded subconfluently in 35 mm μ-dishes (Ibidi, Munich, Germany). Cells were microinjected with L-Ala-D-γ-Glu-meso-diaminopimelic acid (TriDAP; 2 μg ml^{-1} in PBS from AnaSpec, San Jose, USA) using Eppendorf Femtotips II capillaries and an Eppendorf FemtoJet with an injection pressure (pi) of 80 hPa. For identification of injected cells, the goat anti-rabbit-IgG-Alexa 488 antibody (0.5 mg ml^{-1}) was co-injected with TriDAP. Control cells were injected with the IgG-Alexa 488 antibody alone. After microinjection, growth medium containing 50 μM monensin was added. After 3 hours, cells were fixed, stained for IL-8, and analyzed with a Revolution XD

17

spinning disk confocal microscope (Andor technology, Belfast, Ireland). For dye transfer experiments, Caco-2 cells were microinjected with a solution containing LY and the anti-rabbit-IgG-Alexa 594 antibody. LY transfer to neighboring cells was analyzed 10-15 minutes after microinjection.

Flow chamber experiments

Caco-2 cells were seeded in a flow chamber (Ibidi, Munich, Germany) and used at confluency. For infection, bacteria were added to cells and the chamber centrifuged at 37°C for 10 minutes. A constant perfusion of pre-warmed assay medium was then immediately started at a flow rate of 1.5 ml min^{-1}. After 1 hour, this solution was replaced by a solution containing 50 μM monensin and 100 μg ml^{-1} gentamicin. After 2 more hours, cells were fixed and stained for IL-8.

Quantification of the propagation of IL-8 expression during *S. flexneri* infection of A431 and A431-Cx43 cells

Quantification of the propagation of IL-8 across infection foci was performed by automated image analysis as follows. The "MeasureObjectNeighbors" analysis module of CellProfiler was used to classify cells into different subgroups based on their position relative to the infected cell: uninfected cells in direct contact with the infected cell belong to the subgroup "Position 1" (P1), uninfected cells in contact with P1 cells belong to P2, outer uninfected cells in contact with P2 cells belong to P3 et cetera. For each subgroup, the fraction of IL-8 positive cells was measured and compared between the two cell lines.

18

Quantification of the propagation of IL-8 expression in mixed A431 and A431-Cx43 cell populations

In order to test whether Cx43 expression was required in bystander cells, the propagation from *S. flexneri* infected A431-Cx43 cells to either A431-Cx43 or A431 cells, was analyzed. Cells were mixed prior seeding in the A431/A431-Cx43 ratios (70/30) and (10/90) and infected with *S. flexneri* at MOI 0.5 the next day. One hour after adding bacteria, cells were treated with monensin to trap IL-8 intracellularly. Following infection, cells were stained by immunofluorescence for IL-8 and Cx43, used here to identify A431 and A431-Cx43 cells (Cx43 negative: A431 cells, Cx43 positive: A431-Cx43 cells). Cells surrounding *S. flexneri* infected A431-Cx43 cells were exclusively considered. For all these bystander cells, the position relative to the infected cell (positions 1 to 4 were only considered for analysis), as well as the identification of their neighbors, were defined by the "MeasureObjectNeighbors" analysis module of CellProfiler. In addition, the intensity of Cx43 and IL-8 was quantified for all cells. The propagation from infected A431-Cx43 to bystander A431-Cx43 cells (A431/A431-Cx43 ratio 10/90) was quantified by measuring IL-8 expression in A431-Cx43 cells that were in direct contact with infected cells (position 1) or were connected to infected cells via other A431-Cx43 cells (positions 2,3,4 of the "A431-Cx43 path"). Alternatively, the propagation from infected A431-Cx43 to A431 cells (A431/A431-Cx43 ratio 70/30) was quantified by measuring IL-8 expression in A431 cells having direct contact with infected A431-Cx43 cells (position 1) or in adjacent A431 cells connected to infected cells exclusively via A431 cells (positions 2,3,4 of the "A431 path"). A431 cells in contact with uninfected A431-Cx43 producing IL-8 cells were excluded from

19

our analysis. A sketch illustrating the algorithm used for analysis is illustrated

in Figure S7H.

20

SUPPLEMENTAL REFERENCES

Carpenter, A.E., Jones, T.R., Lamprecht, M.R., Clarke, C., Kang, I.H., Friman, O., Guertin, D.A., Chang, J.H., Lindquist, R.A., Moffat, J.*, et al.* (2006). CellProfiler: image analysis software for identifying and quantifying cell phenotypes. Genome Biol *7*, R100.
Datsenko, K.A., and Wanner, B.L. (2000). One-step inactivation of chromosomal genes in Escherichia coli K-12 using PCR products. Proc Natl Acad Sci U S A *97*, 6640-6645.
Murphy, K.C., and Campellone, K.G. (2003). Lambda Red-mediated recombinogenic engineering of enterohemorrhagic and enteropathogenic E. coli. BMC Mol Biol *4*, 11.

Abbreviations

AKT	v-akt murine thymoma viral oncogene homolog
AP-1	activator protein 1
APC	antigen-presenting cell
ARP	actin-related protein
ASC	apoptosis-associated speck like protein
ATF2	Activating transcription factor 2
ATP1A1	Na^+/K^+-ATPase
BIR	baculoviral inhibitory repeat
cAMP	cyclic adenosine monophosphate
CARD	caspase recruitment domain
CCL2	chemokine (C-C motif) ligand 2
CDC42	Cell division control protein 42
cGAMP	cyclic GMP-AMP
cGAS	cyclic GMP-AMP (cGAMP) synthase
cGMP	cyclic guanosine monophosphate
cIAP	inhibitor of apoptosis protein homolog C
CLR	C-type lectin receptor
CX	Connexin
CXCL	chemokine (C-X-C motif) ligand
DAG	diacylglycerol
DAMP	danger-associated molecular pattern
dsDNA	double-stranded DNA
E1	ubiquitin activating enzyme
E2	ubiquitin conjugating enzyme
E3	ubiquitin ligase
EGF	epidermal growth factor
EGFR	EGF receptor
ER	endoplasmatic reticulum
ERK	extracellular signal-regulated kinase
FAE	follicle associated eithelium
F-actin	filamentous actin
FHA	forkhead-associated domain
GEF	guanine-nucleotide exchange factor
GFP	green fluorescent protein
GJIC	gap junctional intercellular communication
GM-CSF	Granulocyte macrophage colony-stimulating factor

Abbreviations

GTP	Guanosintriphosphat
HIV	human immunodeficiency virus
IAP	inhibitor of apoptosis protein
IEC	intestinal epithelial cell
iE-DAP	γ-D-glutamyl-meso-diaminopimelic acid
IκBα	inhibitor of NF-κB
IL	interleukin
IL-8	interleukin 8
IKK	inhibitor of κ light polypeptide gene enhancer in B-cells kinase
INF	interferon
IP$_3$	inositol trisphosphate
Ipa	invasion plasmid antigens
Ipg	invasion plasmid gene
IRAK	IL-1 receptor-associated kinase
IRF	interferon regulatory factor
JNK	JUN N-terminal kinase
LC-HRMS	liquid chromatography high resolution mass spectrometry
LPS	lipopolysaccharide
LRR	leucine-rich repeat
M-cells	microfold cells
MAP2 kinase	mitogen-activated protein kinase kinase
MAP3 kinase	mitogen-activated protein kinase kinase kinase
MAP kinase	mitogen-activated protein kinase
MD-2	myeloid differentiation protein-2
MDP	muramyl dipeptide
MOI	multiplicity of infection
MSK	mitogen- and stress-activated kinase
Mxi	membrane expression of Ipa
MYD88	myeloid differentiation primary response gene (88)
NACHT	domain has been named after NAIP, CIITA, HET-E and TP-1; also called NOD
NAD	NACHT-associated domain
NF-κB	nuclear factor of κ light polypeptide gene enhancer in B-cells
NK	natural killer
NOX4	NADPH oxidase
NLR	Nod-like receptor
NLRA	acidic domain containing NLR
NLRB	BIR domain containing NLR
NLRC	CARD domain containing NLR
NLRP	pyrin domain containing NLR

NLRX	no strong N-terminal homology NLR
NOD	nucleotide-binding and oligomerization domain; also called NACHT
N-WASP	neural Wiskott-Aldrich syndrome protein
Osp	outer *Shigella* proteins
PAI	pathogenicity Island
PAMP	pathogen-associated molecular pattern
PDG	peptidoglycan
PI3K	phosphoinositide-3-kinase
PI5P	phosphatidylinositol 5-phosphate
PIP2	phosphatidylinositol 4,5-bisphosphate
PKA	protein kinase A
PKC	protein kinase C
PKG	protein kinase G
PLC γ1	phospholipase Cγ1
PMN	polymorphnuclear cell
PRR	pathogen recognition receptor
PYD	pyrin domain
RAC	ras-related C3 botulinum toxin substrate
RHO	ras homolog
RIPK2	receptor-interacting protein 2
RLR	RIG-I-like receptor
RNAi	RNA interference
ROS	reactive oxygen species
SARM	sterile alpha and HEAT-Armadillo motifs
siRNA	small interfering RNA
Spa	surface presentation of antigen
SRC	v-src sarcoma viral oncogene homolog
ssRNA	single-stranded RNA
T3SS	type 3 secretion system
TAK1	TGFβ-activated kinase
TAB	TAK1-binding protein
TIFA	TRAF-interacting protein with a forkhead-associated (FHA) domain
TIR	Toll-IL-1 receptor
TLR	Toll-like receptor
TNF	tumor necrosis factor
TRAF	TNF receptor-associated factor
TRAM	TRIF-related adaptor molecule
TriDAP	L-alanyl-γ-D-glutamyl-meso-diaminopimelic acid
TRIF	TIR domain containing adaptor inducing interferon-β

Abbreviations

WHO	World Health Organization
XIAP	X-linked inhibitor of apoptosis protein
ZO	zonula occludens

References

1. Kotloff, K.L., et al., *Global burden of Shigella infections: implications for vaccine development and implementation of control strategies.* Bull World Health Organ, 1999. **77**(8): p. 651-66.
2. Bardhan, P., et al., *Decrease in shigellosis-related deaths without Shigella spp.-specific interventions, Asia.* Emerg Infect Dis, 2010. **16**(11): p. 1718-23.
3. Pazhani, G.P., et al., *Molecular characterization of multidrug-resistant Shigella species isolated from epidemic and endemic cases of shigellosis in India.* J Med Microbiol, 2008. **57**(Pt 7): p. 856-63.
4. Ewing, W.H., *Shigella Nomenclature.* J Bacteriol, 1949. **57**(6): p. 633-8.
5. DuPont, H.L., et al., *Inoculum size in shigellosis and implications for expected mode of transmission.* J Infect Dis, 1989. **159**(6): p. 1126-8.
6. Niyogi, S.K., *Shigellosis.* J. Microbiol., 2005. **43**(2): p. 133-143.
7. Sousa, M.A., et al., *Shigella in Brazilian children with acute diarrhoea: prevalence, antimicrobial resistance and virulence genes.* Mem Inst Oswaldo Cruz, 2013. **108**(1): p. 30-5.
8. Ashkenazi, S., et al., *Growing antimicrobial resistance of Shigella isolates.* J Antimicrob Chemother, 2003. **51**(2): p. 427-9.
9. Schroeder, G.N. and H. Hilbi, *Molecular pathogenesis of Shigella spp.: controlling host cell signaling, invasion, and death by type III secretion.* Clin Microbiol Rev, 2008. **21**(1): p. 134-56.
10. Buchrieser, C., et al., *The virulence plasmid pWR100 and the repertoire of proteins secreted by the type III secretion apparatus of Shigella flexneri.* Molecular Microbiology, 2000. **38**(4): p. 760-771.
11. Mavris, M., et al., *Regulation of transcription by the activity of the Shigella flexneri type III secretion apparatus.* Mol Microbiol, 2002. **43**(6): p. 1543-53.
12. Gall, T.L., et al., *Analysis of virulence plasmid gene expression defines three classes of effectors in the type III secretion system of Shigella flexneri.* Microbiology, 2005. **151**(3): p. 951-962.
13. Parsot, C., *Shigella spp. and enteroinvasive Escherichia coli pathogenicity factors.* FEMS Microbiol Lett, 2005. **252**(1): p. 11-8.
14. Tamano, K., et al., *Supramolecular structure of the Shigella type III secretion machinery: the needle part is changeable in length and essential for delivery of effectors.* EMBO J, 2000. **19**(15): p. 3876-87.
15. Blocker, A., et al., *Structure and composition of the Shigella flexneri "needle complex", a part of its type III secreton.* Mol Microbiol, 2001. **39**(3): p. 652-63.
16. Cordes, F.S., et al., *Helical structure of the needle of the type III secretion system of Shigella flexneri.* J Biol Chem, 2003. **278**(19): p. 17103-7.
17. Tobe, T., et al., *Temperature-regulated expression of invasion genes in Shigella flexneri is controlled through the transcriptional activation of the virB gene on the large plasmid.* Mol Microbiol, 1991. **5**(4): p. 887-93.
18. Nakayama, S. and H. Watanabe, *Involvement of cpxA, a sensor of a two-component regulatory system, in the pH-dependent regulation of expression of Shigella sonnei virF gene.* J Bacteriol, 1995. **177**(17): p. 5062-9.
19. Payne, S.M., et al., *Iron and pathogenesis of Shigella: iron acquisition in the intracellular environment.* Biometals, 2006. **19**(2): p. 173-80.

References

20.   Porter, M.E. and C.J. Dorman, *A role for H-NS in the thermo-osmotic regulation of virulence gene expression in Shigella flexneri.* J Bacteriol, 1994. **176**(13): p. 4187-91.

21.   Parsot, C., et al., *A secreted anti-activator, OspD1, and its chaperone, Spa15, are involved in the control of transcription by the type III secretion apparatus activity in Shigella flexneri.* Mol Microbiol, 2005. **56**(6): p. 1627-35.

22.   Gorden, J. and P.L. Small, *Acid resistance in enteric bacteria.* Infect Immun, 1993. **61**(1): p. 364-7.

23.   Islam, D., et al., *Downregulation of bactericidal peptides in enteric infections: a novel immune escape mechanism with bacterial DNA as a potential regulator.* Nat Med, 2001. **7**(2): p. 180-5.

24.   Mounier, J., et al., *Shigella flexneri enters human colonic Caco-2 epithelial cells through the basolateral pole.* Infect Immun, 1992. **60**(1): p. 237-48.

25.   Sansonetti, P.J., et al., *Infection of rabbit Peyer's patches by Shigella flexneri: effect of adhesive or invasive bacterial phenotypes on follicle-associated epithelium.* Infect Immun, 1996. **64**(7): p. 2752-64.

26.   Wassef, J.S., D.F. Keren, and J.L. Mailloux, *Role of M cells in initial antigen uptake and in ulcer formation in the rabbit intestinal loop model of shigellosis.* Infect Immun, 1989. **57**(3): p. 858-63.

27.   Zychlinsky, A., et al., *IpaB mediates macrophage apoptosis induced by Shigella flexneri.* Mol Microbiol, 1994. **11**(4): p. 619-27.

28.   Zychlinsky, A., et al., *Interleukin 1 is released by murine macrophages during apoptosis induced by Shigella flexneri.* J Clin Invest, 1994. **94**(3): p. 1328-32.

29.   Suzuki, S., et al., *Shigella type III secretion protein MxiI is recognized by Naip2 to induce Nlrc4 inflammasome activation independently of Pkcdelta.* PLoS Pathog, 2014. **10**(2): p. e1003926.

30.   Sansonetti, P.J., et al., *Role of interleukin-1 in the pathogenesis of experimental shigellosis.* J. Clin. Invest., 1995. **96**(2): p. 884-892.

31.   Sansonetti, P.J., et al., *Caspase-1 activation of IL-1beta and IL-18 are essential for Shigella flexneri-induced inflammation.* Immunity, 2000. **12**(5): p. 581-90.

32.   Perdomo, J.J., P. Gounon, and P.J. Sansonetti, *Polymorphonuclear leukocyte transmigration promotes invasion of colonic epithelial monolayer by Shigella flexneri.* J Clin Invest, 1994. **93**(2): p. 633-43.

33.   Sansonetti, P.J., et al., *Multiplication of Shigella flexneri within HeLa cells: lysis of the phagocytic vacuole and plasmid-mediated contact hemolysis.* Infect Immun, 1986. **51**(2): p. 461-9.

34.   Bernardini, M.L., et al., *Identification of icsA, a plasmid locus of Shigella flexneri that governs bacterial intra- and intercellular spread through interaction with F-actin.* Proc Natl Acad Sci U S A, 1989. **86**(10): p. 3867-71.

35.   Girardin, S.E., et al., *Nod1 Detects a Unique Muropeptide from Gram-Negative Bacterial Peptidoglycan.* Science, 2003. **300**(5625): p. 1584-1587.

36.   Pedron, T., C. Thibault, and P.J. Sansonetti, *The Invasive Phenotype of Shigella flexneri Directs a Distinct Gene Expression Pattern in the Human Intestinal Epithelial Cell Line Caco-2.* J. Biol. Chem., 2003. **278**(36): p. 33878-33886.

37.   Philpott, D.J., et al., *Invasive Shigella flexneri Activates NF-{kappa}B Through a Lipopolysaccharide-Dependent Innate Intracellular Response and Leads to IL-8 Expression in Epithelial Cells.* J Immunol, 2000. **165**(2): p. 903-914.

38.   Sansonetti, P.J., et al., *Interleukin-8 Controls Bacterial Transepithelial Translocation at the Cost of Epithelial Destruction in Experimental Shigellosis.* Infect. Immun., 1999. **67**(3): p. 1471-1480.

39. Kasper, C.A., et al., *Cell-cell propagation of NF-kappaB transcription factor and MAP kinase activation amplifies innate immunity against bacterial infection.* Immunity, 2010. **33**(5): p. 804-16.

40. Franchi, L., et al., *The inflammasome: a caspase-1-activation platform that regulates immune responses and disease pathogenesis.* Nat Immunol, 2009. **10**(3): p. 241-7.

41. Lamkanfi, M. and V.M. Dixit, *Inflammasomes and their roles in health and disease.* Annu Rev Cell Dev Biol, 2012. **28**: p. 137-61.

42. Lafont, F., et al., *Initial steps of Shigella infection depend on the cholesterol/sphingolipid raft-mediated CD44-IpaB interaction.* Embo J, 2002. **21**(17): p. 4449-57.

43. Simons, K. and W.L. Vaz, *Model systems, lipid rafts, and cell membranes.* Annu Rev Biophys Biomol Struct, 2004. **33**: p. 269-95.

44. Lillemeier, B.F., et al., *Plasma membrane-associated proteins are clustered into islands attached to the cytoskeleton.* Proc Natl Acad Sci U S A, 2006. **103**(50): p. 18992-7.

45. Simons, K. and D. Toomre, *Lipid rafts and signal transduction.* Nat Rev Mol Cell Biol, 2000. **1**(1): p. 31-9.

46. Parton, R.G. and A.A. Richards, *Lipid rafts and caveolae as portals for endocytosis: new insights and common mechanisms.* Traffic, 2003. **4**(11): p. 724-38.

47. Helms, J.B. and C. Zurzolo, *Lipids as targeting signals: lipid rafts and intracellular trafficking.* Traffic, 2004. **5**(4): p. 247-54.

48. Golub, T., S. Wacha, and P. Caroni, *Spatial and temporal control of signaling through lipid rafts.* Curr Opin Neurobiol, 2004. **14**(5): p. 542-50.

49. Skoudy, A., et al., *CD44 binds to the Shigella IpaB protein and participates in bacterial invasion of epithelial cells.* Cell Microbiol, 2000. **2**(1): p. 19-33.

50. Watarai, M., S. Funato, and C. Sasakawa, *Interaction of Ipa proteins of Shigella flexneri with alpha5beta1 integrin promotes entry of the bacteria into mammalian cells.* J Exp Med, 1996. **183**(3): p. 991-9.

51. Brotcke Zumsteg, A., et al., *IcsA is a Shigella flexneri adhesin regulated by the type III secretion system and required for pathogenesis.* Cell Host Microbe, 2014. **15**(4): p. 435-45.

52. Handa, Y., et al., *Shigella IpgB1 promotes bacterial entry through the ELMO-Dock180 machinery.* Nat Cell Biol, 2007. **9**(1): p. 121-8.

53. Alto, N.M., et al., *Identification of a bacterial type III effector family with G protein mimicry functions.* Cell, 2006. **124**(1): p. 133-45.

54. Terry, C.M., et al., *The C-terminus of IpaC is required for effector activities related to Shigella invasion of host cells.* Microb Pathog, 2008. **45**(4): p. 282-9.

55. Mounier, J., et al., *The IpaC carboxyterminal effector domain mediates Src-dependent actin polymerization during Shigella invasion of epithelial cells.* PLoS Pathog, 2009. **5**(1): p. e1000271.

56. Bourdet-Sicard, R., et al., *Binding of the Shigella protein IpaA to vinculin induces F-actin depolymerization.* Embo J, 1999. **18**(21): p. 5853-62.

57. Niebuhr, K., et al., *Conversion of PtdIns(4,5)P(2) into PtdIns(5)P by the S.flexneri effector IpgD reorganizes host cell morphology.* Embo J, 2002. **21**(19): p. 5069-78.

58. Clerc, P.L., et al., *Plasmid-mediated early killing of eucaryotic cells by Shigella flexneri as studied by infection of J774 macrophages.* Infect Immun, 1987. **55**(3): p. 521-7.

59. Picking, W.L., et al., *IpaD of Shigella flexneri is independently required for regulation of Ipa protein secretion and efficient insertion of IpaB and IpaC into host membranes.* Infect Immun, 2005. **73**(3): p. 1432-40.

60. High, N., et al., *IpaB of Shigella flexneri causes entry into epithelial cells and escape from the phagocytic vacuole.* EMBO J, 1992. **11**(5): p. 1991-9.

References

61. Barzu, S., et al., *Functional analysis of the Shigella flexneri IpaC invasin by insertional mutagenesis.* Infect Immun, 1997. **65**(5): p. 1599-605.

62. Fernandez-Prada, C.M., et al., *Shigella flexneri IpaH(7.8) facilitates escape of virulent bacteria from the endocytic vacuoles of mouse and human macrophages.* Infect Immun, 2000. **68**(6): p. 3608-19.

63. Goldberg, M.B., et al., *Unipolar localization and ATPase activity of IcsA, a Shigella flexneri protein involved in intracellular movement.* J Bacteriol, 1993. **175**(8): p. 2189-96.

64. Goldberg, M.B. and J.A. Theriot, *Shigella flexneri surface protein IcsA is sufficient to direct actin-based motility.* Proc Natl Acad Sci U S A, 1995. **92**(14): p. 6572-6.

65. Yoshida, S., et al., *Microtubule-severing activity of Shigella is pivotal for intercellular spreading.* Science, 2006. **314**(5801): p. 985-9.

66. Ogawa, M., et al., *IcsB, secreted via the type III secretion system, is chaperoned by IpgA and required at the post-invasion stage of Shigella pathogenicity.* Mol Microbiol, 2003. **48**(4): p. 913-31.

67. Ogawa, M., et al., *Escape of intracellular Shigella from autophagy.* Science, 2005. **307**(5710): p. 727-31.

68. Rathman, M., et al., *Myosin light chain kinase plays an essential role in S. flexneri dissemination.* J Cell Sci, 2000. **113 Pt 19**: p. 3375-86.

69. Sansonetti, P.J., et al., *Cadherin expression is required for the spread of Shigella flexneri between epithelial cells.* Cell, 1994. **76**(5): p. 829-39.

70. Takeuchi, O. and S. Akira, *Pattern recognition receptors and inflammation.* Cell, 2010. **140**(6): p. 805-20.

71. Chen, G.Y. and G. Nunez, *Sterile inflammation: sensing and reacting to damage.* Nat Rev Immunol, 2010. **10**(12): p. 826-37.

72. Kim, E.K. and E.J. Choi, *Pathological roles of MAPK signaling pathways in human diseases.* Biochim Biophys Acta, 2010. **1802**(4): p. 396-405.

73. Vallabhapurapu, S. and M. Karin, *Regulation and function of NF-kappaB transcription factors in the immune system.* Annu Rev Immunol, 2009. **27**: p. 693-733.

74. Battistini, A., *Interferon regulatory factors in hematopoietic cell differentiation and immune regulation.* J Interferon Cytokine Res, 2009. **29**(12): p. 765-80.

75. Mogensen, T.H., *Pathogen recognition and inflammatory signaling in innate immune defenses.* Clin Microbiol Rev, 2009. **22**(2): p. 240-73, Table of Contents.

76. O'Neill, L.A., D. Golenbock, and A.G. Bowie, *The history of Toll-like receptors - redefining innate immunity.* Nat Rev Immunol, 2013. **13**(6): p. 453-60.

77. O'Neill, L.A. and A.G. Bowie, *The family of five: TIR-domain-containing adaptors in Toll-like receptor signalling.* Nat Rev Immunol, 2007. **7**(5): p. 353-64.

78. Kawai, T. and S. Akira, *Toll-like receptors and their crosstalk with other innate receptors in infection and immunity.* Immunity, 2011. **34**(5): p. 637-50.

79. Franchi, L., et al., *Function of Nod-like receptors in microbial recognition and host defense.* Immunol Rev, 2009. **227**(1): p. 106-28.

80. Ting, J.P., et al., *The NLR gene family: a standard nomenclature.* Immunity, 2008. **28**(3): p. 285-7.

81. Iwasaki, A. and R. Medzhitov, *Toll-like receptor control of the adaptive immune responses.* Nat Immunol, 2004. **5**(10): p. 987-95.

82. Haas, T., et al., *The DNA sugar backbone 2' deoxyribose determines toll-like receptor 9 activation.* Immunity, 2008. **28**(3): p. 315-23.

83. Kenny, E.F. and L.A. O'Neill, *Signalling adaptors used by Toll-like receptors: an update.* Cytokine, 2008. **43**(3): p. 342-9.

84. Schroder, K. and J. Tschopp, *The inflammasomes.* Cell, 2010. **140**(6): p. 821-32.

85.   Bergsbaken, T., S.L. Fink, and B.T. Cookson, *Pyroptosis: host cell death and inflammation.* Nat Rev Microbiol, 2009. **7**(2): p. 99-109.

86.   Ting, J.P., J.A. Duncan, and Y. Lei, *How the noninflammasome NLRs function in the innate immune system.* Science, 2010. **327**(5963): p. 286-90.

87.   Travassos, L.H., et al., *Nod1 and Nod2 direct autophagy by recruiting ATG16L1 to the plasma membrane at the site of bacterial entry.* Nat Immunol, 2010. **11**(1): p. 55-62.

88.   Watanabe, T., et al., *NOD1 contributes to mouse host defense against Helicobacter pylori via induction of type I IFN and activation of the ISGF3 signaling pathway.* J Clin Invest, 2010. **120**(5): p. 1645-62.

89.   Chamaillard, M., et al., *An essential role for NOD1 in host recognition of bacterial peptidoglycan containing diaminopimelic acid.* Nat Immunol, 2003. **4**(7): p. 702-7.

90.   Opitz, B., et al., *Listeria monocytogenes Activated p38 MAPK and Induced IL-8 Secretion in a Nucleotide-Binding Oligomerization Domain 1-Dependent Manner in Endothelial Cells.* J Immunol, 2006. **176**(1): p. 484-490.

91.   Girardin, S.E., et al., *Nod2 is a general sensor of peptidoglycan through muramyl dipeptide (MDP) detection.* J Biol Chem, 2003. **278**(11): p. 8869-72.

92.   Strober, W., et al., *Signalling pathways and molecular interactions of NOD1 and NOD2.* Nat Rev Immunol, 2006. **6**(1): p. 9-20.

93.   Werts, C., et al., *Nod-like receptors in intestinal homeostasis, inflammation, and cancer.* J Leukoc Biol, 2011. **90**(3): p. 471-82.

94.   Barnich, N., et al., *Membrane recruitment of NOD2 in intestinal epithelial cells is essential for nuclear factor-{kappa}B activation in muramyl dipeptide recognition.* J Cell Biol, 2005. **170**(1): p. 21-6.

95.   Gutierrez, O., et al., *Induction of Nod2 in myelomonocytic and intestinal epithelial cells via nuclear factor-kappa B activation.* J Biol Chem, 2002. **277**(44): p. 41701-5.

96.   Rosenstiel, P., et al., *TNF-alpha and IFN-gamma regulate the expression of the NOD2 (CARD15) gene in human intestinal epithelial cells.* Gastroenterology, 2003. **124**(4): p. 1001-9.

97.   Philpott, D.J., et al., *NOD proteins: regulators of inflammation in health and disease.* Nat Rev Immunol, 2014. **14**(1): p. 9-23.

98.   Viala, J., et al., *Nod1 responds to peptidoglycan delivered by the Helicobacter pylori cag pathogenicity island.* Nat Immunol, 2004. **5**(11): p. 1166-74.

99.   Hruz, P., et al., *NOD2 contributes to cutaneous defense against Staphylococcus aureus through alpha-toxin-dependent innate immune activation.* Proc Natl Acad Sci U S A, 2009. **106**(31): p. 12873-8.

100.   Marina-Garcia, N., et al., *Clathrin- and dynamin-dependent endocytic pathway regulates muramyl dipeptide internalization and NOD2 activation.* J Immunol, 2009. **182**(7): p. 4321-7.

101.   Lee, J., et al., *pH-dependent internalization of muramyl peptides from early endosomes enables Nod1 and Nod2 signaling.* J Biol Chem, 2009. **284**(35): p. 23818-29.

102.   Laroui, H., et al., *L-Ala-gamma-D-Glu-meso-diaminopimelic acid (DAP) interacts directly with leucine-rich region domain of nucleotide-binding oligomerization domain 1, increasing phosphorylation activity of receptor-interacting serine/threonine-protein kinase 2 and its interaction with nucleotide-binding oligomerization domain 1.* J Biol Chem, 2011. **286**(35): p. 31003-13.

103.   Grimes, C.L., et al., *The innate immune protein Nod2 binds directly to MDP, a bacterial cell wall fragment.* J Am Chem Soc, 2012. **134**(33): p. 13535-7.

104.   Mo, J., et al., *Pathogen sensing by nucleotide-binding oligomerization domain-containing protein 2 (NOD2) is mediated by direct binding to muramyl dipeptide and ATP.* J Biol Chem, 2012. **287**(27): p. 23057-67.

References

105. Park, J.H., et al., *RICK/RIP2 mediates innate immune responses induced through Nod1 and Nod2 but not TLRs.* J Immunol, 2007. **178**(4): p. 2380-6.

106. Yang, Y., et al., *NOD2 pathway activation by MDP or Mycobacterium tuberculosis infection involves the stable polyubiquitination of Rip2.* J Biol Chem, 2007. **282**(50): p. 36223-9.

107. Inohara, N., et al., *An induced proximity model for NF-kappa B activation in the Nod1/RICK and RIP signaling pathways.* J Biol Chem, 2000. **275**(36): p. 27823-31.

108. Hasegawa, M., et al., *A critical role of RICK/RIP2 polyubiquitination in Nod-induced NF-kappaB activation.* Embo J, 2008. **27**(2): p. 373-83.

109. Krieg, A., et al., *XIAP mediates NOD signaling via interaction with RIP2.* Proc Natl Acad Sci U S A, 2009. **106**(34): p. 14524-9.

110. Bertrand, M.J., et al., *Cellular inhibitors of apoptosis cIAP1 and cIAP2 are required for innate immunity signaling by the pattern recognition receptors NOD1 and NOD2.* Immunity, 2009. **30**(6): p. 789-801.

111. Estornes, Y. and M.J. Bertrand, *IAPs, regulators of innate immunity and inflammation.* Semin Cell Dev Biol, 2014.

112. Girardin, S.E., et al., *CARD4/Nod1 mediates NF-κB and JNK activation by invasive Shigella flexneri.* EMBO Rep., 2001. **2**(8): p. 736-742.

113. Wang, C., et al., *TAK1 is a ubiquitin-dependent kinase of MKK and IKK.* Nature, 2001. **412**(6844): p. 346-51.

114. Holtmann, H., et al., *Induction of Interleukin-8 Synthesis Integrates Effects on Transcription and mRNA Degradation from at Least Three Different Cytokine- or Stress-Activated Signal Transduction Pathways.* Mol. Cell. Biol., 1999. **19**(10): p. 6742-6753.

115. Saccani, S., S. Pantano, and G. Natoli, *p38-dependent marking of inflammatory genes for increased NF-[kappa]B recruitment.* Nat Immunol, 2002. **3**(1): p. 69-75.

116. Fritz, J.H., et al., *Synergistic stimulation of human monocytes and dendritic cells by Toll-like receptor 4 and NOD1- and NOD2-activating agonists.* Eur J Immunol, 2005. **35**(8): p. 2459-70.

117. Masumoto, J., et al., *Nod1 acts as an intracellular receptor to stimulate chemokine production and neutrophil recruitment in vivo.* J Exp Med, 2006. **203**(1): p. 203-13.

118. Uehara, A., et al., *Various human epithelial cells express functional Toll-like receptors, NOD1 and NOD2 to produce anti-microbial peptides, but not proinflammatory cytokines.* Molecular Immunology, 2007. **44**(12): p. 3100-3111.

119. Keestra, A.M., et al., *Manipulation of small Rho GTPases is a pathogen-induced process detected by NOD1.* Nature, 2013. **496**(7444): p. 233-7.

120. Fukazawa, A., et al., *GEF-H1 mediated control of NOD1 dependent NF-kappaB activation by Shigella effectors.* PLoS Pathog, 2008. **4**(11): p. e1000228.

121. Zhao, Y., et al., *Control of NOD2 and Rip2-dependent innate immune activation by GEF-H1.* Inflamm Bowel Dis, 2012. **18**(4): p. 603-12.

122. Magalhaes, J.G., et al., *Nod2-dependent Th2 polarization of antigen-specific immunity.* J Immunol, 2008. **181**(11): p. 7925-35.

123. Fritz, J.H., et al., *Nod1-mediated innate immune recognition of peptidoglycan contributes to the onset of adaptive immunity.* Immunity, 2007. **26**(4): p. 445-59.

124. Thornberry, N.A., et al., *A novel heterodimeric cysteine protease is required for interleukin-1 beta processing in monocytes.* Nature, 1992. **356**(6372): p. 768-74.

125. Ghayur, T., et al., *Caspase-1 processes IFN-gamma-inducing factor and regulates LPS-induced IFN-gamma production.* Nature, 1997. **386**(6625): p. 619-23.

126. Gu, Y., et al., *Activation of interferon-gamma inducing factor mediated by interleukin-1beta converting enzyme.* Science, 1997. **275**(5297): p. 206-9.

127. Martinon, F., K. Burns, and J. Tschopp, *The inflammasome: a molecular platform triggering activation of inflammatory caspases and processing of proIL-beta.* Mol Cell, 2002. **10**(2): p. 417-26.

128. Fink, S.L. and B.T. Cookson, *Caspase-1-dependent pore formation during pyroptosis leads to osmotic lysis of infected host macrophages.* Cell Microbiol, 2006. **8**(11): p. 1812-25.

129. Broz, P., et al., *Caspase-11 increases susceptibility to Salmonella infection in the absence of caspase-1.* Nature, 2012. **490**(7419): p. 288-91.

130. Kayagaki, N., et al., *Non-canonical inflammasome activation targets caspase-11.* Nature, 2011. **479**(7371): p. 117-21.

131. Hiscott, J., et al., *Characterization of a functional NF-kappa B site in the human interleukin 1 beta promoter: evidence for a positive autoregulatory loop.* Mol Cell Biol, 1993. **13**(10): p. 6231-40.

132. Franchi, L., T. Eigenbrod, and G. Nunez, *Cutting edge: TNF-alpha mediates sensitization to ATP and silica via the NLRP3 inflammasome in the absence of microbial stimulation.* J Immunol, 2009. **183**(2): p. 792-6.

133. Miao, E.A., et al., *Innate immune detection of the type III secretion apparatus through the NLRC4 inflammasome.* Proc Natl Acad Sci U S A, 2010. **107**(7): p. 3076-80.

134. Abreu, M.T., et al., *Decreased Expression of Toll-Like Receptor-4 and MD-2 Correlates with Intestinal Epithelial Cell Protection Against Dysregulated Proinflammatory Gene Expression in Response to Bacterial Lipopolysaccharide.* J. Immunol., 2001. **167**(3): p. 1609-1616.

135. Abreu, M.T., *Toll-like receptor signalling in the intestinal epithelium: how bacterial recognition shapes intestinal function.* Nat Rev Immunol, 2010. **10**(2): p. 131-44.

136. Hornef, M.W., et al., *Intracellular recognition of lipopolysaccharide by toll-like receptor 4 in intestinal epithelial cells.* J Exp Med, 2003. **198**(8): p. 1225-35.

137. Hornef, M.W., et al., *Toll-like receptor 4 resides in the Golgi apparatus and colocalizes with internalized lipopolysaccharide in intestinal epithelial cells.* J Exp Med, 2002. **195**(5): p. 559-70.

138. Cario, E. and D.K. Podolsky, *Differential alteration in intestinal epithelial cell expression of toll-like receptor 3 (TLR3) and TLR4 in inflammatory bowel disease.* Infect Immun, 2000. **68**(12): p. 7010-7.

139. Kim, J.G., S.J. Lee, and M.F. Kagnoff, *Nod1 is an essential signal transducer in intestinal epithelial cells infected with bacteria that avoid recognition by toll-like receptors.* Infect Immun, 2004. **72**(3): p. 1487-95.

140. Sanada, T., et al., *The Shigella flexneri effector OspI deamidates UBC13 to dampen the inflammatory response.* Nature, 2012. **483**(7391): p. 623-6.

141. Ashida, H., et al., *Shigella deploy multiple countermeasures against host innate immune responses.* Curr Opin Microbiol, 2011. **14**(1): p. 16-23.

142. Ogawa, M., et al., *The versatility of Shigella effectors.* Nat Rev Micro, 2008. **6**(1): p. 11-16.

143. Ashida, H., et al., *A bacterial E3 ubiquitin ligase IpaH9.8 targets NEMO/IKKgamma to dampen the host NF-kappaB-mediated inflammatory response.* Nat Cell Biol, 2010. **12**(1): p. 66-73; sup pp 1-9.

144. Okuda, J., et al., *Shigella effector IpaH9.8 binds to a splicing factor U2AF35 to modulate host immune responses.* Biochem. Biophys. Res. Commun., 2005. **333**(2): p. 531-539.

145. Ashida, H., H. Nakano, and C. Sasakawa, *Shigella IpaH0722 E3 ubiquitin ligase effector targets TRAF2 to inhibit PKC-NF-kappaB activity in invaded epithelial cells.* PLoS Pathog, 2013. **9**(6): p. e1003409.

References

146.   Kim, D.W., et al., *The Shigella flexneri effector OspG interferes with innate immune responses by targeting ubiquitin-conjugating enzymes.* Proc Natl Acad Sci U S A, 2005. **102**(39): p. 14046-51.

147.   Newton, H.J., et al., *The type III effectors NleE and NleB from enteropathogenic E. coli and OspZ from Shigella block nuclear translocation of NF-kappaB p65.* PLoS Pathog, 2010. **6**(5): p. e1000898.

148.   Zurawski, D.V., et al., *Shigella flexneri type III secretion system effectors OspB and OspF target the nucleus to downregulate the host inflammatory response via interactions with retinoblastoma protein.* Mol Microbiol, 2009. **71**(2): p. 350-68.

149.   Sperandio, B., et al., *Virulent Shigella flexneri subverts the host innate immune response through manipulation of antimicrobial peptide gene expression.* J Exp Med, 2008. **205**(5): p. 1121-32.

150.   Lowell, G.H., et al., *Antibody-dependent cell-mediated antibacterial activity: K lymphocytes, monocytes, and granulocytes are effective against shigella.* J Immunol, 1980. **125**(6): p. 2778-84.

151.   Brinkmann, V., et al., *Neutrophil extracellular traps kill bacteria.* Science, 2004. **303**(5663): p. 1532-5.

152.   Alexander, D.B. and G.S. Goldberg, *Transfer of biologically important molecules between cells through gap junction channels.* Curr Med Chem, 2003. **10**(19): p. 2045-58.

153.   Sohl, G. and K. Willecke, *Gap junctions and the connexin protein family.* Cardiovasc Res, 2004. **62**(2): p. 228-32.

154.   Herve, J.C., et al., *Gap junctional complexes: from partners to functions.* Prog Biophys Mol Biol, 2007. **94**(1-2): p. 29-65.

155.   Dbouk, H.A., et al., *Connexins: a myriad of functions extending beyond assembly of gap junction channels.* Cell Commun Signal, 2009. **7**: p. 4.

156.   Shimizu, K. and M. Stopfer, *Gap junctions.* Curr Biol, 2013. **23**(23): p. R1026-31.

157.   Giepmans, B.N., *Gap junctions and connexin-interacting proteins.* Cardiovasc Res, 2004. **62**(2): p. 233-45.

158.   Leybaert, L. and M.J. Sanderson, *Intercellular Ca(2+) waves: mechanisms and function.* Physiol Rev, 2012. **92**(3): p. 1359-92.

159.   Hamada, N., et al., *Intercellular and intracellular signaling pathways mediating ionizing radiation-induced bystander effects.* J Radiat Res (Tokyo), 2007. **48**(2): p. 87-95.

160.   Ablasser, A., et al., *Cell intrinsic immunity spreads to bystander cells via the intercellular transfer of cGAMP.* Nature, 2013. **503**(7477): p. 530-4.

161.   Patel, S.J., et al., *DNA-triggered innate immune responses are propagated by gap junction communication.* Proc Natl Acad Sci U S A, 2009. **106**(31): p. 12867-72.

162.   Raqib, R., et al., *Cytokine secretion in acute shigellosis is correlated to disease activity and directed more to stool than to plasma.* J Infect Dis, 1995. **171**(2): p. 376-84.

163.   Dolowschiak, T., et al., *Potentiation of epithelial innate host responses by intercellular communication.* PLoS Pathog, 2010. **6**(11): p. e1001194.

164.   Girardin, S.E., et al., *Nod1 detects a unique muropeptide from gram-negative bacterial peptidoglycan.* Science, 2003. **300**(5625): p. 1584-7.

165.   Makino, S., et al., *A genetic determinant required for continuous reinfection of adjacent cells on large plasmid in S. flexneri 2a.* Cell, 1986. **46**(4): p. 551-5.

166.   Singhirunnusorn, P., et al., *Critical roles of threonine 187 phosphorylation in cellular stress-induced rapid and transient activation of transforming growth factor-beta-activated kinase 1 (TAK1) in a signaling complex containing TAK1-binding protein TAB1 and TAB2.* J Biol Chem, 2005. **280**(8): p. 7359-68.

167. Nembrini, C., et al., *The kinase activity of Rip2 determines its stability and consequently Nod1- and Nod2-mediated immune responses.* J Biol Chem, 2009. **284**(29): p. 19183-8.

168. Dorsch, M., et al., *Identification of a regulatory autophosphorylation site in the serine-threonine kinase RIP2.* Cell Signal, 2006. **18**(12): p. 2223-9.

169. Schmutz, C., et al., *Systems-level overview of host protein phosphorylation during Shigella flexneri infection revealed by phosphoproteomics.* Mol Cell Proteomics, 2013. **12**(10): p. 2952-68.

170. Landstrom, M., *The TAK1-TRAF6 signalling pathway.* Int J Biochem Cell Biol, 2010. **42**(5): p. 585-9.

171. Huang, C.C., et al., *Intermolecular binding between TIFA-FHA and TIFA-pT mediates tumor necrosis factor alpha stimulation and NF-kappaB activation.* Mol Cell Biol, 2012. **32**(14): p. 2664-73.

172. Brigotti, M., et al., *Effects of osmolarity, ions and compatible osmolytes on cell-free protein synthesis.* Biochem J, 2003. **369**(Pt 2): p. 369-74.

173. Tran Van Nhieu, G., et al., *Connexin-dependent inter-cellular communication increases invasion and dissemination of Shigella in epithelial cells.* Nat Cell Biol, 2003. **5**(8): p. 720-726.

174. Ramel, D., et al., *Shigella flexneri infection generates the lipid PI5P to alter endocytosis and prevent termination of EGFR signaling.* Sci Signal, 2011. **4**(191): p. ra61.

175. Kim, M.L., et al., *IKKalpha contributes to canonical NF-kappaB activation downstream of Nod1-mediated peptidoglycan recognition.* PLoS One, 2010. **5**(10): p. e15371.

176. Carpenter, A., et al., *CellProfiler: image analysis software for identifying and quantifying cell phenotypes.* Genome Biol., 2006. **7**(10): p. R100.

177. Kawai, T. and S. Akira, *Toll-like receptor downstream signaling.* Arthritis Res Ther, 2005. **7**(1): p. 12-9.

178. Dupont, N., et al., *Shigella phagocytic vacuolar membrane remnants participate in the cellular response to pathogen invasion and are regulated by autophagy.* Cell Host Microbe, 2009. **6**(2): p. 137-49.

179. Takatsuna, H., et al., *Identification of TIFA as an adapter protein that links tumor necrosis factor receptor-associated factor 6 (TRAF6) to interleukin-1 (IL-1) receptor-associated kinase-1 (IRAK-1) in IL-1 receptor signaling.* J Biol Chem, 2003. **278**(14): p. 12144-50.

180. Ea, C.K., et al., *TIFA activates IkappaB kinase (IKK) by promoting oligomerization and ubiquitination of TRAF6.* Proc Natl Acad Sci U S A, 2004. **101**(43): p. 15318-23.

181. Fujishiro, S.H., et al., *ERK1/2 phosphorylate GEF-H1 to enhance its guanine nucleotide exchange activity toward RhoA.* Biochem Biophys Res Commun, 2008. **368**(1): p. 162-7.

182. Tang, L., et al., *Expression of TRAF6 and pro-inflammatory cytokines through activation of TLR2, TLR4, NOD1, and NOD2 in human periodontal ligament fibroblasts.* Arch Oral Biol, 2011. **56**(10): p. 1064-72.

183. Minoda, Y., et al., *A novel Zinc finger protein, ZCCHC11, interacts with TIFA and modulates TLR signaling.* Biochem Biophys Res Commun, 2006. **344**(3): p. 1023-30.

184. Fujimoto, Y., et al., *Peptidoglycan as Nod1 ligand; fragment structures in the environment, chemical synthesis, and their innate immunostimulation.* Nat Prod Rep, 2012. **29**(5): p. 568-79.

185. Pradipta, A.R., et al., *Characterization of natural human nucleotide-binding oligomerization domain protein 1 (Nod1) ligands from bacterial culture supernatant for elucidation of immune modulators in the environment.* J Biol Chem, 2010. **285**(31): p. 23607-13.

186. Chamaillard, M., et al., *An essential role for NOD1 in host recognition of bacterial peptidoglycan containing diaminopimelic acid.* Nat. Immunol., 2003. **4**(7): p. 702-707.

References

187.   Wang, H., et al., *Ouabain assembles signaling cascades through the caveolar Na+/K+-ATPase.* J Biol Chem, 2004. **279**(17): p. 17250-9.

188.   Yuan, Z., et al., *Na/K-ATPase tethers phospholipase C and IP3 receptor into a calcium-regulatory complex.* Mol Biol Cell, 2005. **16**(9): p. 4034-45.

189.   Nigro, G., et al., *Muramylpeptide shedding modulates cell sensing of Shigella flexneri.* Cell Microbiol, 2008. **10**(3): p. 682-95.

190.   Girardin, S.E., et al., *Identification of the critical residues involved in peptidoglycan detection by Nod1.* J Biol Chem, 2005. **280**(46): p. 38648-56.

191.   Rosse, C., et al., *PKC and the control of localized signal dynamics.* Nat Rev Mol Cell Biol, 2010. **11**(2): p. 103-12.

192.   Zhang, S., et al., *Distinct role of the N-terminal tail of the Na,K-ATPase catalytic subunit as a signal transducer.* J Biol Chem, 2006. **281**(31): p. 21954-62.

Acknowledgements

I would like to express my greatest gratitude to the people who have helped and supported me throughout my project:

- My supervisor Prof. Cécile Arrieumerlou who gave me the opportunity to work on this great and challenging project, for her patient guidance and for providing me with excellent ideas.

- My committee members Prof. Christoph Dehio and Prof. Matthias Wyman who showed great interest in my work and gave me useful advice and input.

- My colleagues Isabel Sorg and Christoph Kasper, who showed enormous interest in the project, shared their broad knowledge and excellent ideas with me, who performed many experiments and were always encouraging and last but not least, for the critical reading of my manuscript.

- My colleague Christoph Schmutz for reading the manuscript and for giving me a lot of fruitful input.

- The group members, Marlies Amstuz, Michaela Hanisch and Simon Ittig, for the great atmosphere, all the fun we had, their help and support throughout my PhD.

- The former group members Veronika Reiterer, Sonja Weichsel, Gregory Melroe, Man Lyang Kim, Lars Grossniklaus and Roland Dreier for being great colleagues.

- Rusudan Okujava for making the two cell lines stably expressing GFP that made my live so much easier.

- Maxime Québatte for sharing his broad knowledge about qRT-PCR with me and for his assistance with Microsoft word.

- Christoph Dehio and all group members, who shared lab and office space with me, were very helpful and generous, and created ideal conditions for me to finish my PhD.

- Petra Chiquet and David Kentner for sharing their protocols and for their assistance during sample preparation.

- Prof. Julia Vorholt, Nathanael Delmotte and Patrick Kiefer for being great and helpful collaborators.

- Martina Liuzzo, my trainee, who did a great job and was extremely helpful.

List of publications

- Kasper CA, Sorg I, Schmutz C, **Tschon T**, Wischnewski H, Kim ML, Arrieumerlou C. Cell-cell propagation of NF-κB transcription factor and MAP kinase activation amplifies innate immunity against bacterial infection. *Immunity*, 33(5):804–16, 2010.

- Reiterer V, Grossniklaus L, **Tschon T**, Kasper CA, Sorg I, Arrieumerlou C. *Shigella* flexneri type III secreted effector OspF reveals new crosstalks of proinflammatory signaling pathways during bacterial infection. *Cell Signal*, 23(7):1188–96, 2011.

- Schmutz C, Ahrne E, Kasper CA, **Tschon T**, Sorg I, Dreier RF, Schmidt A, Arrieumerlou C. Systems-level overview of host protein phosphorylation during *Shigella* flexneri infection revealed by phosphoproteomics. *Molecular & cellular proteomics*, 12(10): 2952-2968, 2013.

Curriculum vitae

Personal data

Name: Therese Tschon-Müller
Date of birth: 19th of November, 1962
Place of birth: Aarau AG
Place of citizenship: Füllinsdorf BL

Education

Oct. 2010 – Nov. 2014:   PhD Thesis
                            Thesis committee: Prof. Dr. Cécile Arrieumerlou (PI),
                            Prof. Dr. Christoph Dehio, Prof. Dr. Matthias Wymann
                            Focal Area Infection Biology
                            Biozentrum, University of Basel
Sep. 2007 - Jan. 2009:   Master of Science in Molecular Biology
                            Major in Cell Biology
                            Thesis committee: Prof. Dr. Birthe Fahrenkrog (PI),
                            Prof. Dr. Ueli Aebi
                            Focal Area Structural Biology
                            Biozentrum, University of Basel
Oct. 2003 - Jul. 2007:   Bachelor of Science in Biology
                            Major in Molecular Biology
                            University of Basel
Sept. 1999 - Mar. 2003:   AKAD Zürich ZH
                            Higher education entrance qualification
                            Main subject mathematics